Combustion and co-combustion characteristics of *Searsia lancea* and *Tamarix usneoides* with coal

Prepared by:

Ntsundeni Richiewell Ndou (818662)

Masters dissertation submitted to Faculty of Engineering and the Built Environment, University of the Witwatersrand, Johannesburg, South Africa, in fulfilment of the requirements for the degree of Master of Science in Engineering

Supervisors:

Dr. Samson O. Bada and Prof. Rosemary Falcon

Advisor:

Miss I. Weiersbye

April 2020

DECLARATION

I declare that this dissertation is my own unaided work, unless otherwise stated and acknowledged. It is being submitted for the degree of Master of Science in Engineering to the University of the Witwatersrand, Johannesburg. It has not been submitted before for any degree or examination to any other university.

Signed: …….. on this 22nd day of April, year 2020

ABSTRACT

The co-combustion of coal with biomass is one of the promising technologies that can offer cleaner and sustainable electricity. This option is attractive as it holds the potential to reduce CO_2, NO_x and SO_x emissions from coal combustion, which are associated with climate change. As emission standards and regulations become stricter, existing coal power stations will struggle to comply as various technologies like Flue Gas Desulfurization (FGD) are too expensive to be integrated with an existing power plant. The co-firing of coal with biomass would be a suitable approach for South Africa which is largely dependent on coal, as the country continue using its available coal resources to meet its energy demand, while complying with the stipulated environmental regulations. However, with the poor physicochemical properties of many biomass sources, it is important to investigate the suitability of each biomass species in order to determine their co-firing potential before being used.

Two indigenous South African trees, *Searsia lancea* and *Tamarix usneoides* were planted to control Acid Mine Drainage (AMD) in mining areas. The trees were planted as part of the AngloGold Ashanti (AGA) mine rehabilitation program in collaboration with the University of the Witwatersrand. The tree species were chosen because of their ability to absorb toxic minerals in their different parts, particularly in the leaves. Different parts of the trees were evaluated for their combustion and co-combustion potential with two South African coals, a discard and a run of mine coal. The physicochemical characteristics and thermal properties of the coals, raw biomass and their blends were investigated using a thermogravimetric analyzer (TGA), a bomb calorimeter, and an elemental analyzer (Elementar vario EL cube analyser). The oxides of major and minor elements present in the biomass, coal and their blends were obtained from X-ray Fluorescence (XRF) techniques. The emissions of CO_2, NO_x and SO_x during biomass, coal and coal-biomass co-combustion were monitored using Multi Gas Analyzer (MGA 11).

Significant differences in fuel characteristics were found between both tree species and their divided plant COMPONENTS and the coals used in the co-firing tests. *Searsia lancea*'s leaves possessed a calorific value of 19.21 MJ/kg compared to 16.73 MJ/kg from the discard coal utilized. All the *Searsia lancea* blends, irrespective of trial site location, possessed lower ash contents (3.77

to 6.60%) relative to *Tamarix usneoides* plant blends which were found to have ash contents of 7.48 to 8.98%. The leaves of both tree species were found with the highest ash content and concentrations of alkali elements leading to higher slagging and fouling ratios. The coals utilized were seen to ignite and burnout completely at higher temperatures than biomass. *Searsia lancea* and *Tamarix usneoides* displayed higher combustion reactivity than discard coal and run of mine coal. *Searsia lancea* harvested from the Mispah site and *Tamarix usneoides* harvested from the Madala site are better fuels, in terms of reactivity compared to all other samples. A decrease in ignition temperature was noted for the discard coal when co-fired with both *Searsia lancea* and *Tamarix usneoides.* There was also an increase in the coal reactivity as the percentage of biomass in the blend increased.

The activation energies for the 100% biomass were found to be lower than the activation energies for the coals utilized in this study, indicating that less energy is required for biomass combustion than for coal combustion. The activation energy for the first stage combustion of *Searsia lancea* was 32.98 kJ/mol, and 24.94 kJ/mol for its second stage combustion reaction. *Tamarix usneoides* had an activation energy of 37.39 and 26.23 kJ/mol in its first and second stage combustion, respectively. The biomass used were found with higher amounts of Na_2O and K_2O than discard coal, indicating that the use of biomass alone for power generation might be detrimental to boilers. The addition of coal to the biomass was found to reduce the concentrations of Na_2O and K_2O, thereby lowering the slagging and fouling potential of the biomass. The emitted gases, that is, CO_2, SO_x and NO_x from the discard coal were reduced by the blending and co-firing of the biomass with coal. This study has demonstrated that both indigenous tree species used for the phytoremediation of contaminated mine sites, could serve as a suitable and compatible valuable source of biomass for combustion and co-combustion with South African high ash coal.

ACKNOWLEDGEMENTS

I am highly indebted to the following individuals and organizations for their support throughout the development of this dissertation:

- My supervisors, Dr. Samson Bada and Prof. Rosemary Falcon for their overwhelming support, relentless guidance and enlightening expertise.
- The National Research Foundation (NRF) and Department of Science and Innovation (DSI) for funding and opportunity.
- The Cyril Ramaphosa Educational Trust (CRET) for additional financial and emotional support.
- The Wits University Clean Coal Technology Research group for valuable inputs and experimental assistance.
- The Wits School of Chemical and Metallurgical Engineering for providing research equipment.
- Mr. Andrew Morgan from the Wits School of Mining Engineering for technical support during experiments.
- Miss I. Weiersbye from the Wits School of Animal, Plant and Environmental Sciences for providing the biomass.
- My family and friends for being pillars of strength.
- Lastly, the Almighty God for keeping me sane.

CONTENTS

LIST OF FIGURES

LIST OF TABLES

CHAPTER 1: INTRODUCTION

1.1 Background and motivation

In recent years, South Africa's economy has been damaged by sustained power cuts caused by under-investment in electricity and shortage of generating capacity (Hedden, 2015). Poor people are also suffering from the exorbitant electricity tariffs that increase almost every year. Clearly, there is an energy crisis in South Africa. According to Export.gov. (2019), coal accounts for approximately 85% of South Africa's electricity production. This is likely to remain the same for the next few years. The quality of coal has been deteriorating leading to a decline in the combustion efficiency (Taole, 2014). Climate change and global warming are at their all-time high (Nunez, 2019). Many researchers have indicated that the emissions from coal combustion are a huge contributor to the ongoing environmental problems. Coal combustion releases CO_2 and SO_x that are deemed harmful to the environment (Keating, 2011). Consequently, there is a great need to move to cleaner electricity generating technologies to curb the emissions and climate change (Gil *et al*., 2010).

Many renewable and clean energy alternatives have proved to be inefficient in South Africa (Slabbert, 2017). For example, solar energy is intermittent as it depends on weather conditions. This means that the solar energy should be stored for it to be used efficiently. However, the cost of storing solar energy is very high (Williams, 2013). Similarly, wind energy cannot be depended on since wind power is not guaranteed daily and is hard to store (Johnson, 2014). Lately, a lot of attention has shifted to biomass as an alternative source for energy production (Sahu *et al.*, 2014). Biomass is considered to be a clean energy source as it is carbon neutral, as long as the trees are replanted (Gil *et al*., 2010). Plants use CO_2 during photosynthesis, and the CO_2 emitted from the combustion of these materials makes no net contribution to the accumulation of CO_2 in the atmosphere or to the greenhouse effect (Gil *et al*., 2010). Exclusive biomass combustion would require new, decentralized power plants to be constructed (Heim and Bemptgen, 1998). This would require huge capital investments as well as large storage capacity due to seasonal fuel availability and will also be time-consuming to build the plants (Heim and Bemptgen, 1998).

With large coal reserves still available, the South African government is reluctant to abandon coal as a major energy source (Energy Advocacy, 2015). However, it is determined to find cleaner technologies that will reduce the adverse environmental impact associated with greenhouse gas emissions from coal combustion (Energy Advocacy, 2015). Co-combustion of coal with biomass is one of the promising clean coal technologies (Gil *et al*., 2010). Environmental benefits of co-combustion include reduction of CO_2 emissions by saving on fossil fuel, lower NO_x and SO_x emissions as biomass contains less nitrogen fuel and sulfur (VGB PowerTech, 2008). The main benefit of co-firing is that the traditional or existing coal boilers can be adapted and used for the combustion of the new fuel (biomass-coal blend). This means that power plants that are failing to comply with the emission regulations can lower their emission to an acceptable standard by combusting a blend of biomass with coal (VGB PowerTech, 2008). With the utilization of this new fuel (biomass-coal blend), the lifespan of traditional coal power stations can be increased through co-firing (Bada *et al.*, 2015). Varol *et al.* (2010), performed an investigation on the co-combustion characteristics of low-quality lignite coals with biomass using thermogravimetric analysis. The authors reported that the combustion characteristics of the low-quality lignite coal utilized were improved by the addition of biomass while CO_2 emissions were reduced.

South Africa is one of the global leading gold producers, while the Witwatersrand basin contains the richest gold deposits and low-grade uranium (Kumar, 1995; Weiersbye *et al*., 2006b). Acid mine drainage (AMD) is a global and national problem that has been ongoing for decades. It is one of the most severe mine pollutions, which occur in abandoned mine waste rock or tailings containing sulphide minerals such as pyrite (Akcil *et al.*, 2006). According to Brodie *et al*. (1992), mine rehabilitation objectives are to ensure physical and chemical stability of the environment and to promote land use for the economy and social upliftment of the community. A mine rehabilitation method is chosen based on the above-mentioned objectives. For the rehabilitation of a gold mine in the Witwatersrand basin of South Africa, two indigenous tree species "*Tamarix usneoides* and *Searsia lancea*", among other trees, were planted to control and treat the AMD water from the mine (Weiersbye *et al*., 2006). The process utilized is known as phytoremediation, which involves using plants and soil microflora as well as non-living biomass to improve the quality of a substrate (Weiersbye, 2008). The investigation conducted by Dye and Weiersbye (2010) had shown that both the *Searsia lancea* and *Tamarix usneoides* trees used as co-fired fuels in this study have the

capability to absorb toxic minerals and trace elements from the contaminated water in their deep roots and leave the land in a better condition.

A lot of tree species including *Searsia lancea* and *Tamarix usneoides* were planted for phytoremediation, and between 2003 and 2008 an estimated 320 hectares of trees were planted (Dye and Weiersbye, 2010). According to Mosito, (2016), some of these trees are being used as firewood by the community, but combusting solely or co-firing of these trees with coal or other fossil fuels might be of a greater economic value. Apparently, co-combustion of biomass with coal may extend the lifetime span of an existing power plant and also wipe out the need for retrofitting a power plant with a flue gas desulfurizer (FGD). Therefore, the potential and suitability of these trees, i.e. the wood, roots, twigs, leaves, and their blends were investigated for combustion and co-combustion with coal in this research. In addition, the extent to which both tree species can reduce emissions was also investigated.

1.2 Problem Statement

The problems expected in this research are as follows:

- Many coal-fired power stations emit CO_2, NO_x and SO_x that are above the regulated emission standards (Vhathvarothai *et al.*, 2013). As a result, the lifespan of many coal-fired power stations is threatened as the need to produce clean energy is rising. Co-combustion of coal with biomass is one of the recent technologies that can be used to increase the lifespan of coal-fired power stations without infringing on environmental policies (Gil *et al*., 2010).

- The combustion of biomass alone in coal boilers may cause slagging and fouling (Bada *et al.*, 2014). “The high inorganic content of the biomass such as the alkalis, sodium and potassium, sulphates, chlorides and carbonates in the ash is believed to be the cause for slagging and fouling” (Li *et al.*, 2012; Febrero *et al*., 2015). The blending of coal with the biomass might reduce the slagging propensity of the fuel and lower the concentration of the gases emitted (Li *et al*., 2012; Bada *et al*., 2015).

- The utilization of *Searsia lancea* and *Tamarix usneoides* for combustion and co-combustion might have a negative impact for energy production due to the heavy metals reported in their ash. This needs to be tested.

- The alkali and chloride contents in biomass have been recognized as being the sources of corrosion in boilers. The co-firing of these raw biomass forms with different proportions of coal might reduce the alkali content of the biomass and thereby reduce corrosion and improve on burning compatibility with coal. NB: Both tree species are noted to hyperaccumulate salts in their leaves, but not in their wood. The leaves contain salts at levels ranging from 2 to 10%. The plants excrete these salts via salt glands, primarily in the form of $CaSO_4$ and NaCl, with lesser amounts of other metal sulphates and chlorides depending upon the severity of the AMD water. The blending of these leaves with the roots, twigs and wood could have a negative impact on the combustion of the biomass. This needs to be investigated.

- The presence of NaCl in the leaves might cause emission problems. A study carried out by Lin and Hsieh (1985) during the combustion of oil, showed that NaCl presence in the air enhances the formation of excess O_2, CO and SO_2. In contrast, the authors noted that the emission of CO_2 was reduced. This study will also investigate if the combustion of the leaves with high NaCl, solely or with coal will reduce the CO_2 emission and enhance the formation of CO and SO_2 as stated in the study by Lin and Hsieh (1985) on oil combustion.

1.3 Aim and objectives

The aim of this research is to evaluate the suitability of *Searsia lancea* and *Tamarix usneoides* used for AMD control as a fuel for combustion and co-combustion.

The objectives are to:

- Determine the physico-chemical properties of the roots, branches, leaves and wood of the two tree species and their blends.

- Determine the combustion and co-combustion reaction kinetics when combusting the two tree species with and without coal in various proportions.
- Evaluate trace elements in the feed materials and ash of the combusted trees and their parts.
- Investigate CO_2, SO_x and NO_x emissions when increasing biomass proportions during co-combustion with coal.

1.4 Research questions

- Can *Searsia lancea* and *Tamarix usneoides* planted for AMD control be used as a fuel for combustion and co-combustion?
- Which tree parts are most suitable for combustion and co-combustion?
- How do combustion properties of *Searsia lancea* and *Tamarix usneoides* differ across different AMD affected sites?
- How do the chemical and thermal properties of *Tamarix usneoides* and *Searsia lancea* compare with those of run of mine and discard coals?
- Can discard coal lower the slagging and fouling potential of *Searsia lancea* and *Tamarix usneoides*?
- Will increasing biomass proportion during co-combustion lower the CO_2 and SOx emissions?

1.5 Hypothesis

Searsia lancea and *Tamarix usneoides* planted to control AMD will improve combustion characteristics of coal when co-fired and lower the emissions of GHG from coal combustion.

1.6 Dissertation Outline

This dissertation has 5 chapters which cover various aspects of the research. The background and motivation for this study, along with the aim and objectives together with the hypothesis are presented in Chapter 1. The focus of Chapter 2 was on the literature review, the knowledge and background on coal, biomass, combustion technologies and co-combustion fundamentals. Furthermore, some of the research done in co-combustion are reviewed. Chapter 3 provides the materials and experimental techniques used in this research. Chapter 4 outlined the discussion of results obtained from this research. Lastly, the conclusions drawn from the results in Chapter 4 are presented in Chapter 5. Additionally, Chapter 5 also offer recommendations for future studies.

CHAPTER 2: LITERATURE REVIEW

2.1 Introduction

This section provides an outline of different investigations previously carried out in the field of combustion and co-combustion. A brief background on coal, biomass, the tree species used in this research and co-combustion is provided. The results from published articles that are in line with the co-combustion of biomass are reviewed in detail. The main experimental technique, i.e. thermogravimetric analysis (TGA) used in determining the coal/biomass combustion reactivity, along with the theory behind combustion reaction kinetics were presented in this chapter.

2.2 Coal

2.2.1 Coal type, rank and grade

Coal is a chemically and physically heterogenous sedimentary rock that consists of both organic and inorganic materials (Miller, 2011). The major organic components of coal are carbon, hydrogen and oxygen. Sulfur and nitrogen make up for the remainder of the organic coal components. Apart from the organic compounds, coal also contains inorganic ash-forming minerals. Radenovic (2006) stated that more than one hundred different minerals and almost every element in the periodic table has been found in coal. Figure 2.1 below shows the make-up of coal's inorganic compounds.

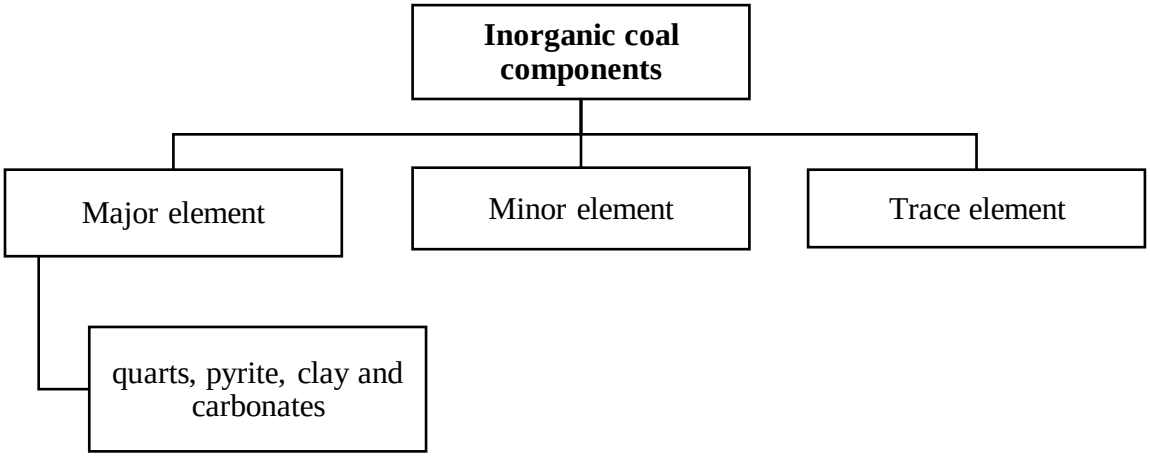

Figure 2. 1: Coal's inorganic compounds (Radenovic, 2006)

Coal is formed from plant remains or materials buried in swamps, which are exposed to the effects of time, temperature and pressure. The geological process that transforms plant remains into coal is called coalification (Miller, 2011). The northern hemisphere (Europe and North America) coal were formed in equatorial conditions during carboniferous times 300 to 350 million years ago (Falcon, 2013). Contrastingly, coal in the southern hemisphere was formed in cold to cool temperature conditions during Persian times, 280 to 300 million years ago. The following factors as outlined below, are responsible for the difference in the quality of Southern African coals from most other coals (Falcon, 2013);

- Between coal basins (age, sedimentary environment, vegetation)
- Between coal fields (rank, type and grade)
- Between seams (climate, vegetation, sedimentary environment)
- Laterally and vertically within one seam.

The main technique for studying the organic and inorganic components of coal is known as petrographic analysis. This technique identifies the reactive capabilities of each material within the coal matrix, and their related industrial applications (Falcon, 1977b). Falcon and Ham (1988) stated that due to differences in the coal organic constituents, coals of similar chemical nature can be found to have significantly different performances under similar operating conditions. These different organic components are referred to as, macerals. Three groups of macerals exist, viz, liptinite, vitrinite, and inertinite. Falcon (1992) and Falcon (1977b) studied the properties of these macerals in different Southern African coals, and the author's findings are summarized below;

- Liptinite

  This maceral has a low reflectance (dark in reflected light), it contains high percentage of aliphatic substances, volatile matter, and hydrogen contents. Liptinite produces heavy tars, bitumens and other hydrocarbon products.

- Vitrinite

  This type of maceral contains moderate volatile matter and moderate to high hydrogen content compared to the inertinite group. On heating, it devolatilizes quickly, becomes

plastic and swells. This maceral group (vitrinite), which is determined by the proportion of light reflecting off the surface of the coal, is used in ranking coal. The rank of coal and its reflectivity denote coal maturity. The reflectivity and coal carbon content increase with coalification whereas volatile matter decreases.

- Inertinite

  This is a maceral with the lowest volatile matter and hydrogen contents relative to the other two maceral groups. However, it has a higher oxygen content. This carbon rich, relatively dense component burns with an intense heat and for longer periods of time than its more porous vitrinite counterpart.

The rank of a coal is a measure of its degree of metamorphism (Shrilekha and Soni, 2015). Coal is classified into three major ranks, namely anthracite, bituminous, and lignite. However, the distinction between the three groups is not clear and coal is also further classified as semi-anthracite, semi-bituminous, and sub-bituminous. Anthracite is the oldest coal from a geological perspective (Shrilekha and Soni, 2015). It is a hard coal composed mainly of carbon with little volatile matter content and virtually no moisture. Contrastingly, lignite is the youngest coal from a geological view. It is a soft coal composed largely of volatile matter and moisture content, but with a low fixed carbon content (Falcon, 1977a). Figure 2.2 below shows how the rank of coal varies. From left to right, the variation is with increasing age.

Figure 2. 2: Variation in coal rank (Falcon, 2013)

The following remarks are made by Falcon, (1977b) on the rank of coal;

- High volatile bituminous coals are ranked according to their moisture content and calorific value (>30% volatile matter on European standards).

- Medium to low volatile bituminous coals are best measured by volatile matter and reflectance of vitrinite (<30% volatile matter on European standards).
- Anthracite are ranked according to the hydrogen content of the coal (8% volatile matter on European standards).
- Rank is important in determining the properties and potential behavior of coal.
- Low rank coals with high volatile matter, oxygen and hydrogen contents, and low carbon content are used for hydrogenation purposes. While coal of different ranks down to medium-bituminous coals can be used for liquefaction. For gasification purposes, coals of different ranks can be utilized depending on the gasification route or process technology.

The grade of coal is a measure of impurities in the coal (Falcon, 2013). In defining "low quality" coal, rank is of little importance (Dong, 2011). There is no single universally accepted definition of low rank or low-grade coal (Mills, 2016). However, a coal can be classified as a low rank or low-grade coal if it possesses high mineral matters, which might limit its application (Mills, 2016). Low rank coals such as sub-bituminous and lignite coals are generally considered to be low grade as they possess high moisture content and low heating value (Mills, 2011). Anthracites and semi-anthracites are sometimes thought to be a low-grade coal due to their delay in ignition and long residence burnout time during combustion. It is difficult to classify bituminous coals as high grade or low-grade coal, but with the characteristics stated below, bituminous coal can be classified as a low-grade coal (Mills, 2016), based on;

- Low heating value implying low efficiency;
- High moisture content, also translating to low efficiency;
- Low volatile matter related to low flame stability;
- High ash content, causing ash-related problems and reducing efficiency;
- High sulfur content, implying high SO_2 emissions and high abatement cost;
- Low ash fusibility, having potential for slagging;
- High alkaline content, having potential for slagging, fouling or corrosion;
- Low Hardgrove Grindability Index, implying high milling power consumption.

Generally, coal is classified as “low grade” or “low quality” if it has properties that are undesirable for its intended end application, especially for power generation (Mills, 2011). A large proportion of low-grade coals are used in power plants that are designed specifically for these kinds of coals, and this is more applicable to the South African coal power plants (Mills, 2016).

2.2.2 Coal utilization

The use of coal dates back to ancient times, although it was only during the industrial revolution that it rose to prominence as a major resource (Miller, 2011). Coal is arguably the most important energy source to drive the first industrial revolution. The use of coal in England grew between 1750 and 1850 due to transport revolution, the iron-industrial revolution and the forest decline (FERC, 2010). Coal is mainly utilized for electricity generation and in the iron and steel production industries (Miller, 2010). Secondary coal use includes locomotives for transport, household heat, and chemicals such as dyes, ammonia and explosives. The four major coal utilization processes are combustion, carbonization, gasification and liquefaction (Miller, 2011). Since this study was based on the combustion of coal and biomass, a thorough literature review was provided on combustion in the next sub-section, while the other three processes are discussed below.

The carbonization of coal, biomass or any organic matter is a process by which these materials are heated up, under a specific condition, and volatile products are driven off both in gaseous and liquid forms, leaving a solid porous residue called char or coke (Miller, 2011). Carbonization can be classified either as a low or high temperature carbonization. Carbonization processes that take place at a temperature greater than 900°C are classified as high temperature carbonization while those occurring below 730°C are known as low temperature carbonization (Satyendra, 2014). High temperature carbonization is mainly applied in the production of metallurgical coke for use in blast furnaces and foundries (Hazra, 2002). Additionally, coke is also used for the manufacture of calcium carbide and electrode carbons, as reductant in ferrous and non-ferrous open-hearth operations, and in foundries to produce cast iron (Miller, 2011). Low temperature carbonization on the other hand is used to provide town gas for residential and street lighting, tars for use in chemical production, and smokeless fuels for domestic and industrial heating (Miller, 2011). The ability of coal to melt upon heating and to form a coherent residue on heating is called caking. This

is a prerequisite for all coking coals. Low rank coals such as lignites and high rank coals such as anthracites do not cake (Tanggara *et al*., 2018). Therefore, these coals are not capable of producing coke.

Gasification is another process used in the upgrading of coal and other carbon solid feedstocks which are difficult to handle by removing unwanted impurities and converting them into gases that can be purified and used directly as a fuel or further processed into other gaseous or liquid products (Miller, 2011). The interest in gasification stems from its attractiveness. Firstly, liquids and gases are easier to handle and use than coal, whether for heating, cooking, or for power generation (Miller, 2017; Luo, 2017). Secondly, impurities in coal can be removed easily through gasification, and with a high carbon conversion ratio rather than through direct combustion (Luo, 2017). Lastly, it is important to note that, synthetic fuels burn more cleanly than coal, releasing less emissions of NO_x and SO_x (Miller, 2011). Carbon dioxide can also be removed readily from the gas stream before gasification products are used or fed into the gas turbine. Gasification is very attractive to countries like South Africa that have coal reserves but lack oil and gas reserves (Zheng *et al.*, 2019). The use of this technology is currently limited (Rycroft, 2019). However, it is expected to rise and be used for future production of electricity, steam, chemicals, and fuels such as hydrogen (MRFR, 2019).

With liquefaction, coal and other feedstocks are converted into liquid products through this approach (Speight, 2017). There are three processes that are used in extracting liquids from coal, these processes are pyrolysis, indirect liquefaction and direct liquefaction. Pyrolysis is not classified under liquefaction although it produces liquid products (Miller, 2011). This is because the liquids in pyrolysis are by-products during coke production and biomass carbonization. By definition, liquefaction is referred to as a process for the conversion of organic solids such as coal, where the primary product is a liquid. In indirect liquefaction, the coal is gasified into a mixture of carbon monoxide and hydrogen (together known as syngas) (de Klerk, 2014; Luque and Speight, 2015). Subsequently, syngas is processed into liquid products using Fischer-Tropsch synthesis. In direct liquefaction, also known as coal hydrogenation, coal is combined with a hydrogen donor solvent and reacted with hydrogen or syngas under elevated pressures and

temperatures to produce a liquid fuel (NETL, 2019). The Fischer-Tropsch process is extensively used in South Africa by Sasol (Speight, 2016; Sasol, 2019).

2.2.3 Influence of coal quality on combustion

Coal quality plays a significant role in the operation and effectiveness of coal-fired power plants (Nalbandian, 2011). In power generation, coal quality affects many operational aspects. The choice of coal plays a major role in the success and economic-viability of a power plant (Mills, 2016). Tables 2.1, 2.2 and 2.3 below show how coal quality affects several aspects of operational and plant design for both new and existing power plants alike.

Table 2. 1: Impact of fuel constituents on combustion (Saxena, 2013; Sharma, 2015)

Fuel constituent	**Impact**
C, H, S and N content	• Change in fuel composition can affect combustion process as boilers are designed for specific fuel compositions. • High C, N or S increase CO_2, NO_x and SO_2 emissions.
Cl content	A high Cl content increases corrosion risk.

Table 2. 2: Impact on emission control systems (Saxena, 2013; Sharma, 2015)

Component	**Impact**
Particulate	• Selection of control equipment is affected by fuel characteristics, boiler type, ash properties, plus particle loading and size. • High ash level can impair effective Electroscopic Precipitation (ESP) operation.
NO_x	• Thermal NO_x might be controlled by reducing combustion zone temperature. • Fuel containing less nitrogen will generate less overall NOx.
SO_2	• SO_2 can be controlled by switching to low sulfur coal or deploying post-combustion systems such as FGD.

Table 2. 3: Influence of coal quality on variation of power plants (Saxena, 2013; Sharma, 2015)

Property	**New plant**	**Existing plant**
High moisture content	• Bigger boiler and pulveriser needed. • Lower boiler efficiency and higher fuel requirement per Megawatt (MW) of output.	• Difficulty in maintaining steam and reheat temperatures. • Reduced boiler efficiency. • Reduced pulveriser capacity. • Reduced outlet temperature.
High ash content	• Increased boiler and pulveriser size. • Higher power requirement. • May require more support oil. • Higher fuel requirement per MW of output. • Large amount of ash for disposal.	• Increased erosion, slagging and fouling of pressure parts and draught fans. • May require more support oil. • Reduced ESP performance. • Overloading of draught fans. • Large amount of ash for disposal.
Volatile Matter (VM) content	• Low volatile matter content may require special boiler design (down-shot). • Impact on boiler turndown ratio and fuel residence time in boiler.	• A sudden decrease in volatile matter can affect flame stability, requiring secondary fuel oil support to manage part-load operations.
Calorific value (CV)	• Low calorific value can impact on size and design of boiler, mills, ESP, draught fans, air and flue gas ducts, fuel handling system, and auxiliary power consumption.	• Lower calorific value means that a greater volume of coal will be needed, as will higher heat transfer into convective surfaces. • Increased de-superheating spray will be required to maintain main steam temperature. • Lower efficiency of boiler, mills, and ESP.
Hardgrove Grindability Index (HGI)	• Mills must be designed to accommodate extreme values, resulting in high equipment costs.	• Coal fineness is affected if HGI value is less than design value. • Increased mill maintenance and downtime. • Reduced boiler efficiency and performance.

2.2.4 Status quo of coal in South Africa

Internationally, coal is currently the most widely used primary fuel, accounting for approximately 27% of global primary energy and 38% of the world's electricity production (IEA, 2018). In South Africa, coal has been a major energy supplier, dating back to the 19th century, when coal from the

Vereeniging area was supplied to the Kimberly diamond fields (Eskom, 2019). Currently, coal accounts for an estimated 77% of South Africa's primary energy needs (Chamber of mines, 2018). This figure is not expected to change significantly in the next decade, as there are no suitable alternative energy sources to coal (Eskom, 2019). Coal's dominance in South Africa's electricity production is highlighted in Figure 2.3 below.

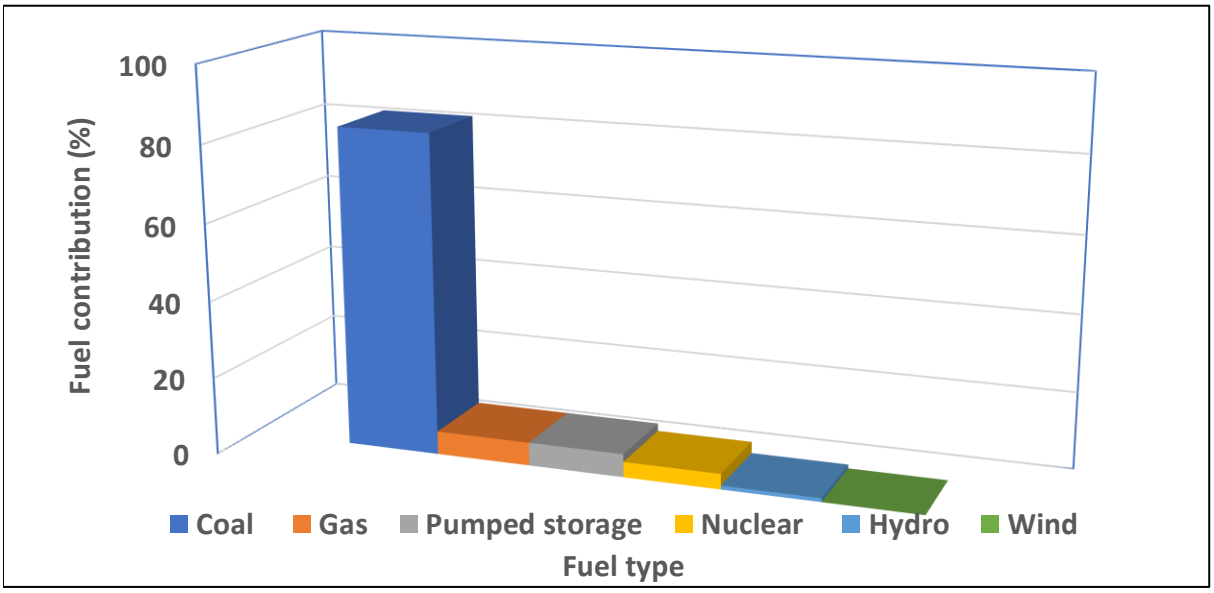

Figure 2. 3: South Africa's fuel contribution to electricity generation in 2017 (Eskom, 2017).

South Africa produces an average of 224 million tonnes of marketable coal annually, making it the 7th largest coal producing country in the world (Coyne, 2018; Eskom, 2019). In 2017 alone, the country produced 252 million metric tonnes of coal, directly contributing 3.3% to the global coal production (Coyne, 2018). South Africa is the 6th largest global coal exporter, with an approximately 5.9% of the total global coal export dollar value in 2018 (Workman, 2019). The remainder of South Africa's coal production feeds the various local industries, with 53% used for electricity generation (Eskom, 2019). The key role played by the country's coal reserves in the economy is illustrated by the fact that Eskom is the 7th largest electricity generator in the world, while Sasol is the biggest coal-to-chemicals producer globally (Eskom, 2019). Figure 2.4 below

shows how coal utilization is distributed in South Africa while the summary of South Africa's contribution to the global coal production is presented in Table 2.4:

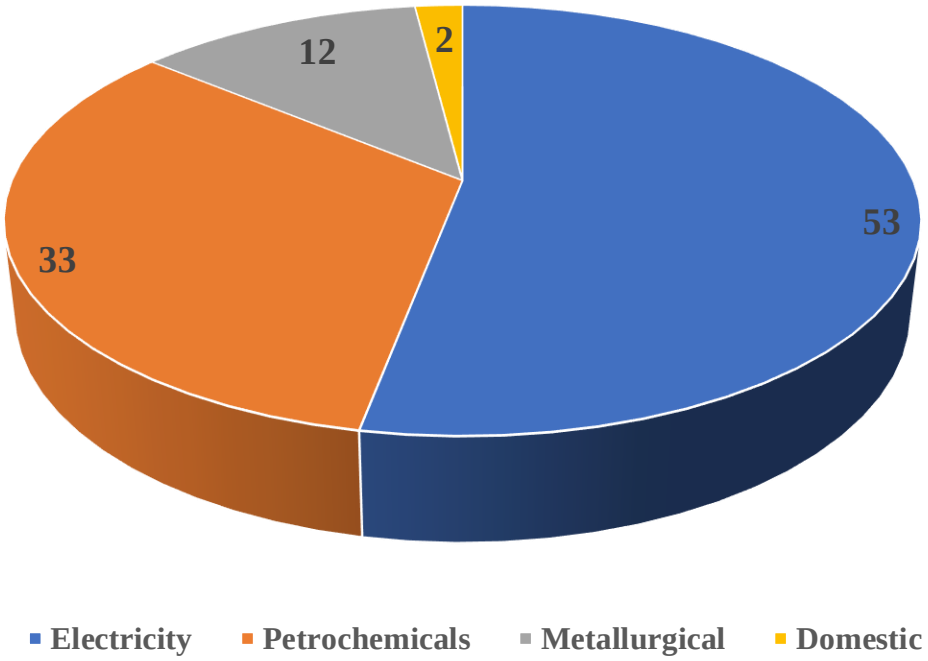

Figure 2.4: Coal utilization in South Africa (Eskom, 2019)

Table 2.4: Summary of coal productions and utilization in South Africa in numbers

Category	Global rank
Production	7
Export	6
Electricity generator (Eskom)	7

There are contrasting reports on the coal reserves in South Africa. Eskom reported an estimated 53 billion tonnes of coal reserves as of July 2019 and further stated that this reserve can supply electricity for the next 200 years at the current production rate of 90 million tonnes per year (Eskom, 2019). The Chamber of Mines on the other hand, reported in their 2018 National Coal Strategy for South Africa that the country is blessed with 30 billion tonnes of coal, accounting for 3.5% of global coal reserves. With the contradiction in the actual reserve number, there is a need for a new study to be conducted in determining the present South Africa's coal reserve and its

quality. Most of the coal mined in the country for domestic and export market has traditionally been from the Witbank and Highveld coalfields (DMR, 2009). The depletion in the coal reserve and quality in this region, and non-ideal mining conditions in the Free State and Springbok Flats has led to exploration and shift by the mining houses to Waterberg coalfield (Jeffrey, 2005; DMR, 2009). The Waterberg coalfield has one of the largest open-cast coal mining fields in the world (Hancox and Gotz, 2014). Grootegeluk mine, situated in the region is one of the most efficient mining operations globally and runs the world's largest coal beneficiation complex (Exxaro, 2018). It is also the only coal producing mine in the coal-rich Waterberg, adjacent to Eskom's existing Matimba and new Medupi power stations (Exxaro, 2018). In 2018, Exxaro produced 47.8 mega tonnes (Mt) of coal, a large portion coming from Grootegeluk mine (Exxaro, 2018).

The average sulfur content in South African coal is approximately 0.9% (Pretorius *et al*., 2015). Coal is known to contain a significant amount of sulfur leading to SO_x emissions (Makgato and Chirwa, 2017), and the SO_2 produced during combustion is one of the most notorious environmental pollutants (Cheng, 2003). Most of the existing power plants in Eskom fleet are not designed to meet the present SO_2 emission standards, as SO_2 emissions were not regulated in the past (Makgato and Chirwa, 2017). Hendrina power station in Mpumalanga, shown in Figure 2.5 below, is one of the Eskom power plants commissioned when SO_2 emission standard was yet to be regulated.

The designing of a new power plant with a desulfurization technology (FGD) and retro-fitting existing power stations to accommodate the technology is one of the options available in reducing the emission of SO_2 into the atmosphere. Studies have shown that the FGD scrubber has the potential to reduce SO_2 emitted from the power plant by 99%, along with the associated gaseous chloride and fluoride present in the flue gases (Srivastava and Jozewicz, 2011; Chandrasekaran, 2017; Lisnic and Jinga, 2018). According to Section 21 of the National Environment Management: Air Quality Act (Act No 39 of 2004), existing South African coal-fired power stations should not exceed 9460 ppm in SO_2 emissions while new power stations' emissions are limited to 1350 ppm (NEMA, 2010). However, there are two major problems with FGDs. One downfall of the technology is that it produces a high concentration of chlorides, magnesium, calcium, and heavy

metals in the effluent which prevents re-use of the effluent (Makgato and Chirwa, 2017). Secondly, the technology is very expensive (RMR, 2019).

The majority of the coal mined at present in South Africa are of very high ash content (Mills, 2016). A recent investigation by Makgato and Chirwa (2017), on the characteristics of the Waterberg coal, shows some coal with an ash content ranging from 29 to 34%. The utilization of these coals for different applications will require it to be beneficiated, in order to improve its quality for domestic application and as an export market product. With beneficiation these coals, different grades of clean coal products are produced, along with coal middlings and discard, which are of poor quality (high ash and sulfur contents). Thus, these middlings and discards, are being utilized by Eskom for electricity generation (Eberhard, 2011).

Figure 2.5: Hendrina Power Station in Mpumalanga, South Africa (Eskom)

According to Mills (2011), bituminous coal is the most abundant energy resource in South Africa. Coal production in South Africa is dominated by five major companies which share more than 80% of the country's annual saleable coal production (DMR, 2014). The companies are: Anglo American Thermal Coal, Exxaro Resources, Sasol Mining, BHP Billiton Energy Coal South Africa

and Xstrata (DMR, 2014). Compared to coals from other regions (international), many South African coals are shallow with thick seams making them easier and cheaper to mine (Mills, 2016). Coals used for electricity generation are amongst the cheapest in the world. These are usually high ash coals with lower calorific value in the case of South Africa than export grades (Mills, 2016). An example of this is the Majuba power station which uses a combination of colliery discards and run of mine coals from several opencast and deep mined sites. The coal as delivered has a nominal calorific value of 21.5 MJ/kg and the properties shown in Table 2.5 below are the average properties of coal used at the Majuba power plant. Some of the coals used in the South African coal power plants and Sasol's coal to liquids operations are from the middlings fraction of the washed export coal (Mills, 2016). This is as a result of the decline in the quality of the South African premium coal, as the high-quality coals have been mined out.

Table 2.5: Average properties of coal used in Majuba power station (Mills, 2016).

Parameters	Average (%)	Range (%)
Ash	35	19-40
Moisture	3.1	1.7-4.4
Sulfur	0.8	0.7-7

2.3 Combustion

2.3.1 Conventional combustion technologies

Almost all the coal mined in the world is used for combustion purposes, for heat and electricity generation (Miller, 2011). The combustion of coal for electricity requires the use of boilers. Harnessing steam for power generation is arguably the most significant technology in the advancement of industrial nations (EIA, 2009). Coal can be burnt in the following three ways (USEA, 2002);

- As large pieces in a fixed bed (stoker)
- As crushed pieces in fluidized bed
- As fine particles in suspension (pulverized coal combustion)

The combustion of coal occurs in multiple steps or stages. Firstly, moisture is driven off as the coal particles are heated up. Subsequently, volatile matter components are driven off in a process called devolatilization, with the combustion of volatile matters occurring in the gas phase. This homogeneous process takes place before or simultaneously with the char combustion (heterogenous reaction), the last step in the process. For most part, these reactions are sequential with the slowest one being the rate-determining reaction (Miller, 2011). The designing of a boiler and furnaces is largely influenced by the volatile matter released by the coal as it is heated (DOE, 2001), while its rate of devolatilization is influenced by temperature and particle size. The final temperature at which the devolatilization is completed is associated with the coal particle size and highest volatile yield. Volatiles yield can also vary with coal rank (Miller, 2011). The devolatilization process is a very fast process measured in milliseconds (Miller, 2011). In contrast, char combustion is much slower, hence it determines the time for complete combustion or burnout (Mills, 2008).

The combustion of coal and the design of boilers or reactors in which it is burnt are determined by the coal type, quality and capacity (Miller, 2011). Fixed-bed combustion includes domestic space heaters, grate furnaces and industrial stokers. Of all the applications of fixed-bed combustion, stokers are of the most interest (Miller, 2011). Generally, stokers are classified into three groups, depending on how the fuel enters the grate of the stoker for burning. The three groups are: underfeed, overfeed and spreader design. In the underfeed stokers, coal is introduced beneath the active fuel bed and is moved from the storage hopper by means of screw or ram into a retort. The underfeed stokers are mainly used for coal in small boilers and are suitable for bituminous and anthracite coals (Eastman, 2003). While the overfeed stokers, also known as mass-burning stokers convey coal from the fuel hopper located at the front of the stoker. These are suitable for burning all ranks of coal. Similarly, spreader stokers can also burn all coal ranks as well as many waste fuels (Prairie State Energy Campus, 2010). It takes fuel from feeders located across the front of the furnace and distribute it uniformly over the grate surface (Eastman, 2003). It can be designed in a wide range of "boiler" sizes and is the most popular of the three stoker types (Miller, 2011).

The most popular combustion system for the past century for large industrial boilers and coal-fired electric generators has largely been pulverized coal combustion (PCC) (Barnes, 2012; Tillman *et*

al., 2012; Zhang *et al*., 2013; Hurskainen and Vainikka, 2016). This is partly because pulverized coal combustors can be constructed to massive sizes (Sarkar, 2015). Pulverized coal combustors have the capacity to produce outputs of between 50 and 1300 MW at efficiencies of 30-36% (IEA, 2018). Furthermore, unlike stoker units which have coal restrictions, pulverized coal combustors can accommodate a wide range of coal quality provided it is designed for such coal specifications (Miller, 2017). However, this technology is not always appropriate for high ash coal (IEA, 2018), but Eskom do utilize this technology in combusting coal of 30 to 35% ash. In pulverized coal combustion, coal is ground to fine powder such that less than 2% is bigger than 300μm and 70-75% is below 75μm for bituminous coal (IEA, 2018). Two types of pulverized coal-fired units exist, based on the furnace design for ash removal: dry-bottom and wet-bottom firing (USEA, 2002). In dry-bottom furnaces, ash is removed from the system in the dry form while in wet-bottom units, ash is removed in a molten form. Dry-bottom furnaces are the most popular of the two types (Miller, 2017). Dry-bottom furnaces are preferred because they are simpler to operate, can accommodate a wider range of fuel properties, and are more reliable than the wet-bottom furnaces (USEA, 2002).

The fluidized bed combustion (FBC) is one of the emerging technologies and also a clean coal technology process for combustion of fossil fuels and other fuels (Sarkar, 2015). This technology is attractive as it holds advantages such as fuel flexibility, low NO_x emissions, co-firing potential, particle size within 1-5 cm and in-situ control of SO_x emissions over conventional pulverized coal combustion (Sarkar, 2015; Miller, 2017). In a fluidized bed combustor, solid, liquid or gaseous fuel, and an inert material such as sand or ash, and limestone are kept suspended through the action of air distributed below the combustor flow (Kaplan, 2010). This action lead to the combustion of the coal or other materials fed into the boiler and the separation of the unburnt carbon from the sand. Fluidized bed combustors can be divided into bubbling fluidized bed combustors (BFB) and circulating fluidized bed combustors (CFB) (Sarkar, 2015). BFB have lower fluidization velocity, which prevent solids elutriating from the bed into convective passes while CFB apply higher velocities to promote solids elutriation (Eastman, 2003). Recently, a lot of interest has shifted to CFBs as this technology is considered the future of coal and biomass combustion (Nuortimo, 2015). The technology is now available in large scale sizes of up to 800 MW (Nuortimo, 2015). With the advancement in CFB technologies, such as the Samcheok Green Power Plant project, the

largest CFB technology-based power plant in the world (4×550 MW), CFB will match pulverized coal combustors in terms of capacity in the near future (Nuortimo, 2015). CFBs can accommodate a wide range of fuels including but not limited to bituminous coal, anthracite, lignite, peat, and biomass (Cai *et al*., 2017). Advantages of this technology over the BFB includes; low bed density, Sub-to Super-critical steam conditions, higher commercial operating scale and extended fuel recirculation (Lyu *et al*., 2017; Eriksson *et al*., 2018). Based on the attributes of the CFB technology, the users can choose the most effective fuel at any given point in time (Nuortimo, 2015). Table 2.6 below shows some of the global projects employing CFB technology.

Table 2.6: Global CFB projects (Nuortimo, 2015; Sumitomo; 2017)

Project	Capacity (MWe)	Facts
GDF Suez Energia Polska, Poland	205	• The world's largest CFB firing 100% biomass.
MGT Teesside Ltd, UK	299	• It will be the world's largest and most efficient biomass (wood chips & pellets) CFB plant. • Operation planned for 2020.
Dainjing, South Korea	105	• Fires coal, palm kernel shell and wood pellets. • Has been in commercial operation since August 2015.
Lahti Energia, Finland	70	• Commercial operation expected in 2020.
Igelsta, Sweden	85	• Started commercial operation in January 2009.
WTE CFB, Sweden	30	• Has been operational since 2011. • Fires refuse derived fuel.
Lagisza, Poland	460	• Started operating in 2009. • Fires Polish bituminous coal.
Novocherkasskaya, Russia	330	• Has been operational since 2015. • Fires Russian anthracite and bituminous coal.
Samcheok, South Korea	4×550	• Started operating in 2015. • Fires Indonesian sub-bituminous coal and biomass.

MWe: Mega Watt electric

2.3.2 Clean coal technologies

There are three main approaches used to reduce emissions and improve air quality in power generation (Morrison, 2012). The first approach aims to reduce emissions of air pollutants and greenhouse gases by increasing the energy efficiency of existing thermal cycles and developing

advanced higher efficiency cycles (Obe, 2017). A higher energy efficiency means less amount of fuel is used to produce electricity, hence less emissions. A second approach involves changing to less carbon-intensive fuels such as natural gas, nuclear power and renewable resources. Under this approach, coal can also be co-fired with fuels containing less carbon and sulfur such as biomass or refuse derived fuel (Miller, 2011). The third approach is the capture, utilization and storage of carbon dioxide from fossil fuel fired power plants (Obe, 2017). There are three technological pathways for CO_2 capture, namely; post combustion capture, oxy-fuel combustion and pre-combustion capture, known as integrated gasification combined cycle (IGCC) (Miller, 2011).

HELE (High Efficiency Low Emission)

In pulverized coal combustion, an increase in the maximum temperature of the steam cycle increases electrical efficiency which lowers both coal consumption and emissions (Barnes, 2018). However, the maximum steam temperature is limited by the materials in which the superheater and heat exchanger tubes can operate on without failure (Barnes, 2018). The HELE combustion technologies are classified as sub-critical, super-critical (SC), ultra-supercritical (USC) or advanced ultra-supercritical (AUSC). These technologies are commercially available and actively deployed in countries such as China, Germany, Japan and Korea (Obe, 2017). Large unit sizes such as 800 MWe and more are the most efficient HELE plants. Efficiencies of HELE plants reach 47% while the global average combustion efficiency is at 35% (Barnes, 2018). The global USC power capacities are summarized in Table 2.7 below. The distinction between these coal combustion technologies is based on the conditions summarized in Table 2.8, and the technologies hold the following advantages over sub-critical units (Barnes, 2018);

- They produce electricity more efficiently by operating at higher temperatures and pressures;
- They provide a significant lifetime operating cost savings despite high initial capital cost as they require less coal per unit of electricity produced;
- New SC and USC units emit 13% and 19% less CO_2 than new sub-critical units, respectively and up to 40% less CO_2 than older sub-critical plants.

Table 2.7: USC coal power capacity worldwide (Barnes, 2018)

Region	In Operation (MWe)	Under construction (MWe)
Asia	201 413	94 575
Europe	24 133	6 045
Middle East	0	3 786
Eurasia	300	0
North America	665	0

Table 2.8: Steam parameters in plant steam cycles (IEA, 2012)

Type of Unit	Superheater temperature (°C)	Superheater pressure (MPa)	Materials in high temperature components	Efficiency (%)
Sub-critical	≤ 540	<22.1	Low alloy CMn and Mo ferritic steels	<35
Super-critical	540-580	22.1-25	Low alloy CrMo steels and 9-12% Cr martensitic steels	35-40
Ultra-supercritical	580-620	22-25	Improved 9-12% Cr martensitic steels and austenitic steels	40-45
Advanced ultra-supercritical	700-725	25-35	Advanced 10-12% Cr steels and nickel alloy	45-52

HELE coal power plants have ultra-modern emission control devices to remove particulates, NO_x and SO_2. Flue gas desulfurization (FGD) is one of the most common emission control technologies employed by the new coal power plants (Eskom, 2018). FGD processes are classified as wet, dry or semi-dry (KC Cottrel, 2016). Limestone is the major reagent used in FGD processes (KC Cottrel, 2016). Figure 2.6 and Figure 2.7 below show the contribution of each FGD process and reagent as applied to the power plants, respectively. Table 2.9 lists the characteristics of each FGD process.

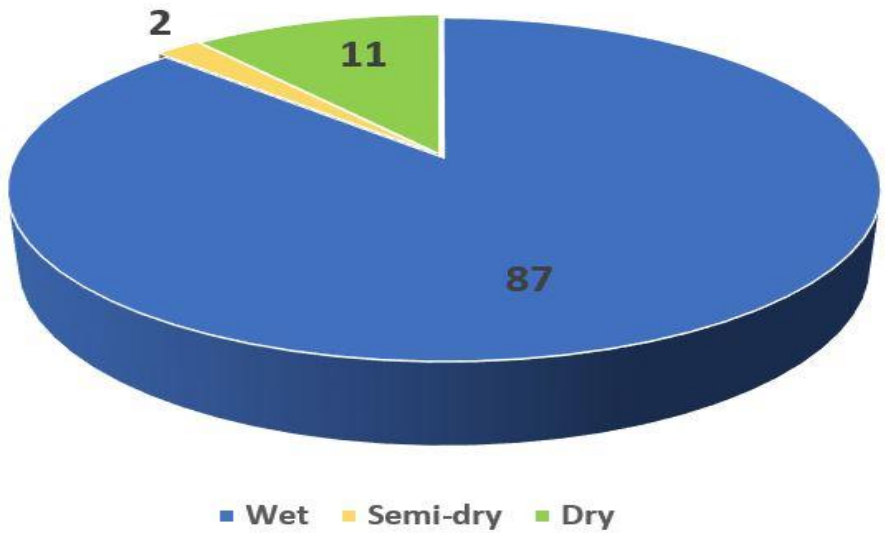

Figure 2.6: Distribution of FGD process per type (KC Cottrel, 2016)

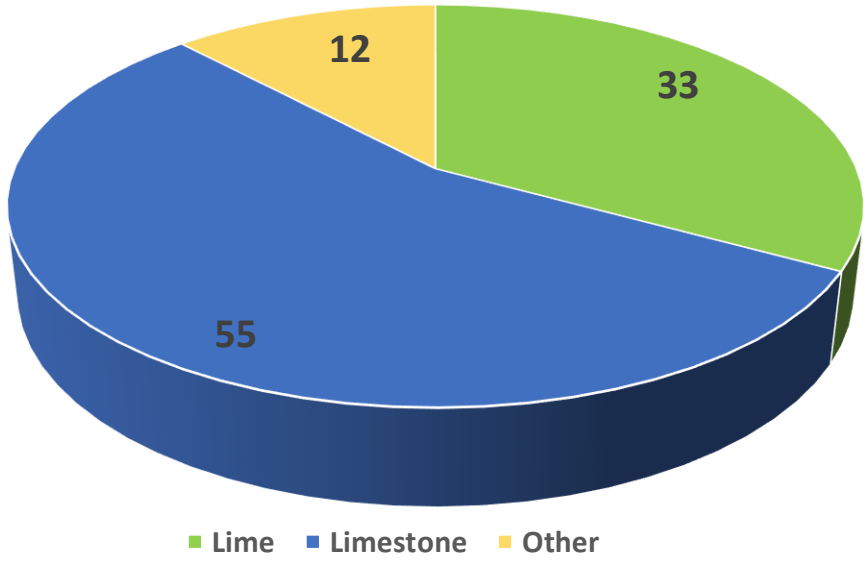

Figure 2.7: Reagent use in FGD processes (KC Cottrel, 2016)

Table 2.9: Summary of FGD processes (Lisnic and Jinga, 2018)

	Dry	**Semi-dry**	**Wet**
Characteristics	Dry powder-Reactor-Dry powder	Slurry/Solution-Reactor-Dry powder	Slurry/Solution-Reactor-Slurry/Solution
Main reactor	Dry injector	Semi-dry reactor	Wet scrubber
Application	Small or medium scale		Large scale
Agents	Magnesium, Calcium and Sodium compounds		
Coal % Sulfur preference	<3%		>3%
Removal efficiency	Up to 95%	Up to 98%	Up to 99%
Water usage	Minimum	Medium	High
Waste water treatment	Unnecessary		Necessary
By-product	Calcium sulfite and sulfate		Gypsum, Ammonium sulfate and Sodium bisulfate
Operation cost	High	Medium	Low

2.3.3 Fundamentals of co-combustion

Power generation from co-combustion of coal/biomass blends is considered a clean coal technology and has gained increasing interest and support, as biomass is considered renewable and carbon neutral (Sahu *et al.*, 2014). Biomass co-firing consists of burning biomass along with coal in coal fired power plants (IEA-ETSAP, 2013). Co-firing technologies include: (i) Direct co-firing, using a single boiler with either common or separate burners, (ii) Indirect co-firing, where a gasifier is used in converting solid biomass into a gaseous fuel, and (iii) Parallel co-firing, where a separate boiler is used for combusting the biomass, and the steam generated is then mixed with the steam from the conventional coal boilers (IEA-ETSAP, 2013). Based on the growing need to utilize biomass for co-firing, it is imperative to evaluate the compatibility of a biomass/coal blend, and the possibility of using such blend in an existing boiler. The co-firing of biomass with coal has proven to reduce the pollutant emissions (Bhuiyan *et al.*, 2016), and Table 2.10 below shows some of the existing combustion technologies available for biomass co-firing.

Table 2.10: Common coal combustion technologies available in biomass co-firing systems (Tillman *et al*., 2012; Sayigh, 2013)

Co-combustion system	Operation requirements	Co-firing percentage (% heat)	Technical features
Pulverized combustion	**Fuel type**: Coal, sawdust and fine shavings. **Particle type**: < 10-20 mm **Moisture content**: < 2%	1-40%	• It can decrease NO_x significantly. • Limited by biomass particle size and moisture content.
Fluidized bed combustion	**Fuel type**: Better suited for woody than herbaceous fuel. **Particle type**: < 80 mm (BFB) < 40 mm (CFB) **Temperature**: < 900°C	CFB: 60-93.5% BFB: 80%	• Most suitable boiler for biomass co-firing. • The soot formation is problematic, especially in CFB.
Packed bed combustion	**Fuel type**: wide range of fuels including coal, peat, straw and woody residue. **Particle type**: Fairly large pieces < 30 mm	3-70%	• Not suitable for direct co-firing, although can be used for parallel or in-direct co-firing.
Cyclone combustion	**Ash content**: > 6% **Volatiles**: > 15% **Moisture content**: > 20%	10-15%	• Suitable for co-firing as minimal modifications are needed.

A recent report from International Energy Agency (IEA) has shown that bioenergy accounts for about 9% of the world's primary energy supply (IEA, 2017). However, more than half of this biomass is rarely commercialized and is used in a more traditional sense. Developing countries, primarily use biomass for cooking and heating, using inefficient open fires or simple cookstoves which impacts negatively on health and the environment (IEA, 2017). In 2016, about 62 countries globally were producing electricity from biomass (Bhuiyan *et al*., 2016). The biggest producer of electricity using biomass is the USA, accounting for 26% of the world's total production. Germany is second with 15%, while Brazil and Japan are tied third with 7% (Bhuiyan *et al*., 2016). In 2015, about 230 combined heat and power (CHP) plants were using co-firing, mostly in northern Europe and the United States, with a capacity of 50 to 700 MW (Rycroft, 2015). Figure 2.8 below shows the capacities of biomass power plants in selected countries. Some of the countries generating power through co-firing in Asia-Pacific are: Australia, China, Indonesia and Thailand. In Europe,

countries such as Denmark, Finland, Germany, Italy, Norway, Spain, Sweden and United Kingdom (UK) are also utilizing this approach. Whilst in Africa, South Africa is the only nation experimenting with the technology (Sahu *et al*., 2014). In the UK, Drax power plant is the largest biomass combustion and co-fired utility in the world. This plant is the cleanest and most efficient coal-fired power station in the UK. It produces 40 000 Mega Watts hour (MWh), and accounts for 7% of Britain's energy production (Power Technology, 2019). Table 2.11 presents a summary of some of the existing co-fired plants in the world.

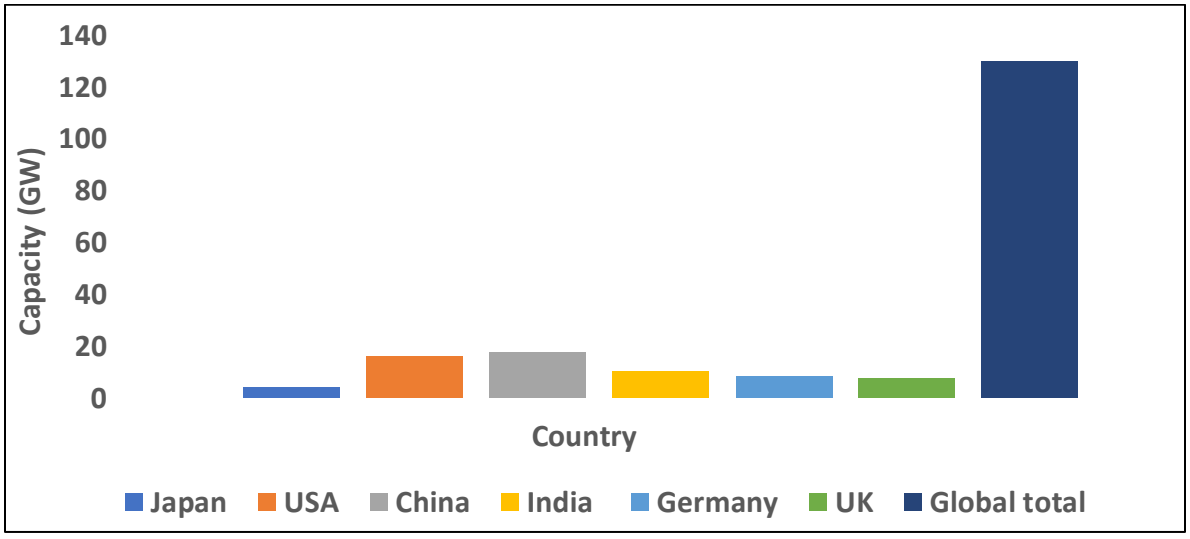

Figure 2.8: Capacities of biomass power plants in selected countries and worldwide (Statista, 2018).

The co-combustion of biomass with coal is cheap, renewable and sustainable (Roni *et al*., 2017). The overall cost of co-firing depends on the plant location and is largely influenced by the availability of biomass (Sahu *et al*., 2014). The cost of biomass depends on biomass type, quantity and geographical location (IEA-ETSAP, 2013). The cost of purchasing biomass pellets globally is more than that of coal, and this is one of the disadvantages of using biomass for power generation. With the upgrade and modification of biomass structure through pelletization and torrefaction, the energy density of biomass can be improved, leading to lower transportation cost (IEA-ETSAP, 2013). The combustion of biomass has been found to lead to the net reduction of CO_2, SO_x, and often NO_x emissions (Roni *et al*., 2017). In addition, the anaerobic release of CH_4, NH_3, H_2S,

amides, volatile organic acids, mercaptans, esters and other chemicals has also been found to be reduced, resulting in several benefits to the environment and the utility (Tillman, 2000). Studies have also shown that biomass co-combustion with coal can reduce the SO_2 emissions by up to 75% (Sahu *et al*., 2014), and traditional pollutants such as NO_x and SO_x (Roni *et al*., 2017). The concentration of NO_x emissions has been found to depend on the biomass type, combustion and co-combustion operating conditions (Baxter, 2005). In the study conducted by Saidur *et al*. (2011), most of the nitrogen present in the biomass was found to be converted to ammonia (NH_3) during combustion.

Table 2.11: Summary of biomass co-firing plants in some selected countries (Roni *et al.*, 2017)

Country	Number of plants co-firing	Average co-firing mixing rates (% biomass)	Co-firing methods	Boiler type	Primary feedstock
Netherlands	10	5-34%	Direct and indirect	PCC, FBC, Grate	Imported wood pellets, palm kernel shells, waste wood and cocoa shells.
Denmark	7	5-100%	Direct and indirect	PCC, FBC	Straw, wood pellets, wood chips and waste wood.
UK	14	3% by heat input	Direct	PCC	Wood pellets, miscanthus, short rotation coppice, olive and palm residues.
Japan	9	3% by mass	Direct	PCC, FBC, IGCC	Wood pellets
Brazil	0	Expected to be around 30%	NA	Test run in pulverized boiler	Rice straw
USA	86	Around 5%	Direct	Stoker, PCC, FBC and Cyclones	Wood pellets, wood chips, wood waste and railroad ties.
Germany	31	5-20%	Direct	Stoker, PCC and FBC	Sewage sludge, straw, wood waste and organic residue.

The main functional groups present in biomass or biomass-derived waste are hemicellulose, cellulose and lignin (Mohan *et al*., 2006). During the devolatilization process, hemicellulose usually decomposes at lower temperatures and release more volatiles, less tar and char. Whilst, lignin does produce more char after devolatilization than that of cellulose or hemicellulose due its amorphous cross-linked resin (Mohan *et al*., 2006). The devolatilization behaviors of coal and biomass differs because of structural differences (Sahu *et al*., 2014). Biomass devolatilization occurs at a much lower temperature than that of coal and releases light hydrocarbons, gases and

tar. Numerous researchers have studied mutual interactions between coal and biomass during devolatilization using thermogravimetric analyzer, fixed bed and an entrained bed reactor (Biagini *et al*., 2002; Kastanaki *et al*., 2002; Tchapda and Pisupati, 2014; Quan and Gao, 2016). A lot of these investigations claimed that interactions between coal and biomass during devolatilization are very insignificant (Sahu *et al*., 2014). Investigation has shown that the devolatilization and thermal degradation of organics in the solid fuels or biomass leads to the production of CO_2, CO, H_2O, H_2, CH_4 and other light hydrocarbons, tar, soot and char (Kabakci, 2017). In the case of lower rank coals, light gases are produced during primary devolatilization due to their lower aromatic carbon and large number of aliphatic groups.

The ignition and flame stability of a solid fuel is pivotal to its carbon burnout and the pollutant formation during combustion (Niksa *et al*., 2003; Taniguchi, 2012). The ignition behavior of solid fuel particles follows two mechanisms, viz, homogenous ignition and heterogenous ignition (Sun and Zhang, 1998). The ignition of the fuel's volatile matters is called homogenous ignition (Riaza *et al*., 2017). However, the direct interaction of oxygen with char or solid fuel resulted into a heterogenous ignition. Factors such as fuel particle size, temperature, heating rate, particle number density, gas composition and fluid flow, do influence the ignition behavior of solid fuel particles (Sun and Zhang, 1998). During the combustion of pulverized coal and biomass, the biomass particles are usually larger than the coal particles (Pederson *et al*., 1996; Grammelis *et al*, 2010). This is due to the difficulty in grinding and milling raw biomass to the same size with coal (Baxter, 2011). The ignition performance of both fuels is expected to be different as a result of the dissimilarity in their physical and chemical properties, which also influences their flame characteristics during co-combustion. The highly volatile matter content in biomass is known to favor the ignition and decomposition of biomass at lower temperatures, thereby generating an intense flame than the coal flame (Gani *et al*., 2005).

In a pulverized coal combustion, the carbon burnout influences the thermal efficiency of the plant and the quality of the fly ash produced (Hurt, 1998). The degree of the carbon burnout depends on the reactivity of the fuel particles, i.e. the fraction of combustible matter available for conversion. This reactivity is influenced by factors such as fuel characteristics, heating rate, temperature and pressure (Hurt, 1998). Many studies have indicated that the reactivity of biomass chars is greater

than that of coal chars (Zolin *et al*., 2002; Lang and Hurt, 2002; Campbell *et al*., 2002; Strydom *et al*., 2015). In a study conducted by Hurt (1998), the catalytic effect of biomass inorganic elements and its porous structure have been found to be responsible for its higher reactivity over coal. In addition, the non-spherical nature of biomass char also influences its aspect ratios, thereby, favors heat transfer and residence time compared to coal particles (Gera *et al*., 2002). Many researchers have shown that the addition of biomass with coal for co-firing can reduce burnout during co-combustion, even in a dedicated coal boiler (Sahu *et al*., 2014; Sung *et al*., 2016; Oladejo *et al*., 2019). The selection of biomass of an ideal particle size and moisture, along with volatile matter and carbon content is of fundamental importance in obtaining a satisfactory burnout in the coal-biomass co-combustion (Splienthoff and Hein, 1998). These fuel characteristics and combustion environment may either increase or decrease the burnout time (Zolin *et al.*, 2002).

Several studies have been carried out on the co-combustion behavior of coal/biomass blends in various scales to evaluate resultant combustion characteristics, heat release patterns, and reaction kinetics among others (Splienthoff and Hein, 1998; Munir *et al*., 2009; Barbanera *et al*., 2018). Thermogravimetric analyzer (TGA) has been used for basic combustion studies, while bench-scale experiments were conducted in a drop tube furnace. TGA is one of the most widely used techniques to investigate and compare thermal characteristics and reaction kinetics of solid fuels during combustion and pyrolysis (Wang *et al*., 2009). The knowledge of the fuel's attributes is required in modelling combustion furnaces for industrial scale application, for both co-firing of biomass with coal and firing of biomass alone (Munir *et al*., 2009). This knowledge is also essential for the design and operation of combustion systems (Cai *et al*., 2008).

A study conducted by Chen and Wu (2009), on the combustion behavior of blends of rice husks and pulverized coal in a TGA showed a three-stage reaction, with a linear relationship found existing between the char yield and the biomass blending ratio. A study by Riaza *et al.* (2017) found that a high volatile matter content in biomass accounted for the lowering of burnout and ignition temperatures during co-combustion. Gil *et al.* (2010) conducted an investigation on the thermal behavior and kinetics of coal/biomass blends during co-combustion. The results obtained by the authors showed that the first order chemical reaction mechanism was responsible for the first stage of biomass oxidation and coal combustion. Several researchers have studied the

activation energy and pre-exponential factor of individual fuels and their blends (Muthuraman *et al*., 2010; Gil *et al.*, 2010; Kok and Ozgur, 2012; Alvarez *et al.,* 2016). Some of the studies in the literature had shown that the activation energy and pre-exponential factor do decrease with an increase in biomass proportion (Wang *et al*., 2009; Muthuraman *et al*., 2010). This trend indicates a positive influence of biomass on the blends during co-firing. The weak chemical bond existing in the biomass compared to the more complex bond in the coal might be responsible for the high reactivity of the biomass.

The influence of thermal treatment on the physicochemical property of bamboo "*Bambusa balcooa*" and its co-firing potential with a South African high ash coal using a thermogravimetric analyzer was conducted by Bada *et al*. (2015). The bamboo species utilized "*Bambusa balcooa"* was pre-treated under torrefaction and low temperature carbonization. The calorific value of the raw bamboo was found increased from 18.53 MJ/kg to 24.02 MJ/kg and 28.20 MJ/kg, under torrefaction and low temperature carbonization, respectively. The ash content in the raw bamboo was found to be 0.49%, and its sulfur content was found undetectable. The activation energies of the raw bamboo ranged from 11.24 to 31.60 kJ/mol across the three reaction stages, while the coal used in the study had an activation energy of 64.12 kJ/mol. Both carbonization and torrefaction was found to have increased the activation energy for the raw bamboo within the range of (67.33-71.71) kJ/mol and (43.70-44.70) kJ/mol, respectively. The authors found that the most effective mechanisms for controlling the combustion process in all samples under stage 3 "carbon combustion" was the chemical reaction models (01, 02 and 03).

The derivative thermogravimetric curves (DTG) also provides the means of identifying the various functional groups in the biomass, in terms of the functional group's response to heat. In a study reported by Bada *et al*. (2015), the authors noted that two peaks were observed as raw bamboo was combusted, while a single peak was noted for the high ash coal. These peaks denote the degradation of hemicellulose at lower temperature and lignin at a higher temperature. A similar observation was made by Park and Jang (2012), Gil *et al*. (2010) and Varol *et al*. (2010) with two peaks obtained from different biomasses. In contrast, one peak was observed for coal combustion. The authors attributed the first of the two peaks, to the decomposition of the hemicellulose and

partial cellulose, while the second peak was attributed to the degradation of the lignin (Mock *et al*., 2018; Hu *et al.*, 2019).

2.3.4 Derivative thermogravimetric profiles

In this study, the DTG curve, known as the derivative thermogravimetric curve, obtained from the combustion and co-combustion of biomass, coal and their blends was used in determining the combustion performance of all the fuels utilized. It is a thermal analytical means of predicting the relative combustion characteristics of fuels proposed as an energy source in a boiler (Norton, 1992). The burning profile of a sample (coal or biomass) is obtained in a TGA after heating the sample at a constant heating rate to 700-900°C in an air environment (Norton, 1992). The weight of the sample (or, alternately, the percentage of the original sample weight) is measured and plotted as a function of either heating time or temperature. This plot is known as a TGA curve. A derivative thermogravimetric (DTG) curve is obtained by plotting the first derivative of the TGA data against temperature, thereby depicting the rate of weight loss as a function of temperature (Norton, 1992). For a fair comparison to be made between different samples, factors such as sample quantity, heating rate, and air flow rate should be the same between the tests. Of these, the air flow rate has the least effect on burning profiles (Norton, 1992).

There are different events observed as the sample temperature increases when burning coal or biomass. The first peak noted, typically at about 100°C or below, is as a result of moisture being released (Norton, 1992). After moisture loss, a negative deflection (weight gain) may be seen, which occurs as a result of the oxidation of the organic matter in the fuel (Cumming and McLaughlin, 1982). With a further increase in temperature, the curve crosses the zero line on the X axis, thereby leading to further weight loss known as “volatile matter initiation temperature” (Cumming and McLaughlin, 1982). Further increase in temperature lead to the initiation of the fixed carbon and char burning, with a rise in the profile curve.

The maximum intensity of the curve (peak), is denoted as the temperature at which the maximum combustion rate occurs (Norton, 1992). This peak temperature (PT) reflects relative reactivities of the fuels and is generally considered to be the most important feature of the DTG curve (Norton,

1992). Solid fuel with its peak temperature occurring at a lower temperature region is expected to ignite first, and start burning at the lower section of the boiler. Whilst, sample with peak temperature occurring at a higher temperature region would require longer residence times or higher temperatures for complete combustion (Wagoner and Winegartner, 1973). The peak height is proportional to burning intensity and the area under the peak is approximately proportional to the total heat liberated (Wagoner and Winegartner, 1973).

The height of the DTG peak is related to reactivity based on the equation below;

$$R = \frac{1}{W_i(\frac{dw}{dt})_{max}} \tag{2.1}$$

where R is the reactivity, W_i is the initial weight of dry, ash-free (DAF) coal (mg), and $\frac{dw}{dt}$, is the maximum rate of weight loss (mg/min) (Ghetti, 1986).

Figures 2.9 and 2.10 below show the stages of coal combustion for a fuel with a single peak and another fuel with a multiple peak respectively. Studies have shown that some low-rank coals, such as lignites, can have two or more major burning peaks. This has been termed “false ignition” because it implies that the coal is ignitable at a relatively low temperature, even though it may not burn completely until higher temperatures are reached (Cumming and McLaughlin, 1982). The double peak seen in Figure 2.10 are well noted in a case of burning biomass alone or biomass co-fired with coal (Gil *et al.*, 2010).

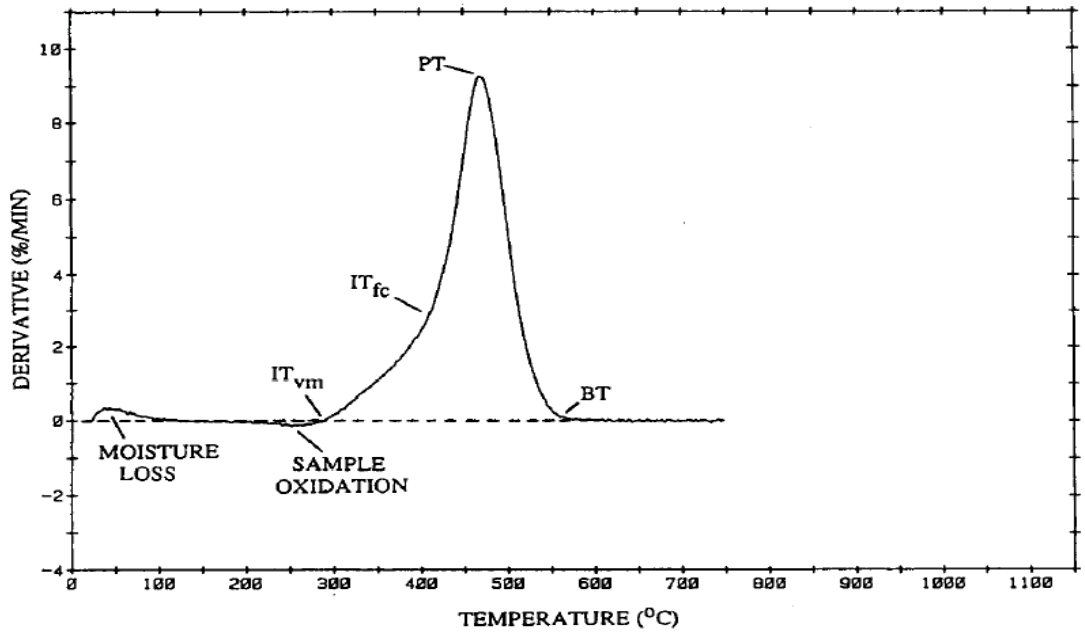

Figure 2.9: A simple burning profile showing moisture loss, sample oxidation, volatile matter initiation temperature (IT_{vm}), fixed carbon initiation temperature (IT_{fm}), peak temperature (PT) and burnout temperature (BT) (Norton, 1992).

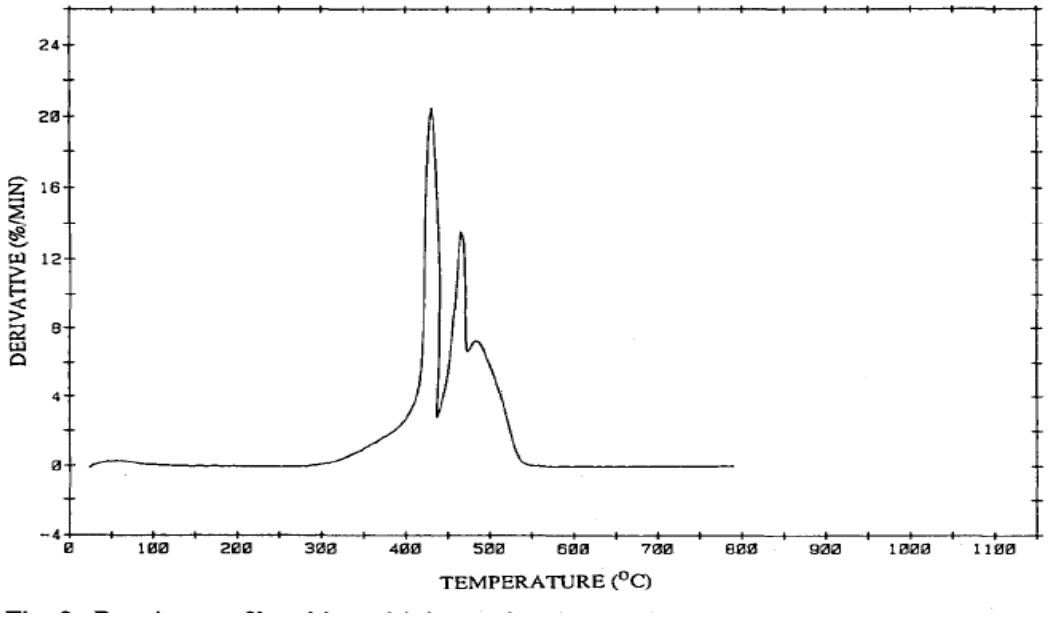

Figure 2.10: Burning profile with multiple combustion peaks due to sample ignition (Norton, 1992).

The burning profiles of fuels provide a detailed information about a fuel from the onset of oxidation to complete burnout (Rostom-Abadi *et al*., 1990). The technique is particularly useful for evaluating unusual fuels in which sample quantities are insufficient for full-scale burning tests (Wagoner and Winegartner, 1973). The DTG profiles of the coals can be used to provide a clear indication of the combustion behavior of coal in a large boiler, even if the physicochemical properties are the same (Norton, 1992). In addition, with the information obtained from the thermal characteristics of the fuels, the prediction of the furnace size, along with the residence time or height of the boiler and auxiliary fuel requirements can be made (Rostom-Abadi *et al*., 1990).

2.3.5 Environmental aspects of co-combustion

Emissions

Biomass is considered carbon-neutral as it does not lead to a net increase in the amount of CO_2 in the atmosphere. This claim was made because the CO_2 released during biomass combustion was believed to be used by plants in their growth process (Hughes, 2000). In addition, the declaration that biomass is a neutral fuel in regard to emission is only valid if we do not include emissions related to biomass harvesting, transportation, pre-treatment etc., and when the total carbon sequestrated in the atmosphere remains constant (Bracmort, 2016; Harvey and Heikkinen, 2018). The use of dedicated energy crops, which include, short-rotation woody crops (hard wood trees) and herbaceous crops like switch grass would go a long way in curbing emissions. Furthermore, with the use of biomass residues rather than these dedicated energy crops, a further mitigation of greenhouse gases could be achieved by avoiding the release of CH_4 from the otherwise landfilled biomass (EPA, 2011). According to many climate experts, CH_4 is believed to be approximately 84 times more potent over two decades than CO_2 when it comes to global warming impact (National Geographic, 2019). The remaining part of this section provide information on the previous studies available in the literature on the use of biomass for the reduction of greenhouse gases.

An investigation conducted by Sahu *et al*. (2014) on switching a power plant fuel from a hard coal to biomass, has shown that that CO_2 emissions can be reduced by up to 93%. Baxter (2005), also presented a report on the increase in the efficiency of power plant co-fired with waste, and the

reduction in the emission of the plant. The retrofitting of existing coal-fired power station for co-combustion has been found to be less expensive, rather than building a new power plant dedicated to pure biomass or waste combustion (IEA-ETSAP, 2013; Rycroft, 2015; Ko and Lautala, 2018). Some attributes of biomass had made it possible for its co-firing potential in the old power plants, of such properties is its high volatile matter content and oxygen content which act as a catalyst in the ignition of the hard coal (Biagini *et al*., 2005; Riaza *et al*., 2017).

From a study conducted by Liu *et al*. (2002) in a bench scale fluidized bed reactor, the authors found that the co-combustion of coal and biomass can reduce NO_x and N_2O emissions, as the proportion of biomass in the coal-biomass blend increases. Similar study conducted by Pederson *et al*. (1997) in a pilot scale 250 MW utility boiler, using a straw as a fuel, also shows a reduction in the emission of NO and SO_2 as the percentage ratio of the straw increases in the blend. Despite the current feasibility of biomass for reducing emission, it is also important that the ratio of biomass to be added to a specific biomass-coal blend should be investigated. A higher biomass share have been found to indicate lower greenhouse gas emissions, and with the exclusion of an upstream biomass, a 10% biomass share can reduce CO_2 emissions by tenfold (Sahu *et al*., 2014). However, burning of a biomass solely or with a high share poses a potential technical risk such as, slagging, fouling and corrosion (Melissari, 2014; Febrero *et al*., 2015).

In a study conducted by Saleh *et al*. (2014), several wood samples were found to release sulfur dioxide at a different concentration. The concentration of SO_2 emission was found by Ren *et al*. (2016) to be influenced by the amount of sulfur and alkali present in the fuel. A high composition of sulfur in the fuel is expected to lead to a high SO_x emission. However, this does not always hold, as some biomasses contain alkali metals like sodium, calcium and potassium which combine with sulfur to form sulphates, which inhibit SO_x emissions (Rokni *et al*., 2018). Ren *et al*. (2016) investigated emissions of carbon, sulfur and nitrogen from the combustion of pulverized raw and torrefied biomass. The results obtained showed that torrefied biomass had a lower SO_x emission than the raw biomass. This is because a lot of organic sulfur is driven off during low temperature torrefaction. Most of the biomass (raw and torrefied) utilized by the authors were found with sulfur emission below 50 ppm compared to the sub-bituminous coal with an emission level of 180 ppm.

The nitrogen content in biomass is found to vary over a wide range while in coal, it only varies within a narrow range (Flagan and Seinfield, 1998; Rokni *et al*., 2018). Although for most fuels, coal has the highest nitrogen content, but there are cases when the opposite is the case (Rokni *et al.*, 2018). A fuel with high nitrogen content implies a higher NO_x emission (Flagan and Seinfeld, 2012; Ren *et al*., 2016). In the study conducted by Ren *et al*. (2016), all fuels converted less than 40% of their nitrogen content to NO_x. Studies have shown that NO_x emissions decrease strongly with an increase in the fuel volatility, hence, addition of biomass to coal blend has a huge potential to reduce NO_x emissions (Munir *et al*., 2011; Guo and Zhong, 2018).

Ash formation and deposition

Biomass is known to contain two kinds of ash agents (Sahu *et al*., 2014). Firstly, ash-forming elements, also known as inherent ash, which are present as salts bound within the structure of the biomass (Sahu *et al*., 2014). Secondly, ash-forming minerals, particles of dirt or clay, introduced to the biomass fuel during harvesting or transportation. These are known as entrained ash (Kleinhans *et al*., 2018). The compounds in inherent ash are homogeneously dispersed in the fuel and are much more mobile than the compounds in the entrained ash (Kleinhans *et al*., 2018). Therefore, inherent ash is readily volatile and available for reactions in burning char (Obernberger *et al*., 1999). A fraction of the ash-forming compounds in the fuel is volatilized and released to the gas phase during combustion (Obernberger *et al*., 1999). Potassium originating from the inherent ash is the most abundant volatile element in biomass (Van Loo and Koppejan, 2008).

A major concern in co-combustion is ash-related issues such as slagging, fouling, corrosion, and particulate emissions (Singh *et al*., 2017; Ma *et al*., 2018). The primary reason for this is that the secondary fuels applied in co-combustion, generally possess a large amount of alkalis and chlorine that may be easily released to gas phase during combustion and create ash deposition (Sahu *et al*., 2014). Fouling of combustor surfaces plays a huge role in the design and operation of combustion equipment (Demirbas, 2007). Inorganic materials in the fuel are the main contributors to fouling (Febrero *et al*., 2015). The behavior of these inorganic materials is much less understood than those of their organic counterparts (Easterly and Burnham, 1996). Biomass contains a larger variety of inorganic materials than coal (Sahu *et al*., 2014). Hence, issues of slagging, fouling, corrosion, and

pollutant emissions need to be explored. This is important for some agricultural residues, and new tree growth where ash can have relatively high alkaline metal contents, particularly sodium and potassium (Easterly and Burnham, 1996; Caillat and Vakkilainen, 2012). Both potassium and sodium are found to lower the melting point of ash and, thus can increase ash deposition and fouling of boiler tubes (Melissari, 2014). In an investigation conducted by Texeira *et al*. (2012) on fouling and slagging tendency of biomass co-fired with coal in a fluidized bed reactor, the authors found that woody biomass can be successfully used as co-fired fuel without significant slagging and fouling problems.

2.4 Biomass

2.4.1 Overview of biomass and bio-energy

Biomass is any organic material that originates from plants, animals, or any other living organism and it is a renewable energy source (EIA, 2018). Plants contain stored energy from the sun, which is absorbed through a process called photosynthesis. The energy absorbed by plants is therefore used in converting CO_2 from the atmosphere into chemical energy. Biomass can be burned directly or converted to liquid biofuels (ethanol and biodiesel) or biogas that can be used as an energy source. Solid biomass, such as wood and garbage, can be burned directly to produce heat. Biogas is produced from paper, food scraps, and other organic waste which has decomposed over many years in a landfill. It can also be produced from sewage and animal manure in special vessels called digesters. Ethanol is made from crops such as corn and sugar cane that are fermented to produce fuel ethanol for use in vehicles. Biodiesel is produced from vegetable oils and animal fats and can be used in vehicles and as heating oil (EIA, 2018). In this study, the overview of the indigenous biomass "*Tamarix usneoides* and *Searsia lancea"* utilized are presented from section 2.4.2 below.

2.4.2 Biomass utilized in the study

Biomass source and plantation

The plant species utilized in this study were harvested from the Witwatersrand Basin Goldfields (WBG), which was highly polluted by tailings storage facilities (TSFs) that are hazardous to the environment and the public (Joubert, 2017). The TSFs is estimated to cover about 400 km^2 within

the WBG. This area was estimated by Weiersbye *et al.* (2006) to be contaminated with about 6 billion tonnes of gold and uranium tailings, and 430 000 tonnes of uranium and 30 million tonnes of sulfur contaminants. The different beneficiation techniques applied in the processing of gold over the years had led to the generation of large volumes of tailings from gold mining activities, since gold only forms a small fraction of the conglomerates that were mined. As the reserve of gold in some of these fields has depleted, these TSFs remained unused and untreated for over a century (Arendze, 2015). Since the TSFs are prone to erosion, generation of acid mine drainage (AMD) and soil contamination, a study was initiated by AngloGold and the University of the Witwatersrand, which required the planting of indigenous tree species between 2003 and 2008 on an estimated 320 hectares of land to address the above-mentioned issues.

In this rehabilitation project, two indigenous tree species "*Tamarix usneoides* and *Searsia lancea*", were amongst other trees planted to control and treat the AMD water from the mine (Weiersbye *et al*., 2006). It is imperative to evaluate the suitability and compatibility of these tree species for co-combustion with coal, as these trees may prove to be a valuable source of biomass.

Tamarix usneoides

Tamarix is native to the Mediterranean countries, former Soviet Union, China, India, North Africa, and Southern Africa (Baum, 1978; Heywood *et al*., 2007). However, there are various species of *Tamarix* in South Africa such as *Tamarix aphylla (L.) Karst*., *Tamarix ramosissima Ledeb*., *Tamarix chinensis Lour*., and *Tamarix parviflora DC* (Bredenkamp, 2003). The *Tamarix* utilized in this investigation is *Tamarix usneoides (T. usneoides)*, also known as *Tamaricaceae* or "The Salt Cider", which was planted on Tailing Storage Facilities (TSFs) and mine waste dumps in the Gauteng, North West and Free State provinces of South Africa (Weiersbye *et al*., 2006). This species is native to Southern Africa and is currently being used in the mines for treating acid mine drainage (AMD), through phytoremediation (Mayonde *et al*., 2013). It is a perennial shrub, that can grow up to 6 m in height (SANBI, 2019). Its leaves are scale-like, about 1.25 mm in length (SANBI, 2019) and typically contain salt glands (Bredenkamp and Phepho, 2008). The fact that it discharges salts enables it to grow in and tolerate soils with high salt concentrations, ranging from 650 to 36000 ppm (Brotherson and Field, 1987).

Studies conducted in South Africa, have shown that *Tamarix usneoides* has the potential for treating waste water generated from the gold mines (Weiersbye *et al*., 2006), as well as treating multiple pollutants such as heavy metals in ground water (Dennis, 2008). *Tamarix usneoides* has been found to lower the concentration of acid mine drainage (AMD) from a South African mine tailing storage facilities (TSFs), and also has the potential to hyper-accumulate NaCl, sulphates, other halogens, and some heavy metals from polluted water and soils (Weiersbye *et al*., 2006; Weiersbye, 2007). The species is likewise known to excrete a range of ions from specialized glandular structures on its leaves (Wilson *et al.*, 2017).

Searsia lancea

The second plant species utilized in this study is *Searsia lancea*, formerly known as *Rhus lancea*, and referred to as Karee tree in English and Rooikaree in Afrikaans language (Wanenge, 2009). *Searsia lancea* is an indigenous tree species with the ability to maintain a high leaf-area throughout the year (Dye *et al*., 2008). It is a multi-stemmed species of bush and tree form with a dense, evergreen canopy, and can grow up to 8 m tall and may be single or multi-stemmed (Plantinfo, 2019). This species was found to tolerate AMD polluted groundwater, the harsh conditions on Highveld mines (fires, frost, wind, drought and AMD polluted soils), and competition from neighboring trees (Joubert, 2017). In addition, it can accumulate high concentrations of sulfur in its leaves, of approximately 1.46-2.83% compared to 0.1-5% from other plants (Wanenge, 2009) which also makes it a good candidate for hydraulic control of seepage from TSFs (Dye *et al*., 2009) and in turn phytoextraction.

The *Searsia lancea* used in this investigation as biomass for coal/biomass co-combustion was planted adjacent to TSFs for phytostabilisation and hydrological control (Dye *et al*., 2008; Dye and Weiersbye, 2010). Studies conducted by Joubert (2017), had shown that *Searsia lancea* is an accumulator of sulfur, chlorine, and calcium with levels of 2 509, 2 501 and 16 733 mg/kg, respectively. An investigation conducted by Lange *et al*. (2012) also established that *Searsia lancea* is a perfect pioneer tree species for quickening the recovery of disturbed vegetation sites. In addition to the ecological value offered by *Searsia lancea*, the tree also boasts of countless traditional uses, ranging from building material to using the fruits for beer brewing (Venter and

Venter 1996; Palgrave, 2002). The use of this species on previously disturbed sites is expected to be of commercial and social value to the community.

2.5 Kinetic analysis

For non-isothermal experiments, the change in the sample mass is recorded against temperature and time. Mathematically, the rate of conversion dx/dt can be seen in equation 2.2 (Gil *et al*., 2010);

$$\frac{dx}{dt} = k(T)f(x) \tag{2.2}$$

The single step kinetic is represented in equation (2.2) above, and this defines the kinetic analysis in combustion reactions. In this equation, t is the time, T is the absolute temperature, x is the extent of conversion, $K(T)$ is the temperature dependent rate constant and $f(x)$ is the temperature-independent reaction model. With the use of a suitable reaction model, the kinetic parameters of the thermal decomposition process can be obtained from TGA data/profiles (Ozawa, 1965; Gil *et al*., 2010; El May *et al*., 2011). In an Arrhenius equation, k as a function of temperature can be written as:

$$k(T) = Ae^{\left(-\frac{E}{RT}\right)} \tag{2.3}$$

Where A is the pre-exponential or frequency factor, E is noted as the reaction activation energy and R is the universal gas constant (8.314 J/ (mol K)). The pre-exponential factor, the activation energy and the reaction model $f(x)$ are collectively known as the kinetic triplet. The characteristics of combustion are defined using these three parameters. The function $f(x)$ is expressed as:

$$f(x) = (1 - x)^n \tag{2.4}$$

The reaction order is represented as n, while the sample conversion, x can be seen in equation 2.5 as previously expressed by Agrawal and Chakraborty (2013) and Meng *et al*. (2013):

$$x = \frac{x_i - x_t}{x_i - x_\infty} \quad (2.5)$$

The x_i is noted as the initial mass of the sample, x_t is the mass of the sample at a time t and x_∞ is the final mass of the sample after the reaction. The combination of equation (2.3) to (2.5) gives:

$$\frac{dx}{dt} = Ae^{\left(-\frac{E}{RT}\right)}(1-x)^n \quad (2.6)$$

At a constant heating rate,

$$\beta = \frac{dT}{dt} \quad (2.7)$$

Equation (2.5) can be written as:

$$\frac{dx}{(1-x)^n} = \frac{A}{\beta} e^{(-E/RT)}\ dT \quad (2.8)$$

The integration from of equation (2.8) is shown in equation (2.9) as:

$$G(x) = \int_0^x \frac{dx}{f(x)} = \frac{A}{\beta}\int_{T_0}^{T} e^{\left(-\frac{E}{RT}\right)} dT \quad (2.9)$$

$$T = T_0 + \beta T \quad (2.10)$$

According to Chen *et al*. (2013), T_o is noted as the starting temperature.

The methods for determining the kinetic parameters involved in a reaction can be grouped into two; model-free methods also known as iso-conversion kinetic methods and model-fitting methods which depend on kinetic models (Vyazovkin and Wight, 1999; Wang *et al*, 2005). The model-free methods can be used to determine the activation energy of a reaction without the knowledge of the reaction model $f(x)$ (Yao *et al*., 2008) whilst the model-fitting methods can be used for predicting

activation energy without the knowledge of the reaction mechanism (Agrawal and Chakraborty, 2013). As stated by Meng *et al.* (2013), the model-free method has the advantage of determining activation energy without prior knowledge of the $G(x)$ function. In contrast, model-fitting methods are used in calculating the activation energy by fitting non-isothermal TGA data to a hypothetical reaction model. The difference in the two approaches for the kinetic analysis of isothermal and non-isothermal data have been reported by many researchers. A study by Vyazovkin and Wight (1999) noted that model-fitting approaches give accurate fits for both isothermal and non-isothermal data, but the Arrhenius parameters yielded by this approach are extremely ambiguous when applied to non-isothermal data. This is because x and T change simultaneously during non-isothermal experiment and model-fitting fails to obtain clean separation between the temperature dependency of $K(x)$ and the reaction model $f(x)$. According to Vyazovkin and Wight (1999), with the iso-conversional approach these shortcomings can be avoided, and this why the approach can be used to obtain reliable and consistent kinetic information for both isothermal and non-isothermal data.

Application of iso-conversional approaches is based on either applied differential methods or integral methods. Differential methods are thought to be the worst of the model-free methods, even though they do not assume any approximations (Bai *et al*., 2015). For differential iso-conversion method, equation 2.6 is linearized by taking logarithms, resulting in equation 2.11:

$$\ln\left(\frac{dx}{dt}\right) = \frac{-E}{RT} - \ln\big(f(x)\big) \qquad (2.11)$$

By considering a constant heating rate β, equation (2.11) can be transformed to:

$$\ln\left(\frac{dx}{dT}\beta\right) = \frac{-E}{RT} - \ln\big(f(x)\big) \qquad (2.12)$$

The activation energy can be derived from equation (2.11) by plotting $\ln\left(\frac{dx}{dT}\beta\right)$ versus $1/T$ which is a straight-line plot with a slope $-E/R$. Friedman method is a perfect example of this differential

iso-conversional method (Wang *et al.*, 2005 and Bai *et al.*, 2015). The integral method is derived by rearranging equation 2.6 for constant heating rate leading to the integral equation below:

$$\int_0^x \left(\frac{dx}{f(x)}\right) = \frac{A}{\beta}\int_{T_o}^{T} e^{\left(\frac{-E}{RT}\right)}\, dT \qquad (2.13)$$

From equation 2.13, the integral methods like the Coats-Redfern method (Coats and Redfern, 1964) or Flynn-Wall-Ozawa method could be applied to integrate the expression and determine the activation energy (Yao *et al*, 2008). Although, the iso-conversional methods can determine the activation energy E for the reaction independent of the reaction model but cannot determine the pre-exponential factor and the reaction model. Several researchers had proposed different reaction mechanisms for the modelling of biomass and biomass-coal blends, with many proposing first order reactions (Nassar, 1999; Zhou *et al*, 2006; and Gil *et al*, 2010).

The kinetic reactions of biomass and biomass-coal blends are heterogeneous. In the investigation conducted on the pyrolysis of different biomasses, more than one thermal event was identified by Zhou *et al.* (2006). Similarly, Gil *et al.* (2010) identified two thermal events using the same approach. The authors demonstrated that the first order reaction is the most effective mechanism for the devolatilization stage, and diffusion was found to be responsible for the biomass char reaction. Ozawa (1992), also found that the conversion at the maximum rate is constant and autonomous of the heating rate and in the case where heating is linear the rate constant follows the Arrhenius law. Following this, it is assumed that the dominating reaction is at a conversion conforming to the maximum rate of decomposition for a single first order reaction when the material is heated up at a constant rate.

A two-stage reaction kinetics scheme consisting of two independent reactions was proposed for the thermal decomposition of biomass under an oxidative atmosphere by Liu *et al.* (2002) and Shen *et al*. (2009). The kinetic scheme includes two separate reactions:

$$A(solid) \rightarrow B(char) + C1(gas)\ (First\ stage) \qquad (2.14)$$

$$B(char) \rightarrow C2(gas) + D(ash)\ (Second\ stage) \qquad (2.15)$$

2.5.1 Coats-Redfern method

The kinetic model applied in this study was derived from equation (2.9), which was integrated to obtain the Coats-Redfern method:

$$\ln\left(\frac{g(x)}{T^2}\right) = \ln\left(\frac{AR}{\beta E}\left(1-\frac{2RT}{E}\right)\right) - \frac{E}{RT} \qquad (2.16)$$

Since it can be proved that for most values of E and for the temperature range of combustion, the expression $\ln\left(\frac{AR}{\beta E}\left(1-\frac{2RT}{E}\right)\right)$ in Eq. (2.9) is essentially constant (Zhou *et al*., 2006), a straight line should be obtained by plotting $\ln\left(\frac{g(x)}{T^2}\right)$ versus $1/T$. Furthermore, if the correct $g(x)$ is used, the plot of $\ln\left(\frac{g(x)}{T^2}\right)$ versus $1/T$ should result in a straight line with a high correlation coefficient of linear regression analysis, from which the values of E and A can be calculated. Firstly, the activation energy can be derived from the slope of the line $-E/R$. Additionally, the pre-exponential factor can also be calculated by taking the temperature $m_t = (m_i + m_f)/2$ as the intercept of equation 2.16, (Zhou *et al*., 2006).

The function $g(x)/f(x)$ is dependent on the mechanism controlling the reaction, the size and shape of the reacting particle (Gil *et al*., 2010). With these functions, it is possible to estimate the reaction mechanisms controlling the thermal degradation of the samples from the TGA curves. The form of $g(x)$ that gives a straight line with the highest correlation coefficient will be considered the function of the model that best represents the kinetics of mass loss for each separate reaction (Gil *et al*., 2010). Most dynamic studies conducted using TGA frequently use the first-order chemical reaction assumption (O1 model). Additionally, other chemical reaction (O2 and O3 models), boundary-controlled reactions (R2 and R3 models) and diffusion mechanisms (D1, D2, D3 and D4 models) are commonly applied to describe the combustion reactions of biomass. The results obtained by Gil *et al*. (2010) indicated that the first order chemical reaction is the most effective mechanism for the first step of biomass oxidation and for coal combustion. However, diffusion mechanisms were found to be responsible for the second step of biomass combustion.

Table 2.12 below shows expressions of $g(x)$ for the kinetic models employed in solid-state reactions.

Table 2.12: Expressions of the function $g(x)$ for the kinetic models employed in solid-state reactions

Mechanism and model	$\boldsymbol{g(x)}$
Reaction order	
01	$-\ln(1-x)$
02	$(1-x)^{-1}$
03	$(1-x)^{-2}$
Phase boundary-controlled reactions	
R2	$1-(1-x)^{1/2}$
R3	$1-(1-x)^{1/3}$
Diffusion	
D1	x^2
D2	$(1-x)ln(1-x)+x$
D3	$(1-(1-x)^{\frac{1}{3}})^2$
D4	$1-2x/3-(1-x)^{2/3}$

CHAPTER 3: RESEARCH METHODOLOGY

In this chapter, the materials used in this study, their properties and sample preparation standards utilized are presented. The analytical methods and instruments used to achieve the research objectives outlined are also reported. Figure 3.1 below summarizes the research methodology as applied to this research.

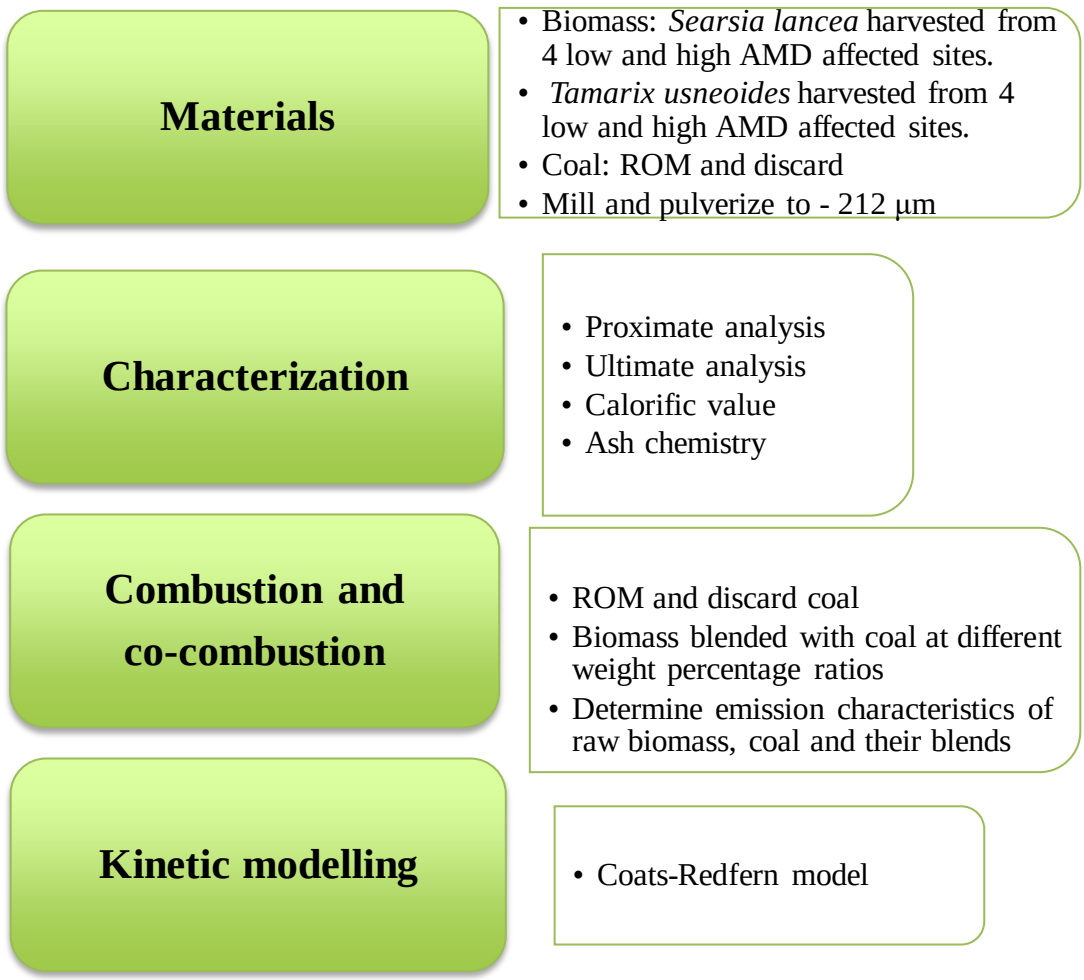

Figure 3.1: Overview of research methodology

3.1 Material

3.1.1 Biomass

The two tree species used in this study are *Searsia lancea* and *Tamarix usneoides*. The two tree species were 12 years old when harvested from four different trial test sites in the Vaal and Wits gold mines of South Africa. The locations of the sites are AngloGold Ashanti's (AGA) West Wits mine operation near Carletonville (26°26' 12"S 27°21' 12"E) and AGA's Vaal River mine operation near Klerksdorp (26°59'57"S 26°46'28"E). The Vaal River (VR) and West Wits (WW) mine sites are located 112 km apart. Figure 3.2 shows the location of the Vaal River and the West Wits mining operations. From the Carletonville (WW) mine, trees were harvested from the Red soil and Madala sites, while from the Klerksdorp (VR) mine, trees planted on the Mispah and West complex sites were also harvested as the source fuels.

From each site, two trees of both *Searsia lancea* and *Tamarix usneoides* were harvested (8 trees for each species and 16 trees in total), and divided into different plant sections representing the leaves, roots, twigs, wood, stump and rootball, as depicted in Figure 3.3a to 3.3g. After dividing the trees into different sections, all the tree sections were dried, and cut into different sections using a band saw. The sections were further reduced in a Retch 200 SM mill manufactured in Germany before being pulverized to about 70% passing -212 μm. The Retsch 200 SM mill is shown in Figure 3.4 while Tables 3.1 and 3.2 below show different parts of the tree that were collected per sample.

NOTE: The sites from which the trees were taken were noted to contain different levels of AMD concentration, soil nutrient levels and micro-organisms. In addition, investigation conducted by Weiersbye and Witkowski (2006) have shown that the *Tamarix usneoides* leaves contain high levels of salt (NaCl) ranging from 2 to 10%, therefore such high salt concentrations would be detrimental in any combustion situation. For the combustion test conducted in this study, the leaves were excluded from the blends of coal with biomass.

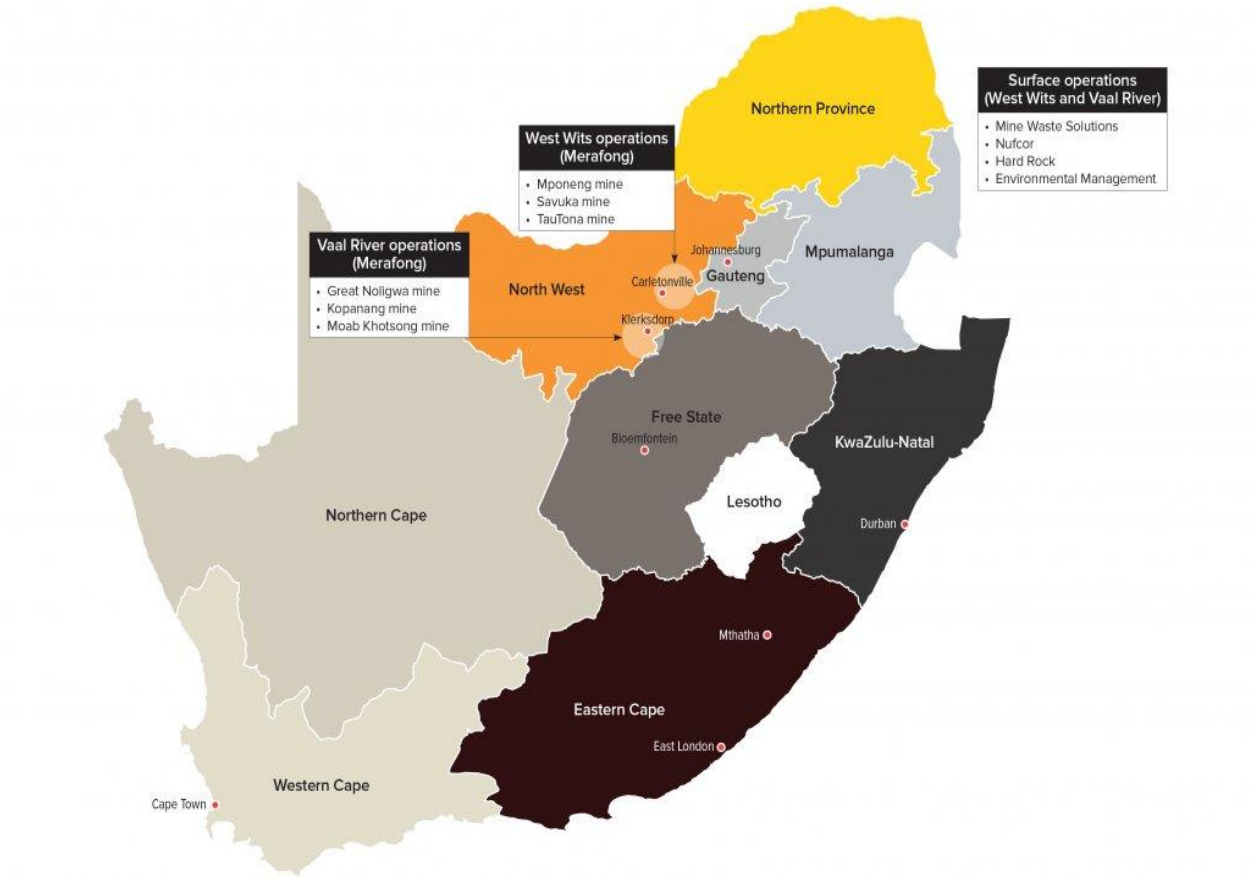

Figure 3.2: Location of Vaal River and West Wits Mining Operations (Mining Weekly, 2016)

Figure 3.3: Different biomass parts for *Searsia lancea* and *Tamarix usneoides*

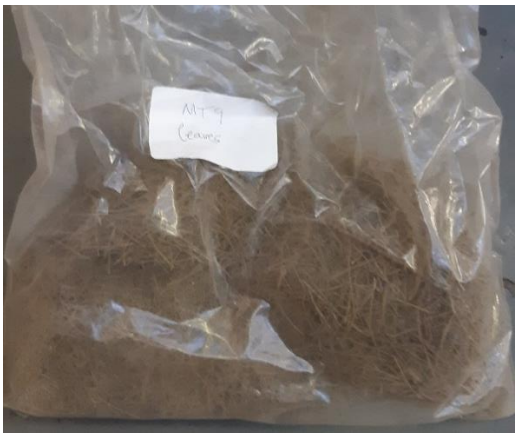

Figure 3.3a: Leaves

Figure 3.3b: Twigs

Figure 3.3c: Wood

Figure 3.3d: Dry biomass

Figure 3.3e: Roots

Figure 3.3f: Rootball

Figure 3.3g: Stump

Figure 3.4: Retsch SM 200 (Retsch, n.d.)

Table 3.1: Tree parts collected from West Wits mining sites

Site	Tree identity	Parts collected
Madala	T1	• Leaves • Twigs • Wood • Dry biomass • Roots
	T3	• Leaves • Twigs • Dry biomass • Stump
	S1	• Leaves • Twigs • Wood • Dry biomass • Stump
	S3	• Leaves • Twigs • Wood • Dry biomass • Roots
Red soil	T4	• Twigs • Wood • Roots
	T6	• Wood • Dry biomass • Roots
	S4	• Leaves • Twigs • Dry biomass • Roots
	S5	• Leaves • Twigs • Wood • Dry biomass • Stump

T: *Tamarix usneoides;* S: *Searsia lancea*

Table 3.2: Tree parts collected from Vaal River mining sites

Site	Tree identity	Parts collected
West Complex	T7	• Leaves • Twigs • Wood • Roots • Rootball
	T9	• Leaves • Twigs • Wood
	S7	• Leaves • Twigs • Wood • Dry biomass • Root • Rootball
	S8	• Leaves • Twigs • Wood • Dry biomass • Roots
Mispah	T11	• Leaves • Twigs • Wood • Roots • Rootball
	T12	• Leaves • Twigs • Wood • Roots • Rootball
	S11	• Leaves • Twigs • Wood • Dry biomass • Roots
	S12	• Leaves • Twigs • Wood • Dry biomass • Stump • Roots and Rootball

T: *Tamarix usneoides;* S: *Searsia lancea*

3.1.2 Coal

The two South African coals utilized in this study were sourced from a coal mine located within the Witbank coal field. The samples are run of mine (ROM) coal and discard coal. The samples were first milled in a hammer mill and then pulverized to -212 μm. Representative fractions of these samples were prepared for different analyses such as proximate, ultimate analysis, emission test, and combustion and co-combustion tests.

3.2 Analytical methods

The proximate analyses for all samples were conducted in accordance with the ASTM D-5142 (ASMT International, 2019), with approximately 1 g used in determining the inherent moisture, ash content and volatile matter present. The calorific value was determined for both tree species and coal using a Leco AC 500 calorimeter in accordance with ASTM D5865-04 (ASMT International, 2019). The system uses an electronic thermometer with an accuracy of 0.0001°C to measure the temperature every six seconds, with the results obtained within 4.5 to 7.5 minutes. The ultimate and sulfur analyses of all samples were performed according to ASTM D 5373-02 and ASTM D 4239-05 for CHN and sulfur content, in an Elementar vario EL cube analyser, with approximately 5 mg for each sample (ASMT International, 2019). The XRF analysis for the selected ash samples were conducted using an Ametek SPECTRO XEPOS HE analyser with about 5 g of each ash sample loaded into a sample cup for this analysis. The particle size of the samples was measured using a laser-based particle size analyzer, namely a Mastersizer (2000) of Malvern Instruments Ltd. The emission was measured using MGA 11 mobile gas analyzer, manufactured by Dr Födisch, Germany. Analytical instruments used are listed in Figures 3.5 to 3.9 below.

Figure 3.5: Leco AC 500 oxygen bomb calorimeter (LECO, n.d.)

Figure 3.6: The Elementar vario EL cube (Elementar, n.d.)

Figure 3.7: Ametek SPECTRO XEPOS HE analyser (SPECTRO XEPOS HE, n.d.)

Figure 3.8: Malvern Mastersizer 2000 particle size analyser (MalvernPanalytical, n.d.)

Figure 3.9: Multi Gas Analyser (MGA) 11 (Oy Anatek Instrument Ab, n.d.)

3.3 Ash Oxide Analyses

The coal samples were ashed in an atmosphere of air according to the ISO standard 1171:2010 for *'Solid mineral fuels - Determination of ash*' (ISO, 2019), and the compositional analysis of the major elements in the coal ash was determined using Ametek Spectro X-lab pro. The collection of oxides analyzed include: SiO_2, Al_2O_3, CaO, K_2O, Na_2O, Fe_2O_3, MgO, TiO_2, SO_3^{2-} and P_2O_5. The biomass samples, along with their coal blends were ashed in accordance with the CEN/TS 14775:2009 standard for '*Solid biofuels - Determination of ash content*' (BSI group, 2019) and major elements in the ash determined using the same procedure above. In terms of application, the ash analyses indicate the likelihood of abrasion, wear in mills and ducts, and the slagging or fouling potential of the coal on heating.

The fouling index, F_u, which was used to determine the fouling potential of the coal and biomass was calculated based on the base to acid ratio according to equation (3.1) as follows:

$$F_u = R_{B/A} \times (N_2O + K_2O) \quad (3.1)$$

The base to acid ratio was determined by equation (3.2) as follows:

$$R_{B/A} = \frac{(Fe_2O_3 + CaO + MgO + K_2O + Na_2O)}{(SiO_2 + TiO_2 + Al_2O_3)} \quad (3.2)$$

Low fouling potential, when $F_u \leq 0.6$, medium for $0.6 < F_u \leq 1.6$, high for $1.6 < F_u \leq 40$, and extremely high with tendency to deposits sintering when $F_u > 40$ (Texeira *et al.*, 2012).

The slag ratio was determined according to equation (3.3) as follows:

$$S_R = \frac{SiO_2}{SiO_2 + Fe_2O_3 + CaO + MgO} \times 100 \quad (3.3)$$

Low slagging if $S_R > 72$, medium if $65 < S_R \leq 72$ and high when $S_R < 65$ (Febrero *et al*., 2014).

3.4 Differential Thermogravimetry (DTG) and Emission Test

The thermogravimetric analysis (TG) and DTG test was conducted in a TGA, in an air atmosphere, ratio of 21% oxygen and 79% nitrogen. A 100 mg representative sample was feed into the TGA for each combustion test at a heating rate of 6°C/min, from 25°C to 850°C and held until there is constancy in weight loss. All the samples tested were subjected to these step parameters. The combustion characteristics of the raw fuels and their blends with coal at three different ratios of coal to biomass (3:1, 1:1 and 1:3) were determined from the DTG curves generated. Table 3.3 below explicitly shows all the samples used for combustion and co-combustion. All the samples

were tested twice for reproducibility, also note in Table 3.3, that 100% discard and 100% ROM appear only in one block as they do not change with site.

Table 3.3: Samples for combustion and co-combustion tests

	Sample ID	
Site	**Searsia lancea**	**Tamarix usneoides**
Madala	100% S 75% S + 25% D 50% S + 50% D 25% S + 75% D 100% D 75% S + 25% ROM 50% S + 50% ROM 25% S + 75% ROM 100% ROM	100% T 75% T + 25% D 50% T + 50% D 25% T + 75% D 100% D 75% T + 25% ROM 50% T + 50% ROM 25% T + 75% ROM 100% ROM
Red soil	100% S 75% S + 25% D 50% S + 50% D 25% S + 75% D 75% S + 25% ROM 50% S + 50% ROM 25% S + 75% ROM	100% T 75% T + 25% D 50% T + 50% D 25% T + 75% D 75% T + 25% ROM 50% T + 50% ROM 25% T + 75% ROM
West complex	100% S 75% S + 25% D 50% S + 50% D 25% S + 75% D 75% S + 25% ROM 50% S + 50% ROM 25% S + 75% ROM	100% T 75% T + 25% D 50% T + 50% D 25% T + 75% D 75% T + 25% ROM 50% T + 50% ROM 25% T + 75% ROM
Mispah	100% S 75% S + 25% D 50% S + 50% D 25% S + 75% D 75% S + 25% ROM 50% S + 50% ROM 25% S + 75% ROM	100% T 75% T + 25% D 50% T + 50% D 25% T + 75% D 75% T + 25% ROM 50% T + 50% ROM 25% T + 75% ROM

S: Searsia lancea; T: Tamarix usneoides; D: Discard; ROM: Run of mine

These thermographs provided information on the sample weight loss, key temperatures at which ignition, devolatilization and peak temperature stages were reached, and changes in reaction time

for both species, coal and coal-biomass blends. A Leco TGA 701 can be seen in Figure 3.10 below.

Figure 3.10: The Leco TGA 701 (MARC, n.d.)

The schematic diagram of combustion experimental system is displayed in Figure 3.11. The experiments were carried out in a stainless-steel reactor inserted in an Elite 1200°C, horizontal tube furnace (TSH12/38/500), mullite work tube with an internal diameter of 40 mm and a length of 750 mm. The tube furnace was heated from room temperature to the targeted temperature of 850℃ for the combustion and co-combustion test, with the furnace temperature monitored with an EUROTHERM 2216e temperature controller. The experiment was conducted in air atmosphere (21% oxygen/79% nitrogen) with an air flow rate of 300 ml/min. The air, with a purity of 99.9% was purchased from Afrox. Once the tube furnace was heated up to the targeted temperature, blank test was conducted three times with an empty alumina crucible and MGA 11 mobile gas analyzer connected online at 1 scan per second. This was to ascertain the repeatability of the analyzer and the batch test procedure. A test sample of coal, biomass and their blends (0.1) g was fed through port 9 as shown in Figure 3.11, into the tube furnace (11), as a batch test, rather than feeding the sample continuously through the screw feeder (7). Since the experiment was conducted using a

batch test, the reactor gas inlet pipe (10), flush gas inlet port (15) and flush gas outlet port (16) were not utilized.

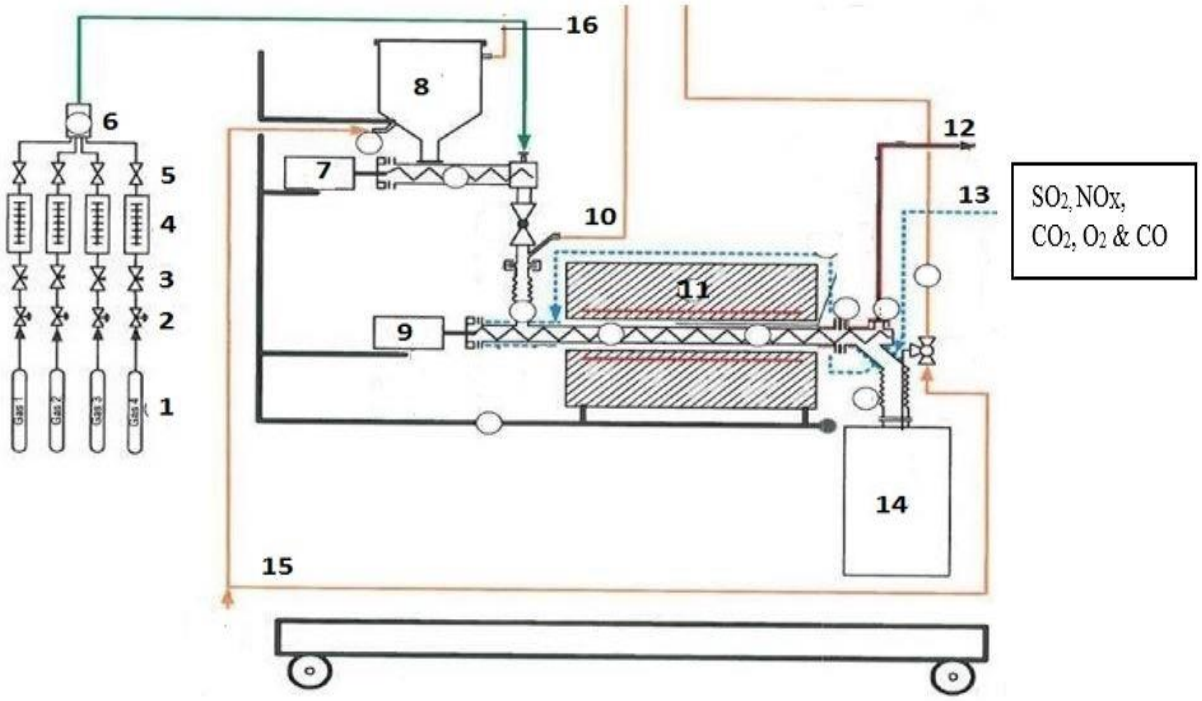

Figure 3.11: The schematic diagram of combustion and co-combution experimental system.

3.5 Kinetic analysis

In this work, the approach used to calculate kinetic parameters was based on Arrhenius equation, which has been used extensively by researchers to obtain kinetic parameters of thermal events under combustion conditions (Gil *et al*., 2010). For non-isothermal experiments, the change in the sample mass is recorded against temperature and time. Mathematically, the rate of conversion dx/dt can be seen in equation 3.4:

$$\frac{dx}{dt} = k(T)f(x) \qquad (3.4)$$

Where, t is the time, T is the absolute temperature, x is the extent of conversion, $K(T)$ is the temperature dependent rate constant and $f(x)$ is the temperature-independent reaction model. The sample conversion, x can be seen in equation 3.5 as previously expressed by Agrawal and Chakraborty (2013) and Meng *et al*. (2013):

$$x = \frac{x_i - x_t}{x_i - x_\infty} \tag{3.5}$$

The x_i is noted as the initial mass of the sample, x_t is the mass of the sample at a time t and x_∞ is the final mass of the sample after the reaction.

In an Arrhenius equation, k as a function of temperature can be written as:

$$k(T) = Ae^{(-\frac{E}{RT})} \tag{3.6}$$

Where A is the pre-exponential or frequency factor, E is noted as the reaction activation energy and R is the universal gas constant (8.314 J/ (mol K). The function $f(x)$ is expressed as:

$$f(x) = (1 - x)^n \tag{3.7}$$

The reaction order is represented as n. The combination of equations (3.4) to (3.7) gives:

$$\frac{dx}{dt} = Ae^{\left(-\frac{E}{RT}\right)}(1 - x)^n \tag{3.8}$$

At a constant heating rate (β),

$$\beta = \frac{dT}{dt} \tag{3.9}$$

Equation (3.8) can be written as:

$$\frac{dx}{(1-x)^n} = \frac{A}{\beta} e^{(-E/RT)}\ dT \tag{3.10}$$

The integral form of equation (3.10) is shown in equation (3.11) as:

$$G(x) = \int_0^x \frac{dx}{f(x)} = \frac{A}{\beta} \int_{T_0}^{T} e^{(-\frac{E}{RT})} dT \tag{3.11}$$

TGA technique consists of pre-heating a sample to a given temperature (T_0), and then starting the experiment at a fixed nominal heating rate (β). Theoretically, temperature (T), can be expressed as a function of heating rate and time as follows:

$$T = T_0 + \beta t \tag{3.12}$$

According to Chen *et al*. (2011), T_o is noted as the starting temperature.

The kinetic model applied in this study was derived from equation (3.11), which was integrated to obtain the Coats-Redfern method:

$$\ln\left(\frac{g(x)}{T^2}\right) = \ln\left(\frac{AR}{\beta E}\left(1 - \frac{2RT}{E}\right)\right) - \frac{E}{RT} \tag{3.13}$$

Since it can be proved that for most values of E and for the temperature range of combustion, the expression $\ln\left(\frac{AR}{\beta E}\left(1 - \frac{2RT}{E}\right)\right)$ in Eq. (3.13) is essentially constant (Zhou *et al*., 2006), a straight line should be obtained by plotting $\ln\left(\frac{g(x)}{T^2}\right)$ versus $1/T$. Furthermore, if the correct $g(x)$ is used, the plot of $\ln\left(\frac{g(x)}{T^2}\right)$ versus $1/T$ should result in a straight line with a high correlation coefficient of linear regression analysis, from which the values of E and A can be calculated. Firstly, the activation energy can be derived from the slope of the line $-E/R$. Additionally, the pre-exponential factor can also be calculated by taking the temperature at which $m_t = (m_i + m_f)/2$ as the intercept of equation (3.13) (Zhou *et al*., 2006).

CHAPTER 4: RESULTS AND DISCUSSIONS

This chapter presents and discusses results of the tests and analysis outlined in Chapter 3. The identities of the sites in which the trees were planted and harvested, the individual trees milled and analyzed are depicted in Figure 4.1 below.

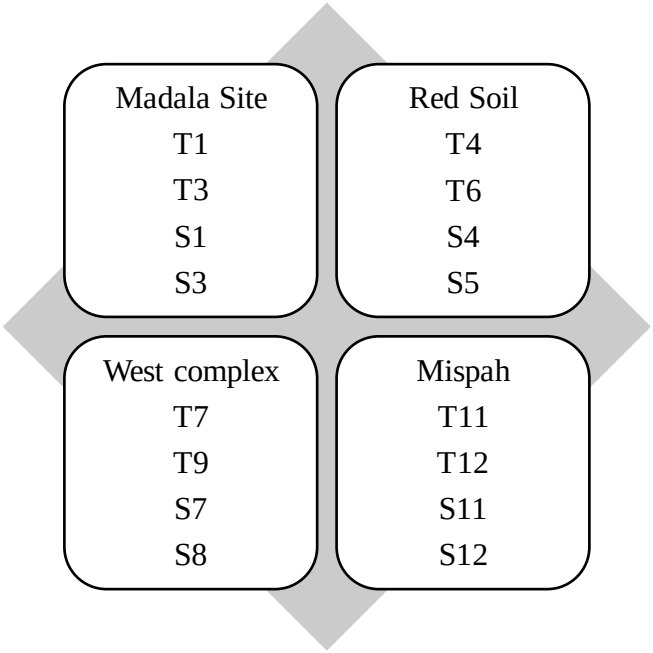

Figure 4.1: Identities of biomass samples tested

4.1 Fuel characterization

4.1.1 Variation of ash content in different tree parts

Proximate analysis was conducted on two trees of both *Searsia lancea* and *Tamarix usneoides* harvested from four sites (Figure 4.1). The sixteen individual trees (two from each sites) were divided into different plant sections representing the leaves, roots, twigs, wood, stump and rootball. Figure 4.2 shows the results from the physicochemical properties of both species with different ash content.

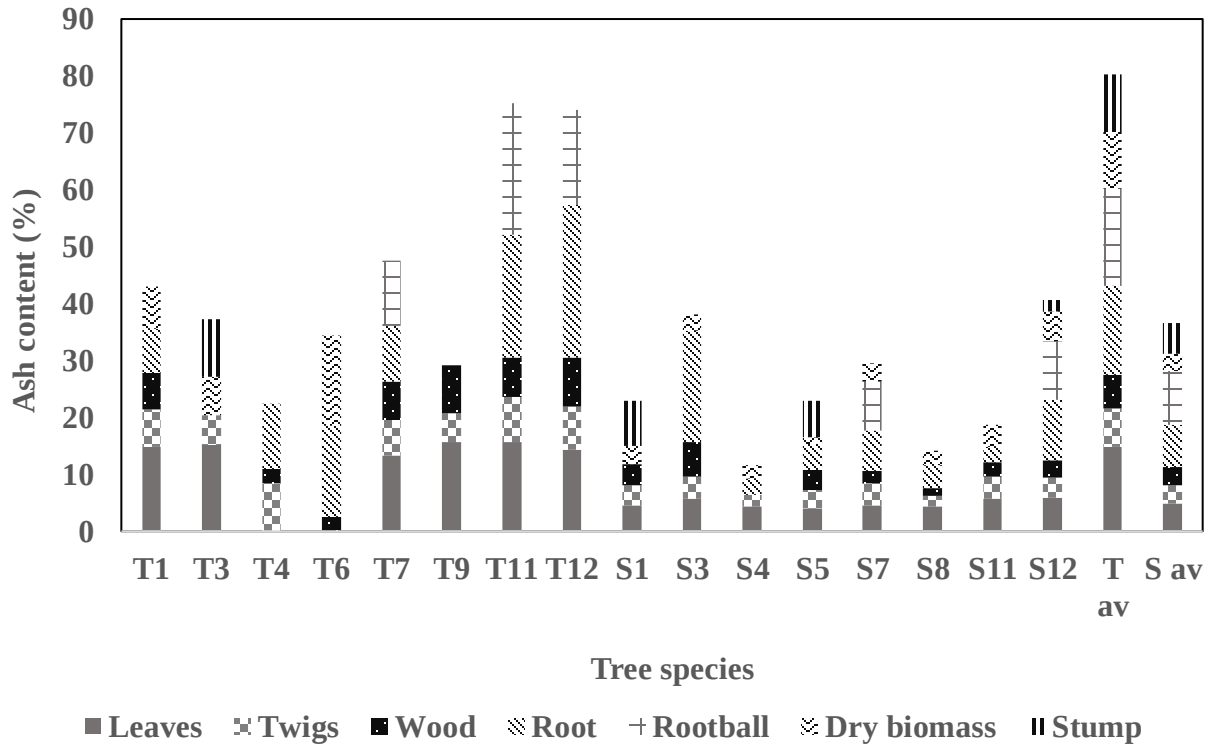

Figure 4.2: Ash content of different tree parts (T av and S av are the average ash contents in the tree part for *Tamarix usneoides* and *Searsia lancea*, respectively).

As shown in Figure 4.2, the root, root ball and leaves from both *Searsia lancea* and *Tamarix usneoides* harvested from the AMD affected sites (Madala, Red soil, West complex and Mispah) are noted to contain high ash compared to the other tree sections. The wood and twigs had the least ash content, i.e. inorganic mineral residue, indicating that these tree compartments might be the most suited for co-firing, in terms of lower propensity to slagging and fouling. *Searsia lancea* was found to have a lower ash content than *Tamarix usneoides* in all the tree compartments as seen in Table 4.1. Its leaves have an average ash content of 4.87% at a range of 3.96 to 5.87% compared to an average of 14.81% for *Tamarix usneoides* leaves from a range of 13.35-15.64%. The high ash noted in *Tamarix* leaves as seen in Table 4.1 was expected, since this was the same species reported by Weiersbye and Witkowski (2007), as having a high level of salt (NaCl) ranging from 2 to 10%.

Table 4.1: Range and average ash content for different tree compartments of *Searsia* and *Tamarix*

	Tamarix usneoides		***Searsia lancea***	
	Average (%)	**Range (%)**	**Average (%)**	**Range (%)**
Leaves	14.81	13.35-15.64	4.87	3.96-5.87
Twigs	6.75	5.16-7.96	3.29	1.94-3.93
Wood	6.00	2.49-8.36	3.16	1.33-6.03
Root	15.60	7.8 -26.87	7.33	2.67-19.57
Rootball	17.09	11.4-23.26	9.43	8.63-10.22
Dry biomass	9.96	6.71-15.78	3.04	1.19-5.21
Stump	10.06	10.06	5.52	2.02-8.01

4.1.2 Fixed carbon variation in different tree compartments

As shown in Figure 4.3, for both *Searsia lancea* and *Tamarix usneoides*, the tree compartments were seen with different fixed carbon content. The *Tamarix usneoides* wood and twigs sections had the highest fixed carbon, averaging 17.08 and 15.66%, respectively while its leaves had the lowest fixed carbon content, averaging 8.93%. Contrastingly, the leaves of *Searsia lancea* were found with the highest fixed carbon content of any tree part for both trees, with an average of 23.02%. The high concentration of carbon noted in these leaves might be as a result of the species being able to sequestrate carbon. A study conducted by Tomimatsu *et al*. (2014) had shown that the carbon content in the leaf of *Dipterocarpus sublamellatus* tree species do increases with high CO_2 concentration. In addition, high fixed carbon in leaves is not uncommon as Bhavsar *et al*. (2018) also found fixed carbon of 15.9 and 16.9% for mango and cashew trees' leaves respectively. The twigs and wood had the second and third most fixed carbon content, averaging 20.59 and 20.36%, respectively for the *Searsia lancea* species. Table 4.2 below summarizes the range and average fixed carbon content for all the tree compartments for both *Searsia lancea* and *Tamarix usneoides.*

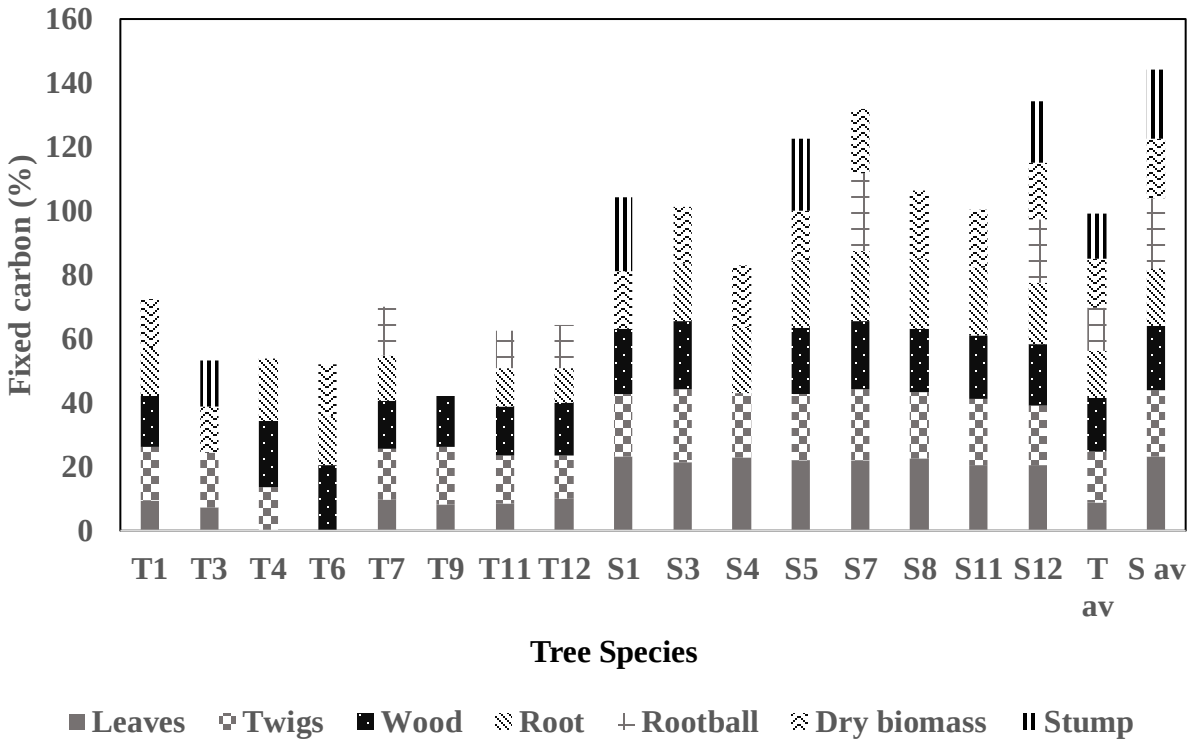

Figure 4.3: Fixed carbon content of different tree parts (T av and S av are the average ash contents in the tree part for *Tamarix usneoides* and *Searsia lancea*, respectively).

Table 4.2: Range and average fixed carbon content for different tree compartments

	Tamarix usneoides		***Searsia lancea***	
	Average (%)	**Range (%)**	**Average (%)**	**Range (%)**
Leaves	8.93	7.45-10.08	23.21	20.61-23.31
Twigs	15.66	13.42-17.8	20.59	18.37-22.81
Wood	17.08	15.02-20.47	20.36	19.2-21.34
Root	14.51	11-19.68	20.85	17.99-22.03
Rootball	13.63	11.85-15.53	21.90	19.62-24.18
Dry biomass	15.25	14.41-16.01	18.50	15.45-21.44
Stump	14.23	14.23	21.72	19.13-23.21

4.1.3 Volatile matter and moisture content variation in different tree compartments

Volatile matter content also varied in different tree compartments for both *Searsia lancea* and *Tamarix usneoides* as seen in Figure 4.4. For *Tamarix usneoides*, twigs and wood had the highest volatile matter content while root and rootball had the least. This is in line with the values of standard biomass as documented by Stahl *et al*. (2004). The authors found the average volatile matter in standard biomass to be around 76% while the wood compartment had about 8% more volatiles. For *Searsia lancea*, dry biomass, wood and twigs had the most volatile matter content while the root and rootball had the lowest.

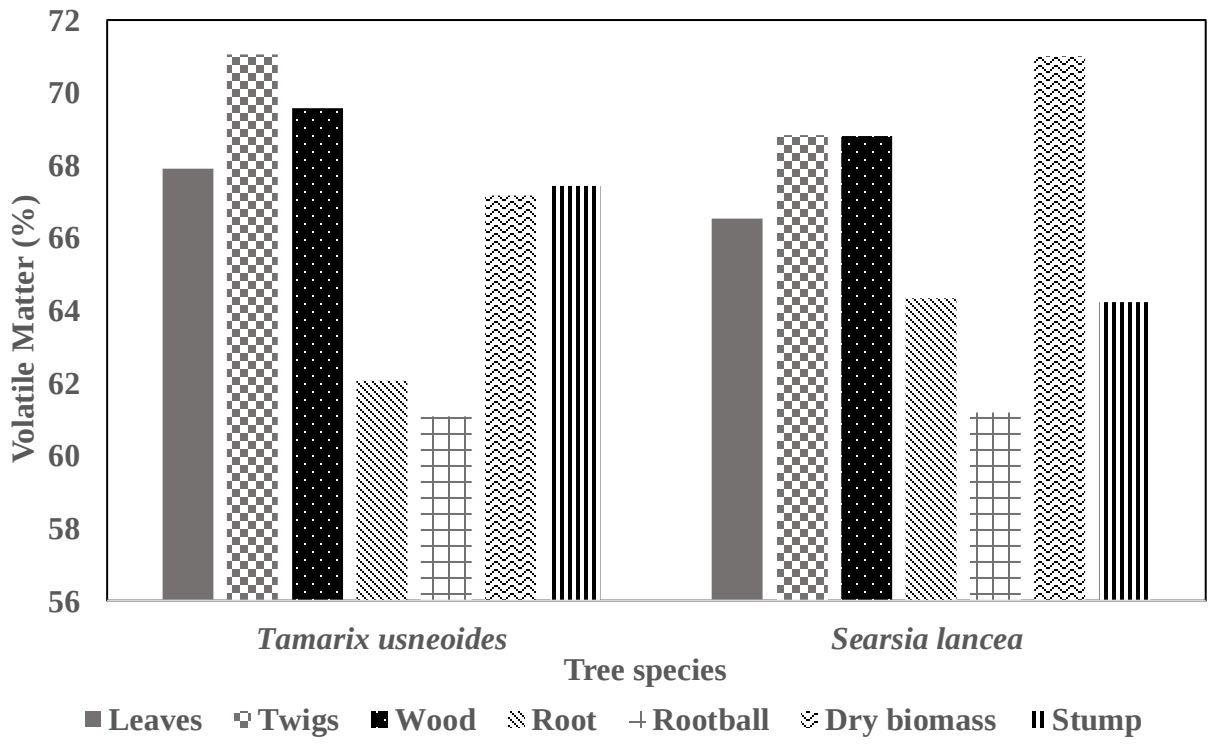

Figure 4.4: Volatile Matter content in different tree parts

Compared to other physicochemical properties, there was little difference in the moisture content across the different tree parts for both species. However, the stump was seen with the highest moisture content in Figure 4.5, as this is the tree part that is least susceptible to losing water as it is buried underground.

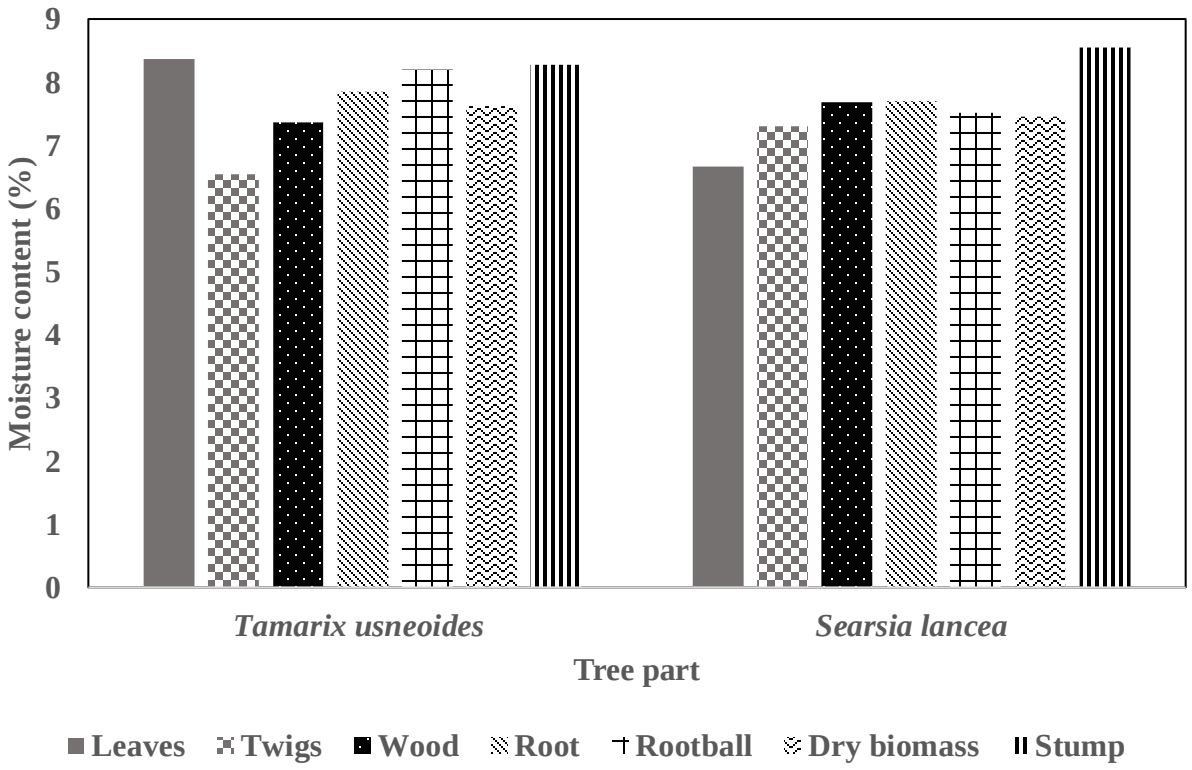

Figure 4.5: Moisture content in different tree parts

4.1.4 Fuel characterization of different AMD affected sites

The proximate and the calorific values results for all the samples from the four sites in which the AMD rehabilitation trial test was conducted are shown in Tables 4.3 to 4.6 according to the plant components for each tree. The sites from which the trees were taken were noted to contain different levels of AMD concentration, ranging from the pH of 5 to 6.2 (Joubert, 2017). All the four sites were also found by Joubert (2017) to contain different level of metal concentrations at different tree compartments. It is expected that there might be a variation in the quality and energy characteristics of the trees and their plant components, detailed analyses were undertaken for all plant materials.

Table 4.3: Proximate analysis and heat content result for *Searsia lancea* (Redsoil)

Sample	Section	M (%)	VM (%)	ASH (%)	FC (%)	CV (MJ/Kg)
S4	**LEAVES**	4.18	68.65	**4.41**	**22.77**	**19.21**
	TWIGS	7.18	70.50	2.03	20.31	18.20
	DB[a]	7.25	71.03	2.35	19.38	16.93
	ROOTS	7.15	69.54	2.78	20.54	17.21
	BLEND 1[b]	6.09	70.27	2.81	20.84	17.32
	BLEND 2[c]	6.94	70.76	2.49	19.83	17.33
S5	**LEAVES**	4.98	69.01	3.96	**22.05**	
	TWIGS	6.84	69.16	3.29	20.72	
	WOOD	8.01	67.98	3.49	20.54	
	DB[a]	6.06	77.32	1.19	15.45	
	STUMP	9.09	61.59	6.52	**22.81**	
	ROOTS	6.97	67.34	4.55	21.16	
	BLEND 1[b]	5.94	70.17	2.94	20.96	
	BLEND 2[c]	7.34	69.00	3.64	20.04	17.34
S4+S5	**BLEND 3**[d]	8.41	66.77	3.77	21.05	17.31

Ad: Air dried basis; VM: Volatile matter; FC: Fixed carbon; M: Moisture; CV: Calorific value; 1^{b}: Blend of all tree sections; 2^{C}: Blend excluding the leaves; 3^{d}: Blend of 2^{C} S4 & S5; DB: dried biomass and ***Redsoil: Less affected AMD site***

Table 4.4: Proximate analysis and heat content result for *Searsia lancea* (West Complex)

Sample	Sections	M (%)	VM (%)	ASH (%)	FC (%)	CV (MJ/Kg)
S7	**LEAVES**	6.87	66.43	4.57	**22.14**	18.66
	TWIGS	5.85	68.12	3.93	22.09	
	WOOD	7.35	69.16	2.16	21.34	
	DB[a]	7.47	69.28	3.07	20.19	
	ROOTS	8.06	62.86	7.06	22.03	
	ROOTBALL	7.48	59.72	8.63	**24.18**	
	BLEND 1[b]	6.92	65.63	4.94	22.53	
	BLEND 2[c]	7.22	65.34	5.40	22.05	17.28
S8	**LEAVES**	5.86	67.18	4.31	**22.65**	18.80
	TWIGS	7.17	70.34	1.94	20.56	
	WOOD	6.65	72.17	1.33	19.87	
	DB[a]	8.07	67.94	2.57	21.44	
	ROOTS	7.87	66.20	3.98	21.95	
	BLEND 1[b]	7.28	68.06	3.20	21.48	
	BLEND 2[c]	7.93	68.52	3.00	20.56	17.29
S7 + S8	**BLEND 3[d]**	8.35	66.45	3.94	**21.28**	**17.27**

Ad: Air dried basis; VM: Volatile matter; FC: Fixed carbon; M: Moisture; CV: Calorific value; 1^{b}: Blend of all tree sections; 2^{C}: Blend excluding the leaves; 3^{d}: Blend of 2^{C} S7 & S8; DB: dried biomass and ***West Complex: High affected AMD site.***

Table 4.5: Proximate analysis and heat content results for *Tamarix usneoides* (Madala)

Sample	Sections	M (%)	VM (%)	ASH (%)	FC (%)	CV (MJ/Kg)
T1	**LEAVES**	8.73	66.99	**14.84**	**9.46**	14.10
	TWIGS	6.97	69.61	6.63	16.81	
	WOOD	7.44	70.29	6.32	15.97	
	DB[a]	7.86	69.44	7.38	15.32	
	ROOTS	7.53	69.80	7.80	14.89	
	BLEND 1[b]	7.57	68.14	9.13	15.17	
	BLEND 2[c]	7.59	69.46	7.25	15.71	16.23
T3	**LEAVES**	7.61	69.75	**15.21**	**7.45**	14.25
	TWIGS	5.14	72.56	5.22	17.09	
	DB[a]	7.00	71.89	6.71	14.41	
	STUMP	8.28	67.44	10.06	14.23	
	BLEND 1[b]	6.87	69.25	9.87	14.02	
	BLEND 2[c]	7.24	69.96	9.12	13.69	15.89
T1 + T3	**BLEND 3[d]**	**8.26**	**68.96**	**8.18**	**14.61**	**16.09**

Ad: Air dried basis; VM: Volatile matter; FC: Fixed carbon; M: Moisture; CV: Calorific value; 1^{b}: Blend of all tree sections; 2^{C}: Blend excluding the leaves; 3^{d}: Blend of 2^{C} T1 & T3; DB: dried biomass and ***Madala: Less affected AMD site***

Table 4.6: Proximate analysis and heat content results for *Tamarix usneoides* (Mispah)

Sample	Sections	M (%)	VM (%)	ASH (%)	FC (%)	CV (MJ/Kg)
T11	**LEAVES**	8.87±	67.01	15.64	**8.48**	16.06
	TWIGS	**7.06**	**69.94**	7.96	15.05	
	WOOD	**8.95**	68.66	**6.96**	**15.44**	
	ROOTS	7.52	59.15	21.47	11.86	
	ROOT BALL	7.83	**57.06**	**23.26**	11.85	
	BLEND 1[b]	8.20	63.22	15.45	13.15	
	BLEND 2[c]	7.91	62.84	15.63	13.64	16.31
T12	**LEAVES**	**8.96**	66.75	14.24	**10.08**	**15.31**
	TWIGS	8.05	**70.88**	**7.67**	13.42	
	WOOD	8.20	66.79	8.61	**16.42**	
	ROOTS	**6.49**	**55.65**	**26.87**	11.00	
	ROOT BALL	8.38	61.50	16.62	13.52	
	BLEND 1[b]	8.22	63.80	15.06	12.92	
	BLEND 2[c]	7.31	63.45	15.30	13.95	16.17
T11 + T12	**BLEND 3[d]**	**8.37**	**68.52**	**7.48**	**15.64**	**16.26**

Ad: Air dried basis; VM: Volatile matter; FC: Fixed carbon; M: Moisture; CV: Calorific value; 1^{b}: Blend of all tree sections; 2^{C}: Blend excluding the leaves; 3^{d}: Blend of 2^{C} T11 & T12; and ****Mispah: High AMD affected site***

From the proximate analysis conducted on the two tree species (Table 4.3-4.6), it is apparent that the trees do indeed have different properties. In Tables 4.3 and 4.4, the moisture contents in the *Searsia lancea* samples planted on the Red soil and West complex sites are shown to range from 4.18 to 9.09%. The bottom section of the tree (roots) possesses the highest moisture content. For the same species (*Searsia lancea*), the ash content of the sample planted on the West complex (High AMD affected site) was found to be 7.06 and 8.63% for the root and rootball, respectively. The root from the Red soil (Less AMD affected site), was found to have a considerably lower ash content of 2.78%. According to Tables 4.5 and 4.6, the ash content from the leaves of *Tamarix usneoides* planted on the Madala and Mispah sites are within the range of 14.24-15.64%. The rootball and root for this species planted on Mispah (High AMD affected site) was within the range of 16.62-26.87%. This is much higher than that obtained from the Madala site (Less AMD affected site). The high ash noted in *Tamarix* leaves is expected, since this was the same species reported by Weiersbye and Witkowski (2007), as having a high level of salt (NaCl) ranging from 2 to 10%. The blend of all sections in *Tamarix usneoides* trees without leaves added shows an ash content

ranging from 7.48-8.98%, while the blend of *Searsia lancea* components was found with an ash content within the range of 3.77-3.94% as seen in Tables 4.3-4.6.

A higher ash content noted in *Tamarix usneoides,* according to Table 4.5 and 4.6 is more likely to cause slagging and fouling issues than *Searsia lancea* (Table 4.3 and 4.4). Of the two species, *Tamarix usneoides* is a greater hyperaccumulator (Weiersbye *et al*., 2006; Weiersbye, 2007). Therefore, it is likely for *Tamarix* to contain greater composition of elements with a high tendency for fuel slagging and fouling compared to *Searsia* or other biomasses that are not planted on an AMD-rich soil. The ash content from both coals were remarkably greater than that of the biomass, as seen in Table 4.6. However, according to Sahu *et al*. (2014) the ash constituents are found to be more responsible for slagging and fouling, rather than the ash quantity. Hence, it is expected that coal will have a lower slagging and fouling propensity compared to biomass despite a higher ash content, and this is due to its lower Fe_2O_3 + CaO + MgO composition and higher alumina and silica composition (Texeira *et al*., 2012; Melissari, 2014; Febrero *et al*., 2015). Moreover, it is expected that the addition of coal will reduce the fouling and slagging propensity of biomass utilized in this study when co-fired with coal.

The calorific values of *Searsia lancea* blends were higher than those of the blends of *Tamarix usneoides*, in line with the higher fixed carbon content in *Searsia lancea*. The blend of *Searsia lancea* in Red soil had a calorific value of 17.31MJ/kg and fixed carbon content of 21.5% while the blend of *Searsia lancea* in West complex had a similar calorific value of 17.27MJ/kg and a fixed carbon content of 21.28%. Meanwhile, the blend of *Tamarix usneoides* from Madala had a calorific value of 16.09MJ/kg and a fixed carbon content of 14.96% while *Tamarix usneoides* from Mispah had a similar calorific value of 16.26MJ/kg and a fixed carbon content of 15.64%. Detailed data on the physicochemical properties of *Searsia lancea* and *Tamarix usneoides* from the four sites and the two coals can be seen on Appendix A.

4.1.5 Physicochemical properties of the tree species and the coal samples

Table 4.7 shows the physicochemical characteristics of *Searsia lancea* and *Tamarix usneoides* blends, discard and run of mine coals. The discard coal utilized as the co-fired fuel has an ash content of 41.95% and calorific value of 16.73 MJ/kg. All the biomass samples utilized are seen with lower ash content and similar calorific value relative to this coal. The fixed carbon content and calorific value of *Searsia lancea* leaves was found to be higher than other parts in that tree (Table 4.7). The volatile matter content of the biomass ranged from 63.90 to 69.40% compared to 20.17 and 22.88% obtained from the discard and run of mine coals, respectively. Many studies have shown the volatile matter content of most biomass species to be greater than 70% (Gil *et al*., 2010; Slopiecka *et al*., 2011; Bada *et al*., 2015). A higher amount of volatile matter in biomass is expected to have a positive impact on the devolatilization process during combustion (Vhathvarothai *et al.*, 2013) while a fuel with a low volatile matter content is associated with low flame stability (Mills, 2016). The highly volatile matter content in biomass will most likely favor the ignition and decomposition of biomass at lower temperatures, thereby generating a flame which is more intense than that of coal at this stage (Gani *et al*., 2005).

Table 4. 7:Physicochemical properties of *Searsia lancea*, *Tamarix usneoides* and coal samples

		Samples										
Analyses		**T1+T3**	**T4+T6**	**T7+T9**	**T11+T12**	**S1+S3**	**S4+S5**	**S7+S8**	**S11+S12**	**S1 Leaves**	**ROM Coal**	**Discard Coal**
Proximate analysis (Wt%, Ad)	Ash	8.18	8.98	8.35	7.48	6.60	3.77	3.94	3.91	4.54	29.42	41.95
	FC	14.61	18.69	14.95	15.54	20.34	21.05	21.28	18.41	20.86	45.48	35.83
	VM	68.96	63.90	68.53	68.52	64.70	66.77	66.45	69.40	66.57	22.88	20.17
	M	8.26	8.45	8.18	8.37	8.37	8.41	8.35	8.30	8.03	2.24	2.06
Ultimate analysis (Wt%, Ad)	C	40.92	42.39	43.55	43.16	45.35	45.16	45.73	45.12	47.93	58.30	48.90
	H	5.91	5.80	6.17	6.38	6.18	6.08	6.20	6.35	5.97	3.19	2.67
	O	35.35	32.58	31.54	32.31	32.96	36.04	35.22	35.78	31.83	4.57	1.93
	N	0.42	0.99	1.05	0.99	0.40	0.44	0.46	0.44	1.60	1.43	1.15
	S	0.96	0.81	1.16	1.31	0.14	< 0.1	< 0.1	< 0.1	< 0.1	0.85	1.34
CV (MJ/Kg)		16.10	16.64	16.53	16.26	17.07	17.31	17.27	17.23	17.75	21.72	16.73

Ad: Air dried basis; VM: Volatile matter; FC: Fixed carbon; M: Moisture; H: Hydrogen; N: Nitrogen; S: Total Sulfur; C: Total carbon; CV: Calorific value and O: Oxygen is by difference [100-(H+C+N+Ash+H_20+S)]

From the ultimate analysis test (Table 4.7), *Searsia lancea* has more total carbon content and hydrogen composition than *Tamarix usneoides* which explains a higher heating value for *Searsia lancea*. The average carbon content for *Searsia lancea* is 45.34% while *Tamarix usneoides* has an

average total carbon content of 42.51%. The hydrogen content of discard (1.83) and run of mine (3.36) were lower than those of biomass. *Tamarix usneoides* had an average oxygen content of 32.95%, while *Searsia lancea* had an average oxygen content of 35.02%. The coal samples had an oxygen content of 1.93% for the discard coal and 4.57% for the run of mine coal. A high oxygen and hydrogen content coupled with low carbon content in biomass compared to coal is responsible for the lower heating value in the biomass. The energy contained in carbon-oxygen and carbon-hydrogen bonds is lower than that of carbon-carbon bonds in coal (Munir *et al*., 2009). Table 4.7 also shows that the *Tamarix usneoides* had an average volatile matter to fixed carbon (VM/FC) ratio of 4.28, while *Searsia lancea* had a VM/FC ratio of 3.31 which are both lower than that of a typical biomass VM/FC of > 5.0 (Tillman, 2000). Both coal samples had a ratio of 0.50 and 0.56 for the run of mine and discard coal, respectively. It is expected that gas-phase oxidation of volatile matter species will be the predominant form of combustion for both *Searsia lancea* and *Tamarix usneoides* (Wang *et al*., 2009). In this study, the leaves were not added to the blends for the combustion test due to the previous findings from Joubert (2017) which stated that the leaves have the ability to accumulate up to 3% sulfur.

The two species are likely to reduce emission when co-fired with coal. As seen in Table 4.7, both species were seen with lower nitrogen and sulfur content compared to coals. The sulfur content in the *Searsia lancea* was found to be less than 0.1, and nitrogen content lower than that of *Tamarix usneoides.* Based on the elemental composition of the two species, it is expected that more NO_x and SO_x will be emitted from the *Tamarix usneoides* combustion that that from the *Searsia lancea*. In addition, it is also expected that the combustion of coal alone will have higher NO_x and SO_x emissions than sole biomass combustion. The co-firing of these coals with *Tamarix usneoides* and *Searsia lancea* may reduce the emissions of NO_x and SO_x.

4.2 Thermal Analysis

4.2.1 Combustion profiles of raw *Searsia lancea, Tamarix usneoides* and coal samples

The differential thermogravimetric (DTG) and thermogravimetric analysis (TGA) thermographs for the *Searsia lancea, Tamarix usneoides* and two different South African coals are depicted in

Figures 4.6 and 4.7. Both curves provide distinctly different reaction regions, as combustion of biomass occurred in stages (Gil *et al*., 2010). Two peaks were observed for biomass combustion compared to one for coal combustion. Bada *et al.* (2015) also observed two peaks during the combustion of raw and thermally treated bamboo. These profiles provide an insight into the combustion and reactivity of the samples.

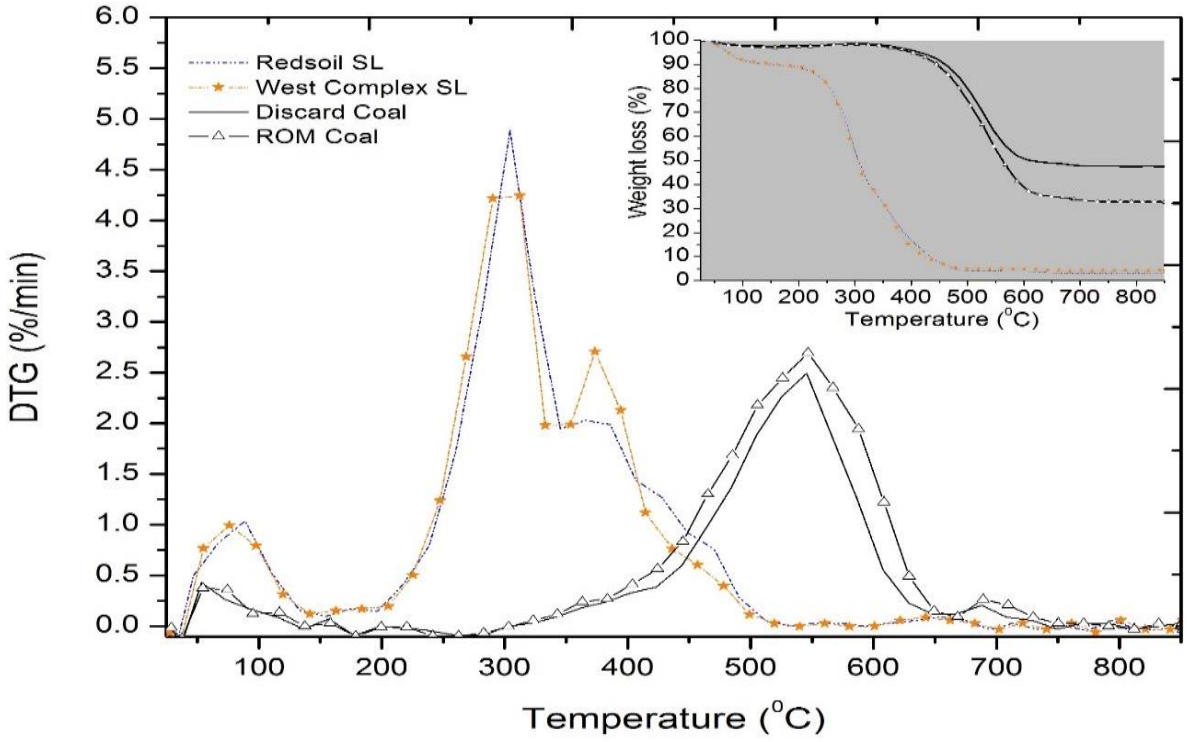

Figure 4.6: DTG curves for *Searsia lancea* planted on two sites with high ash coals

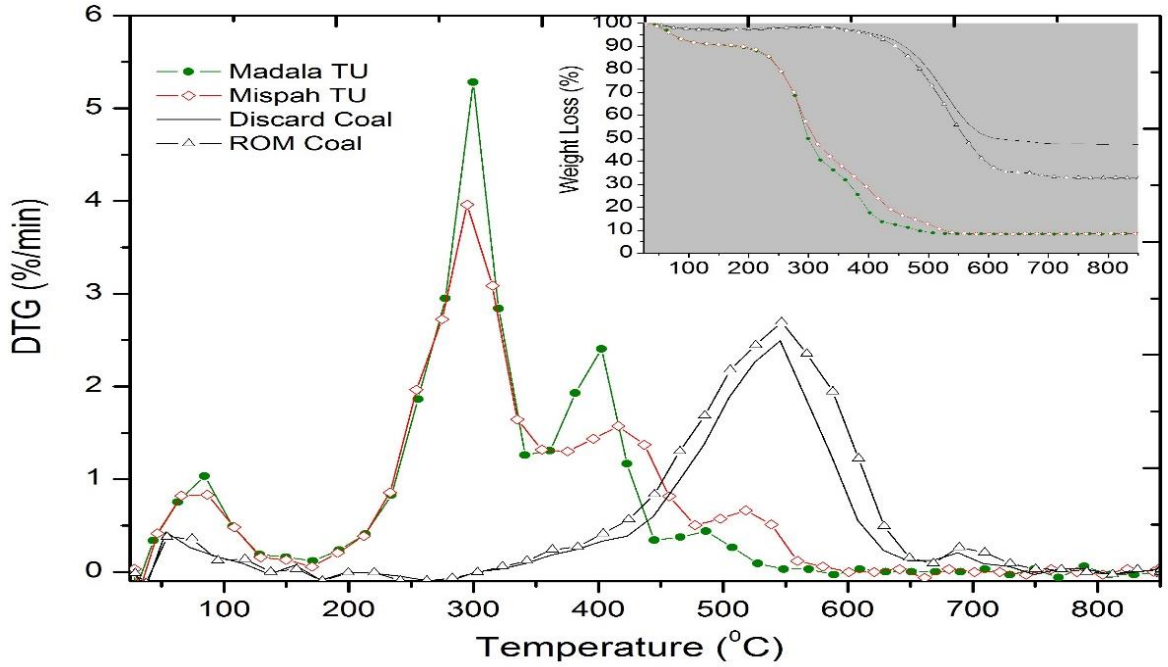

Figure 4.7: DTG curves for *Tamarix usneoides* planted on two sites with high ash coals

The DTG curves in Figures 4.6 and 4.7 show the evaporation of the moisture occurring below the temperature of 100°C for all samples. The initiation of the volatile matters (IT_{vm}) was also seen occurring almost at the same temperature. It was observed that all the *Searsia lancea* samples (Figure 4.6), irrespective of the site harvested, ignited at the same temperature (235°C). *Tamarix usneoides* samples also follow the same trend igniting at a temperature of 233°C. The early ignition of volatiles seen in both biomasses is as a result of their fuel properties, such as volatile matter and oxygen content above 60 and 30%, respectively, compared to the oxygen content in the discard coal at 1.93% (Table 4.7). The *Searsia lancea* planted on the Red soil reaches its peak temperature at around 310°C, with a reactivity of 4.83%.°C /min while the *Tamarix usneoides* samples planted on the Madala site (Figure 4.7) also reaches its peak at a temperature of 301°C, and with a reactivity of 5.3%.°C /min. The second peak observed at the temperature of 376.8°C for *Searsia lancea* harvested from the West complex (Figure 4.6) was more pronounced, indicating higher quantity of lignin in the sample compared to the sample harvested from the Reds soil site. A study conducted by Alvarez *et al*. (2016) had shown that the first peak seen during the combustion of biomass can be attributed to the combustion of cellulose and hemicellulose, while the second peak is related to the combustion of lignin. It can be observed in both Figures (4.6 and 4.7) that the

biomass had a higher reactivity than coal which is in agreement with the findings of Riaza *et al*. (2017).

The coals were ignited at higher temperatures of 410 and 425°C for ROM and discard coal, respectively. This increase in the coal ignition temperature is due to its higher carbon content and more mature maceral components, which resulted in the decrease in the initiation of its fixed carbon (IT_{FC}) and delay in char reactivity compared to that of biomass (Sahu *et al*., 2014). In addition, the discard coal was also seen to have burnt out completely before the ROM coal, due to its lower organic maceral proportion versus ash and low total carbon content (Table 4.7). The difference in the burnout temperatures between the discard coal and both *Searsia lancea* forms was about 220°C. In conclusion, it can be seen below that the biomass is the easiest of the fuel samples to ignite and combust whilst the discard coal is more difficult to combust as it ignites at higher temperature and has the lowest volatile matter content in relative terms (Table 4.7). These findings were similar to the results obtained by Sung *et al.* (2016) and Oladejo *et al*. (2019), where coal was found to have a higher ignition temperature than biomass.

4.2.2 Combustion profiles of *Searsia lancea* and *Tamarix usneoides* harvested from four different AMD rich sites

Figure 4.8 shows the combustion profile of *Searsia lancea* planted and harvested from four different AMD sites; Madala, Red soil, West complex and Mispah. The four *Searsia* samples were seen with similar combustion profiles, similar ignition and burnout temperatures ranging from 511 or 523°C. The *Searsia* harvested from the Mispah was the most reactive biomass, followed by the tree harvested from the Red soil sites, while those planted on Madala and West complex had the least reactivity. All the trees also displayed two combustion peaks as expected of biomass.

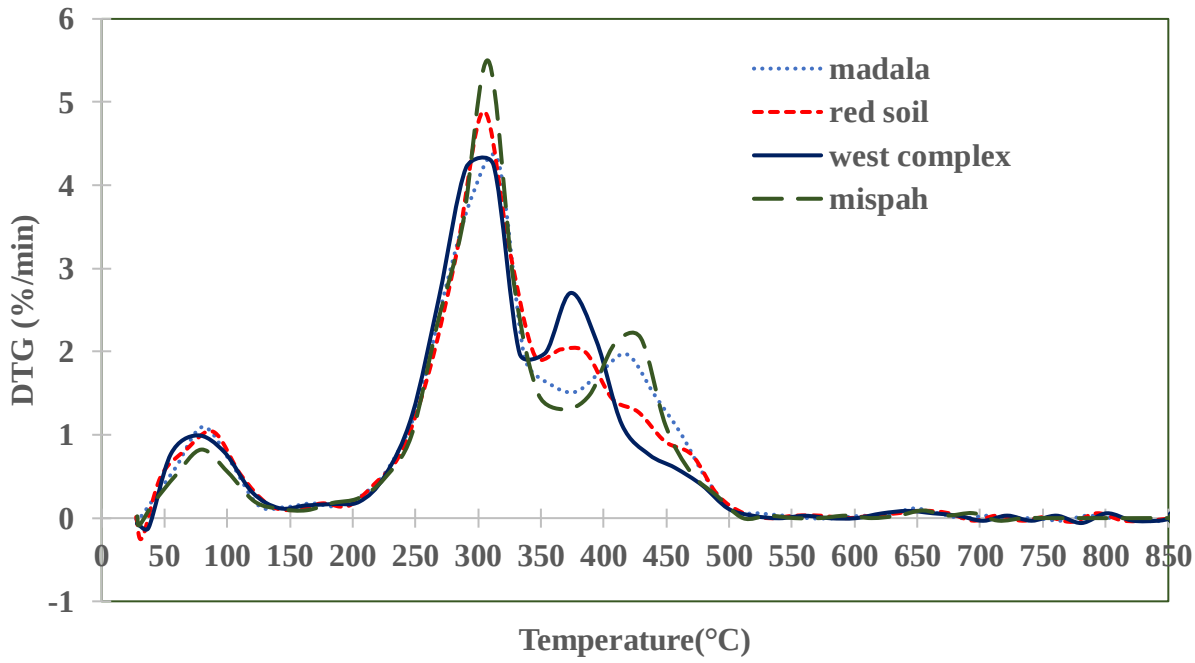

Figure 4.8: Combustion characteristics of *Searsia lancea* on four AMD rich sites

The combustion profiles of raw *Tamarix usneoides* harvested from four different AMD sites; Madala, Red soil, West complex and Mispah are also presented in Figure 4.9. The main critical temperatures from the thermograph are presented again in Table 4.8. The combustion profiles for the four samples followed the same trend, with the *Tamarix* planted on Madala site having the highest reactivity with the rate of mass change of 5.28%/min. The sample was also seen with a more pronounced second peak at a temperature of about 400°C. According to Table 4.8, the same sample was also seen with the lowest burnout temperature out of all *Tamarix* harvested from the four sites. The peak temperature for *Tamarix* in all sites ranged from 300 to 315°C while the burnout temperature ranged from 548 to 580°C. In summary, it should be noted that the *Searsia lancea* harvested from the Mispah site and *Tamarix usneoides* harvested from the Madala site are better fuels, in terms of reactivity compared to all other samples.

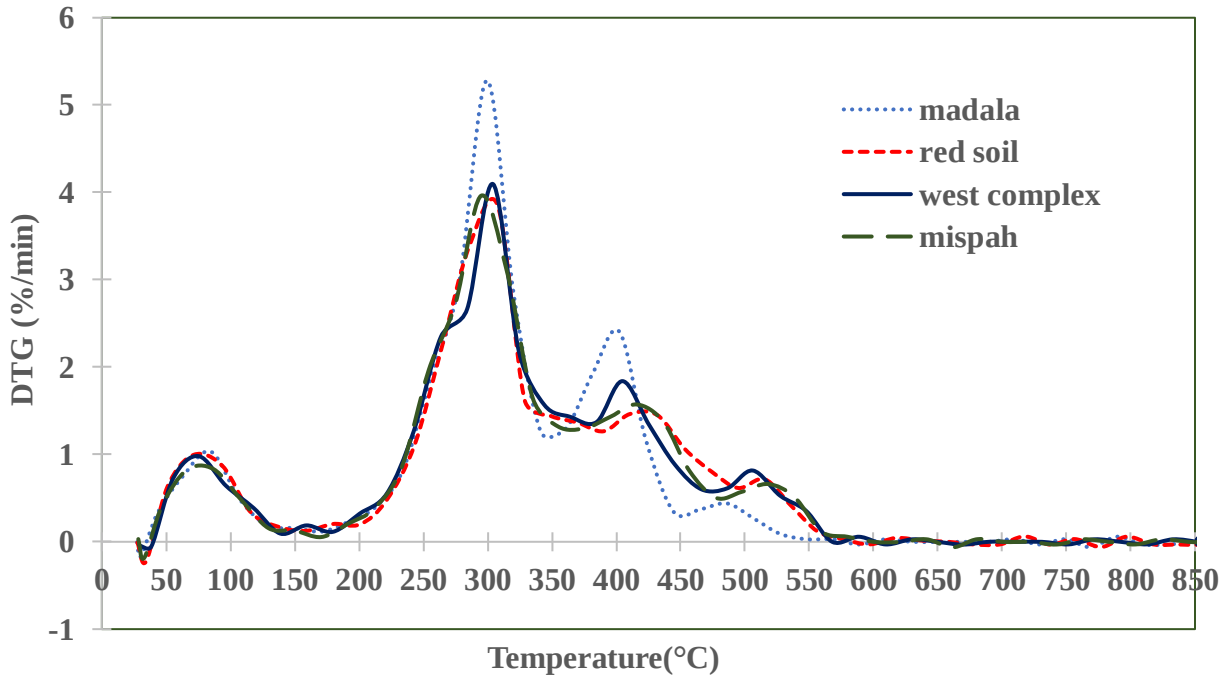

Figure 4.9: Combustion characteristics of *Tamarix usneoides* on four AMD rich sites

Table 4.8: Ignition, peak and burnout temperatures of 100% *Tamarix usneoides* and 100% *Searsia lancea* from four different sites

Site	*Tamarix usneoides*			*Searsia lancea*		
	(IT_{VM}) (°C)	PT (°C)	BT (°C)	(IT_{VM}) (°C)	PT (°C)	BT (°C)
Madala	192	300	548	146	316	523
Red soil	180	308	577	176	304	512
West complex	159	304	568	163	312	519
Mispah	191	315	580	184	308	511

IT_{VM}: Initiation of volatile matter, PT: Peak temperature, BT: Burnout temperature

4.2.3 Co-combustion of *Searsia lancea* planted on Redsoil and West complex with coal discard

The DTG curves for the coal discard in Figures 4.10 and 4.11 present a single reaction profile after the moisture was released compared to other biomass samples with two different and distinctive reaction stages. The initiation of the fixed carbon (IT_{FC}) for the raw *Searsia lancea* harvested from the Redsoil (Figure 4.10), was seen occurring at the lowest temperature of 241°C, similar to the observation made by Bada *et al*. (2014) and Makwarela *et al*. (2017) on the combustion of different raw bamboo species. The same species harvested from the West complex site (Figure 4.11) has an ignition temperature of 248.8°C. In Figure 4.10, the raw biomass sample has the highest peak temperature of 305.3°C, while *Searsia lancea* (Figure 4.11), has a peak temperature of 312.8°C. As the coal percentage in the blend increases, the peak for the combustion of biomass/coal discard decreases, signifying the influence of reducing biomass volatile matter on fuel reactivity. In addition, this also has an influence on the burn-out temperature, with a decrease in the burnout temperature between discard coal and raw biomass at 141°C. According to the thermograph in Figure 4.10, the total decomposition of the hemicellulose, cellulose and lignin in the raw *Searsia lancea* occurs between a shorter temperature range, namely between 198.1 to 512°C, compared to other biomass/coal blend samples.

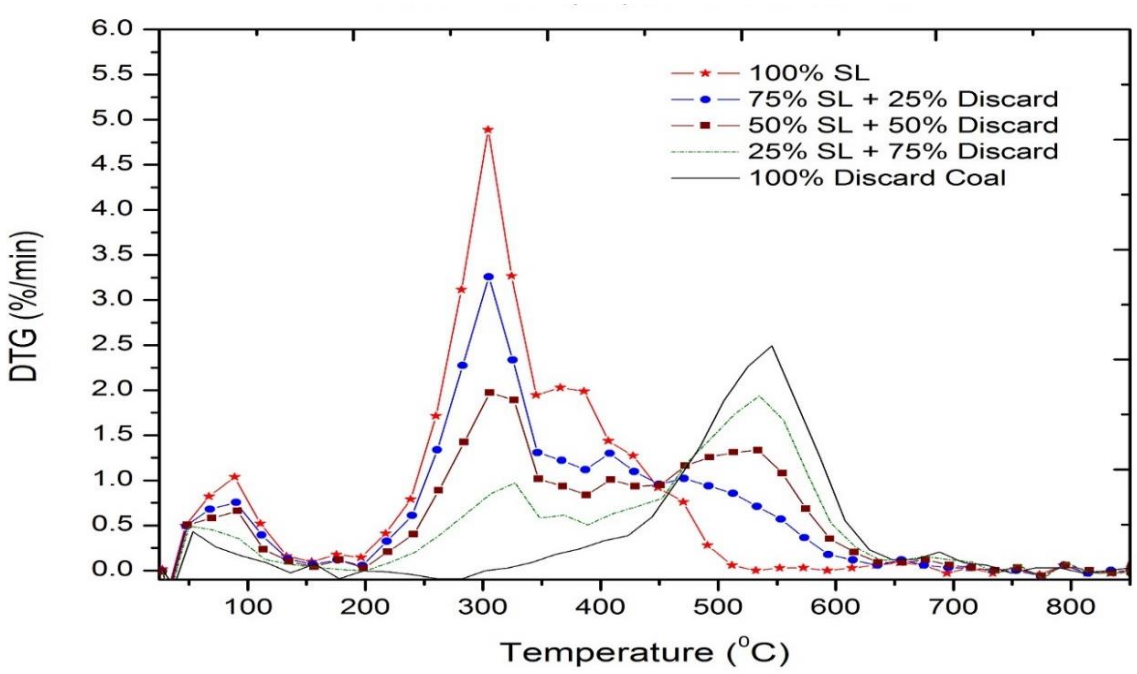

Figure 4.10: DTG curves for *Searsia lancea* planted on Red soil site with discard coal

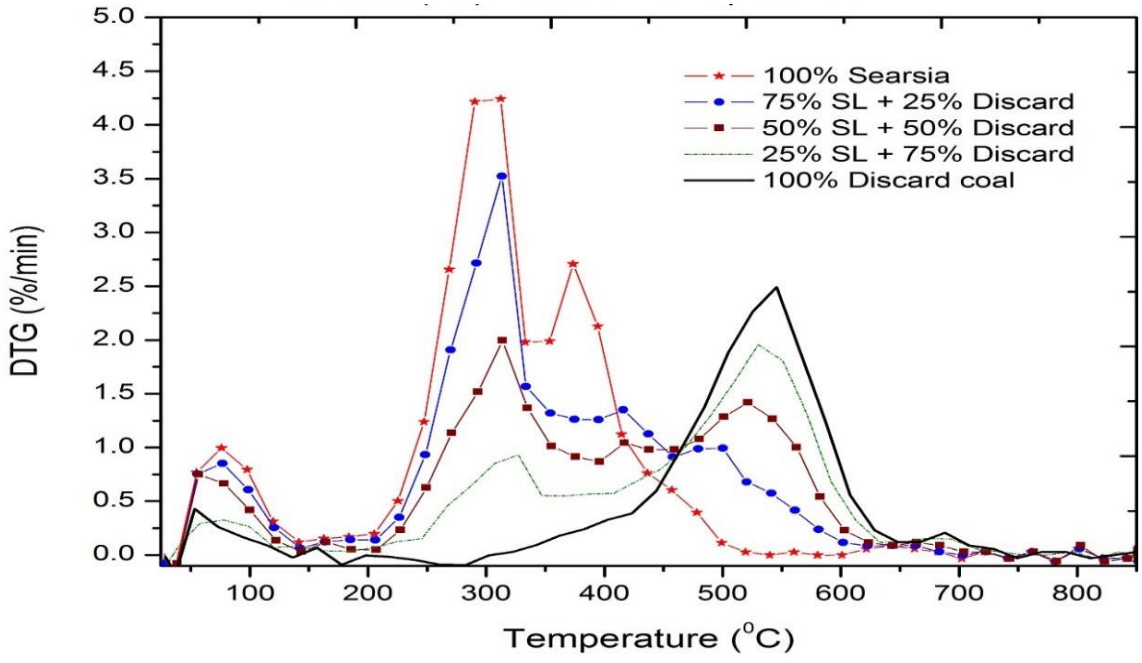

Figure 4.11: DTG curves for *Searsia lancea* planted on West complex site with discard coal

Similar trends are also observed in Figure 4.11 for *Searsia lancea* harvested from the West complex (AMD affected site). The ignition temperature of the raw biomass sample was 246°C compared to discard coal of 425°C while the peak burning temperatures for biomass and coal were 313 and 550°C, respectively. These reductions in ignition, peak and burnout temperatures observed in this investigation are obviously due to the co-firing effect of biomass with discard coal. For both Figures (4.10 and 4.11), the blend of 25% *Searsia lancea* + 75% coal was seen with the highest underlying peaks after coal, signifying that the weight ratio of individual fuel in the blend has a significant influence on the combustion process which in turn, may influence total combustion efficiency when blended together. In conclusion, both forms of *Searsia lancea* are found to be more efficient in combustion than the discard coal, while the thermographs in Figure 4.11 present *Searsia* with a higher second combustion peak, indicating a higher solid carbon and therefore higher lignin decomposition. The latter condition is likely to be linked to the characteristic of the tree in withstanding contaminants in the soil in which that plant grew and attaining similar/higher fixed carbon in all compartments (Table 4.4).

Furthermore, as can be seen in Figures 4.10 and 4.11, as the percentage biomass in the blend increases the initiation of the volatiles and peak burning temperature of the fixed carbon in the discard coal profile moves lower towards that of the biomass species. It is suggested that, with volatile matter content greater than 60% in both biomasses, the co-firing of these biomasses with the discard coal utilized in this study appears to have led to increasingly lower temperatures for release and combustion of volatiles in the coal discard. It is suggested that this is likely to provide a more stable flame for the combustion process in a boiler (Ren *et al*., 2017). The combustion and co-combustion profiles of *Searsia lancea* and *Tamarix usneoides* from all four AMD sites with discard and run of mine coals can be seen in Appendix B.

4.2.4 Co-combustion of *Tamarix usneoides* planted on Mispah and Madala sites with coal discard

The co-combustion of discard coal and *Tamarix usneoides* harvested from two different AMD affected sites, Mispah and Madala, at 25%, 50% and 75% by wt.% was investigated and depicted in Figures 4.12 and 4.13. These figures provide an insight into the combustibility of the *Tamarix usneoides*, coal and their blends. The thermograph in Figure 4.13 shows that the combustion of 100% *Tamarix usneoides* planted on Madala site has a higher reactivity of 5.3%. °C/min compared to the same species of *Tamarix* harvested from the Mispah site (Figure 4.12) with a reactivity of 3.95%. °C /min. It is also noted in the DTG curves from Figure 4.12 and 4.13 that the co-firing of 25%, 50% and 75% biomass samples in the coal blends have higher reactivities occurring at lower temperature regions than the discard coal sample.

An improvement was made to the combustion characteristics of the discard coal when blended with both biomass samples. There was a decrease in the devolatilization and ignition temperature of the blend when discard coal was co-fired with T*amarix usneoides*, *i.e.* from 424°C for the discard coal to approximately 222°C in the co-fired blend. This decrease in ignition temperature as the percentage ratio of biomass in the blend increases is once again considered to be due to the higher quantity of combustible volatiles being emitted from the *Tamarix usneoides* component in the blend which would also be likely to have an impact on the earlier ignition of the coal discard component. Such modifications in the volatilization rate of the different fuels are also reported by Sahu *et al*. (2014). It is also of interest to note that three almost equal peaks of maximum combustion rate exist when 50% biomass is blended with the discard coal. This extends the heat production rate over time and temperature ranges from 330 to 550°C.

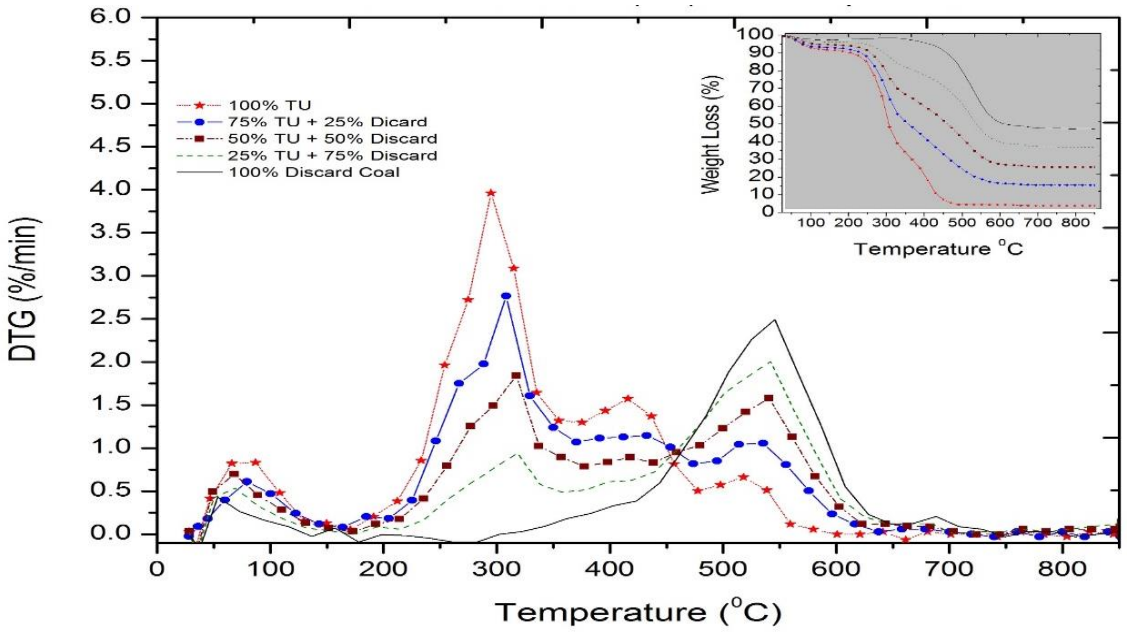

Figure 4.12: DTG curves for *Tamarix usneoides* planted on Mispah site with discard coal

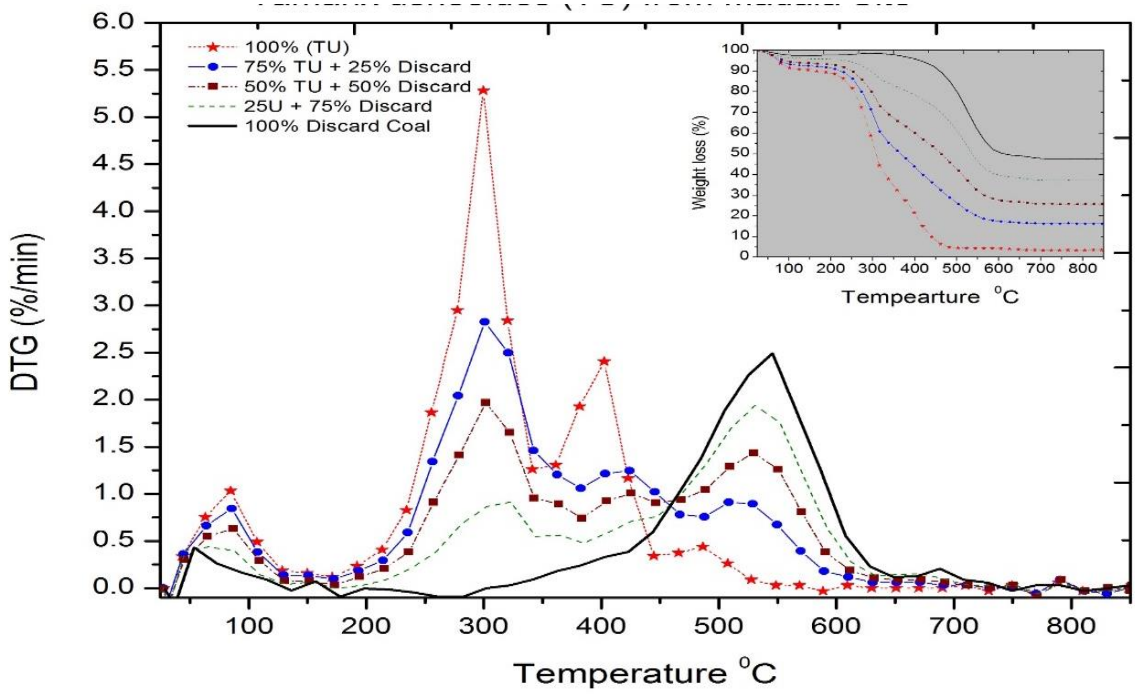

Figure 4.13: DTG curves for *Tamarix usneoides* planted on Madala site with discard coal

From the TG profiles embedded in the top right corners of both Figures 4.12 and 4.13, it was observed that as the biomass weight proportion in the blend increases, the percentage weight residue after combustion decreases. This decrease in combustion residue might be as a result of the heat released from the modification to the volatilization rate of the blends as biomass ratio increases, thereby leading to an increase in reactivity at a lower temperature region for the blends. The 75% *Tamarix* + 25% coal from Mispah site was seen with a weight loss residue of 19.5%, while the 75% *Tamarix* + 25% coal from Madala has a residue of 17.5% after burnout.

The conclusion drawn from these observations is that biomass addition does improve the combustion efficiency of the high ash discard coal utilized in this study. In addition, the difference in the AMD concentration between the two sites does not appear to have had an obvious major effect on the energy and combustion characteristics of the *Tamarix usneoides* samples utilized in this study, apart from the fact that the *Tamarix usneoides* sample planted on Madala was shown to exhibit a 2% higher reactivity and weight loss rate than that grown on the Mispah site. The *Tamarix usneoides* sample planted on the Madala site underwent a weight loss of 50.1% compared to 42.5% from the *Tamarix usneoides* planted on Mispah site at a peak temperature of 400°C.

4.2.5 Influence of discard coal blend on combustion efficiency of *Searsia lancea and Tamarix usneoides* planted on Madala sites

The difference in the combustion efficiency between the two plant species planted on the Madala site was determined from their thermographs. The aim was to provide an insight into the effective utilization of these biomass fuels and the discard coal. The combustion efficiency of the raw plant samples and the coal/biomass blends were determined at four temperatures, namely, at 300°C, 400°C, 500°C and 600°C. The percentage of material combusted (η) from the total combustible sample in each fuel was calculated from the expression provided in equation 4.2, with the aid of data obtained from the TGA & DTG analyses.

$$\eta = \left(\frac{M_{107} - M_T}{M_{107} - M_{BT}}\right) \times 100\% \qquad (4.2)$$

Where, M_T is the combustible mass available for combustion at any temperature, M_{BT} is the residue mass at the burnout temperature for individual fuel, M_{107} is the sample dry mass after moisture released at 107°C.

Combustion efficiency (η) from Equation 4.2 was plotted versus ratio of the coal in the blend on x-axis, with the ration 0.0 representing 100% raw biomass. The x-axis in Figure 4.14 denotes the ratio of the coal in the blend, with the ratio of 0.0 representing 100% raw biomass. It can be observed that at 0.0 on the x-axis, for the temperature of 300°C, the *Tamarix usneoides* was shown to have a combustion efficiency of 8.32% higher than that obtained from *Searsia lancea*. The same raw *Tamarix* sample at 300°C, has a combustion efficiency of 50.4% compared to the high ash discard coal utilized (0%). Raw *Tamarix* was seen to exhibit the highest combustion efficiency as the temperature increases, with 87.3% at 400°C, compared to the discard coal with only 3.08%. Also noted was the fact that, as the ratio of the coal in the blend decreases for any temperature, i.e. from 1.0 on the x-axis to 0.0, the amount of biomass burnt increases, i.e. the combustion efficiency of the blend increases. The increase in biomass functional groups and the presence of more combustible volatile matter derived from the biomass samples in the blend are considered to be responsible for the improved combustion of the discard coal.

Figure 4.14 also presents the influence of temperature on the combustion efficiency of the different plant species with coal, in raw and varying blended mixtures. It can be seen that, at a blend of 75% coal + 25% biomass, there is an increase in combustion efficiency from 14% for *Searsia lancea* at 300°C to 96.2% at 600°C. *Tamarix*, on the other hand, shows a marginally higher efficiency when raw, in lower biomass proportion in the blends, and at lower temperatures but it follows a similar efficiency pattern to the *Searsia* samples thereafter. Both species are also noted to have better combustion efficiency compared to the discard coal between the temperature of 300-500°C, but similar efficiency with the discard coal at 600°C. It is concluded that both plant species can be co-fired with this discard coal in a power plant.

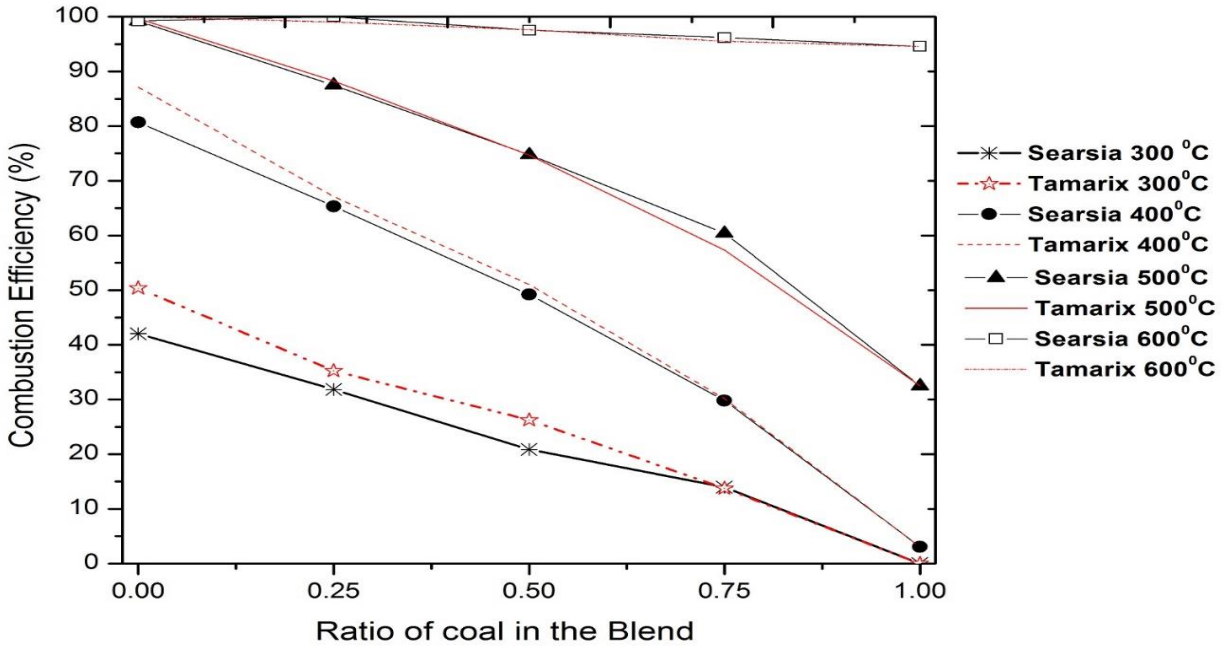

Figure 4.14: Combustion efficiency curve for *Searsia lancea*, *Tamarix usneoides* and discard coal.

4.3 Reaction kinetics

A kinetic study on the combustion of *Searsia lancea* and *Tamarix usneoides*, solely and when co-fired with ROM coal and discard coal was conducted. In this study, the Coats-Redfern method was used to determine the activation energies of the biomass and the coal-biomass combusted at different proportions. The kinetic parameters were determined assuming single separate reaction for a particular stage of thermal conversion. A first order reaction was assumed, meaning an expression of $f(x) = 1 - x$ was used. The activation energies of 100% biomass were compared with those from 100% discard coal and 100% ROM coal. The effect of coal inclusion (at 25%, 50% and 75%) on the kinetic energy of the coal-biomass blend was also investigated. In addition, the activation energies of both *Searsia lancea* and *Tamarix usneoides* harvested from different sites were determined and compared with each other. The DTG curves from the combustion and the co-combustion of the samples, provided the data used in determining the kinetic parameters for all samples, as shown in Figure 4.15.

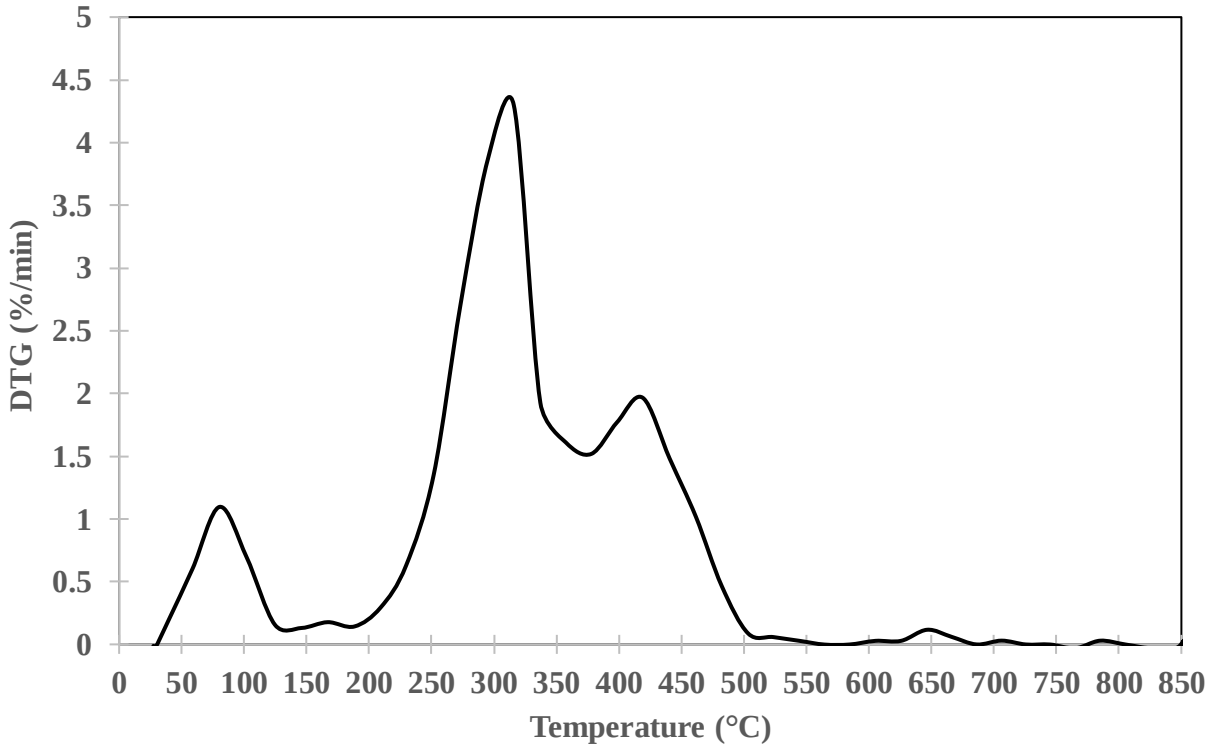

Figure 4.15: DTG curve for 100% *Searsia lancea* planted on Madala site

The plots in Figures 4.16 and 4.17 below were obtained from the first and second combustion stage reactions of 100% *Searsia lancea* planted on Madala site (Figure 4.15) using the Coats-Redfern model under a selected temperature range. Straight lines with high correlation co-efficient of linear regression were obtained. Firstly, the activation energy was calculated from the slope of the line $-E/R$, and the pre-exponential factor was calculated by taking the temperature at which $m_t = (m_i + m_f)/2$ as the intercept of equation (3.13). The same procedure was used to calculate the activation energies of all the other samples.

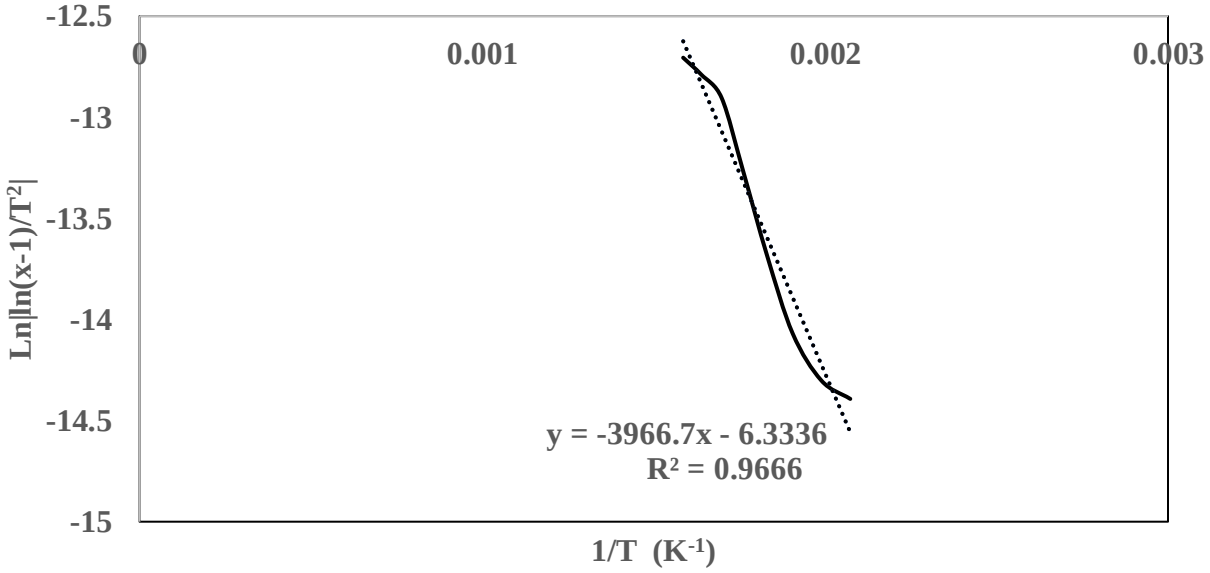

Figure 4.16: Coats-Redfern plot for first stage combustion of *Searsia lancea* planted on Madala site.

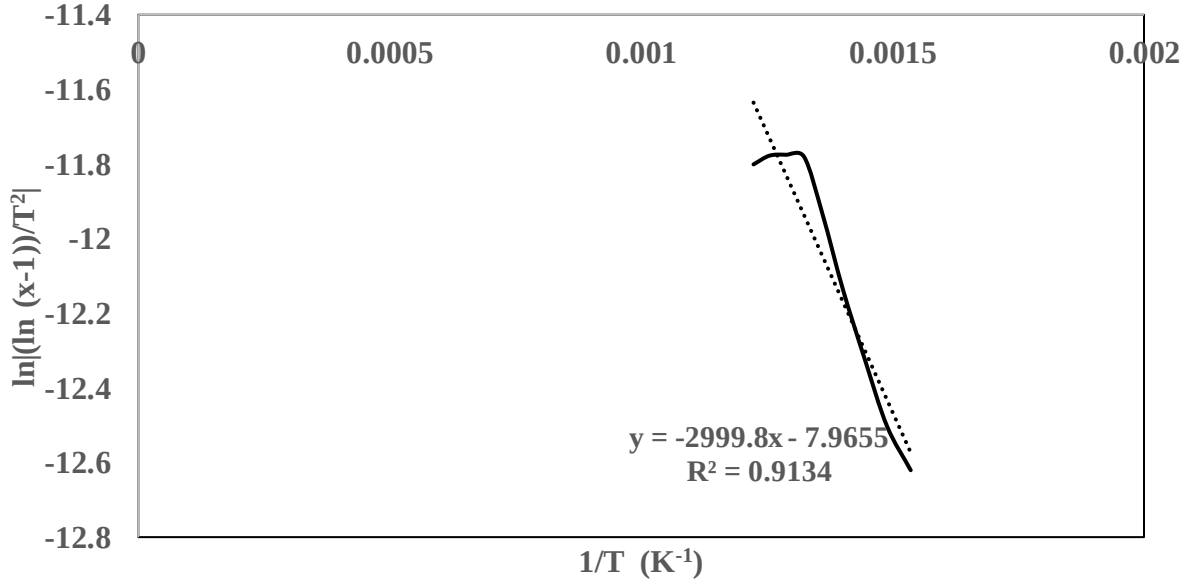

Figure 4.17: Coats-Redfern plot for second stage combustion of 100% *Searsia lancea* planted in Madala site.

Kinetic parameters from the combustion and co-combustion of all samples

The activation energies, pre-exponential factors and the correlation co-efficients of 100% *Searsia lancea*, 100% *Tamarix usneoides*, 100% ROM coal, 100% discard coal, along with their coal-biomass blends were determined using Coats-Redfern methods. The kinetic parameters depicted in Table 4.9 are from biomass species (*Searsia* and *Tamarix*) harvested from the Madala sites. The kinetic parameters for the two coals was determined under a single stage reaction, while other samples were determined by assuming a two-stage reaction under a selected temperature range.

Table 4.9: Kinetic parameters of biomass, coal and their blends

Sample	**First stage**			**Second stage**		
	E(kJ/mol)	**A (s^{-1})**	**R^2**	**E (kJ/mol)**	**A (s^{-1})**	**R^2**
100% S	32.98	1×10^7	0.9666	24.94	2×10^6	0.9134
75% S + 25% D	33.01	1×10^7	0.9652	21.05	1×10^6	0.9798
50% S + 50% D	28.52	4×10^6	0.9795	27.55	4×10^6	0.9514
25% S + 75% D	22.69	2×10^6	0.9737	39.96	3×10^7	0.9598
100% T	37.39	2×10^7	0.9433	26.23	3×10^6	0.9775
75% T + 25% D	26.08	3×10^6	0.9414	14.86	7×10^5	0.9959
50% T + 50% D	21.63	1×10^6	0.9343	11.22	1×10^6	0.9983
25% T + 75% D	20.61	1×10^6	0.9511	41.69	5×10^7	0.9694
ROM coal				60.16	3×10^9	0.9853
Discard coal				64.51	1×10^9	0.9720

S: *Searsia lancea*, T: *Tamarix usneoides*, D: Discard coal, ROM: Run of mine

The activation energies for the 100% biomasses were found to be lower than the activation energies for the coals utilized in this study (Table 4.9), indicating that less energy is required for biomass combustion than for coal combustion. This is in line with the findings of other authors. Vhathvarothai *et al*. (2013) found the activation energies of Cypress wood chips and macadamia nut shells to be lower than that of coal when they investigated thermal behavior of biomass and coal during co-combustion. The lower activation energies values obtained from the combustion of biomass could be attributed to its high volatile matter and lower carbon content compared to coal. The activation energy for the first stage combustion of *Searsia lancea* was 32.98 and 24.94 kJ/mol for its second stage combustion reaction. *Tamarix usneoides* had an activation energy of 37.39 and 26.23 kJ/mol in its first and the second stage combustion, respectively. Bada *et al*. (2015) obtained

activation energies in the range of 11.24-31.60 kJ/mol which is similar to this when they combusted raw *bambusa balcooa*. Subsequently, Alvarez *et al*. (2016) found an activation energy range of 14-86 kJ/mol for 28 different biomass samples. In addition, Cao *et al*. (2017) obtained a range of 5 to 54 kJ/mol for different sizes of straw. Recently, Boumanchar *et al*. (2019) reported average activation energies of 9.54, 44.27 and 13.34 kJ/mol in drying, devolatilization and char combustion, respectively for different biomass wastes. Meanwhile, ROM coal and discard coal had an activation energy of 60.16 and 64.51 kJ/mol, respectively. This is expected, as coal is required to take longer reaction time to oxidize and at much higher temperature compared to biomass with much higher percentage of oxygen and low carbon content, as reported in Table 4.7. A similar activation energy value obtained in this study was reported by Bada *et al*. (2015) for a high ash South African coal. Prior to that, Tahmasebi *et al*. (2013) had found an average activation energy of 37.83 kJ/mol for coal.

It can be noted that at 25% biomass in the blend, the first stage activation energy (E_a) was lower than the second stage activation energy, while as the biomass percentage increases further, the second stage activation energy reduces. Alvarez *et al*. (2016) found that less energy is required in the combustion of lignin and carbon compared to the required energy needed for the combustion of cellulose and hemicellulose, which occurs under the first stage of combustion. In addition, their findings are also in agreement with the study conducted by Wang *et al*. (2016) on the co-combustion of coal and biomass. Wang *et al*. (2016) found that more energy or higher E_a is required in the combustion of the volatiles (volatile combustion), which occurs at the lower temperature environment, compared to the char combustion. This also explained why higher E_a is required under the first stage combustion to combust the 75% biomass inclusion compared to that of 50% and 25% in this study. A study conducted by Chen *et al*. (2015) also confirmed that activation energies in the lower temperature ranges to be higher than those in higher temperature ranges during biomass co-combustion in a fluidized bed reactor.

4.4 Ash analysis

4.4.1 Concentrations of major oxides and chlorine in biomass, discard coal and their blends

The concentration of major and minor elements was obtained from the XRF analysis conducted on the biomass ash, discard coal ash and ash obtained from the coal/biomass blends. The compositions of major oxides: Fe_2O_3, CaO, MgO, K_2O, Na_2O, SiO_2, TiO_2, Al_2O_3 and SO_3^{2-} were then calculated and listed in Table 4.10 below. Vasilev *et al.* (2014) defined major elements in the ash as those with concentrations greater than 1%, while the minor elements are considered to range from 0.1 to 1%. SiO_2, Al_2O_3, Fe_2O_3 and CaO are the predominant oxides found in the discard coal utilized in this study, each with a percentage composition of 50.87%, 36.18%, 9.42% and 6.47% in that order. A study by Mahlaba *et al*. (2011) on physical, chemical and mineralogical characterization of hydraulically disposed fly ash from SASOL Synfuels also found SiO_2, Al_2O_3, Fe_2O_3 and CaO to be the major oxides in South African coal ash. Further studies by Akinyeye *et al*. (2016) on the analysis of coal ash from an electrostatic precipitator of a South African coal power station and Maledi (2017) on the analysis of South African coal discard also found similar oxides to make up the major part of coal ash. Silicon and aluminum are the main inorganic elements in the ash which may indicate abundance of quartz and aminosilicate minerals in the discard coal sample (Akinyeye *et al*., 2016).

Table 4.10: Composition of major oxides and chlorine in *Searsia lancea*, *Tamarix usneoides*, discard coal and their blends

	Composition of major oxides and chlorine (wt.%)									
Sample ID	**Fe_2O_3**	**CaO**	**MgO**	**K_2O**	**Na_2O**	**SiO_2**	**TiO_2**	**Al_2O_3**	**SO_3^{2-}**	**Cl**
100% D	9.42	6.47	1.01	1.09	1.38	50.87	2.51	36.18	3.26	<0.01
100% S	3.70	32.17	16.12	12.19	2.52	12.10	0.38	4.45	8.51	0.47
100% T	0.83	18.87	13.26	5.30	7.45	4.24	0.08	1.32	38.68	0.18
75% S + 25% D	4.64	13.71	5.90	4.43	1.74	36.85	1.73	24.71	13.08	0.07
50% S + 50% D	4.51	8.48	2.72	2.46	1.51	43.18	1.95	30.27	9.96	0.02
25% S + 75% D	4.29	5.90	1.46	1.34	1.23	43.83	1.95	30.92	6.23	<0.01
Tamarix leaves	0.23	28.22	17.79	6.23	16.25	1.59	0.04	1.21	32.59	2.85
Searsia leaves	2.94	26.89	15.43	27.99	1.67	7.91	0.15	2.33	13.53	1.13

S: *Searsia lancea*, T: *Tamarix usneoides*, D: Discard coal

The Fe_2O_3 concentration reported in this research (9.42%) is relatively higher than those observed by other authors, indicating a higher presence of minerals associated with iron in the discard coal leading to a higher Fe_2O_3 content than in the bituminous and sub-bituminous coals used by other authors (Mahlaba *et al*. 2011; Akinyeye *et al*., 2016). The high Fe_2O_3 content together with the high sulfur content in the discard suggests the presence of pyrite (Fe_2S) minerals in this coal. In addition, the presence of high Fe may also come from siderite ($FeCO_3$), chlorite ($Fe_5Al_2Si_3O_{10}(OH)_8$) and jarosite ($(Na,K)Fe_3(SO_4)_2(OH)_6$) minerals (Maledi, 2017). A study by Kotelo (2013), also shows that the presence of basic oxides (CaO and MgO) in the ash may be due to the high concentration of Calcite ($CaCO_3$) and dolomite ($CaMg(CO_3)_2$) minerals in the coal. The presence of TiO_2 suggests that discard coal contains rutile and/or anatase minerals. Rutile accounts for most of the TiO_2 in South African coal while anatase only contributes about 1-2 wt.% (Maledi, 2017).

Alkali metals are known to be a major contributor to fouling and slagging in boilers (Sahu *et al*., 2014). Both potassium and sodium are found to lower the melting point of ash and, thus can increase ash deposition and fouling of boiler tubes (Melissari, 2014). Biomass had higher amounts of Na_2O and K_2O than discard coal, suggesting that the use of biomass in boilers may be detrimental to boilers. The addition of coal used in the study during co-firing reduces the concentrations of Na_2O and K_2O from 12.19 and 2.52% in 100% *Searsia* to 1.34 and 1.23%, respectively in a sample which had 75% coal discard + 25% biomass (Table 4.10). The ash from *Searsia lancea* contained lower concentration of Na_2O than that of *Tamarix usneoides*. The ash obtained from the *Tamarix* leaves was found to possess higher Na_2O, SO_3^{2-}, Cl and Ca than *Searsia* leaves. This supports the findings of Weiersbye and Witkowski (2007), that high levels of salt are absorbed by the leaves of *Tamarix*. Therefore, this result justifies why the leaves from both species, especially *Tamarix* were not added to the tree compartments during blending. Another reason for omitting leaves in the tree blends was high levels of chlorine which are known to cause corrosion in boilers (Texeira *et al*., 2012). The blends of *Tamarix* and *Searsia* at different coal ratio also had higher chlorine levels compared to the discard coal, with less composition than those in the leaves. The presence of chlorine can be attributed to high levels of NaCl absorbed in the leaves of *Tamarix*. The addition of coal reduced the concentration of chlorine from 0.47% in 100% biomass sample to 0.01% in a sample with 75% discard coal + 25% biomass inclusion. In general Na, Cl, S, Ca

and K are all mostly deposited in the leaves than in any other part of the trees (Vasilev *et al*., 2014). Hence, with these high concentrations of alkali metals in the leaves, the combustion of this compartment is likely to be detrimental to any combustion technology.

The ash obtained from *Searsia lancea* was found to contain lower SO_3^{2-} concentrations compared to *Tamarix usneoides*. The high percentage concentration of sulfur observed in *Tamarix* is expected as the literature has shown that this species does have the capability to hyper-accumulate sulphates and some heavy metals (Weiersbye *et al*., 2006 and Weiersbye and Witkowski, 2007). Interestingly, coal ash had less SO_3^{2-} than both *Searsia lancea* and *Tamarix usneoides* blends. This is counterintuitive as discard coal had more elemental sulfur than both *Searsia lancea* and *Tamarix usneoides* in ultimate analysis. The results could mean that most of the sulfur in the coal discard are converted into SO_x as compared to the biomass. According to Rokni *et al*. (2018), sulfur content in the ash depends more on the sulfur retention ability than actual sulfur content of the fuel. Addition of coal to biomass reduced the concentrations of Na, Cl, S and Ca. The result obtained in this study is in line with the findings of Texeira *et al*. (2012), where Al, Fe and Ti in biomass had lower concentrations than in coal.

4.4.2 Concentrations of trace elements in biomass, discard coal and their blends

Vasilev *et al*. (2014) classifies trace elements as those elements with concentrations between 0.1 and 1%. The determination of these trace elements is important as elements like As, Co, Cr, Cu, Hg, Mn, Ni, Sb and V can be potentially toxic (Vasilev *et al*., 2014). Both the volatile parts of trace elements and the non-volatile parts can cause environmental issues. While the volatiles can be emitted to the atmosphere, the non-volatiles contained in coarse ash may lead to problems when used for different application, such as fertilizer in agriculture and waste water treatment (Vasilev *et al*., 2015). The concentrations of trace elements in the ash of *Searsia lancea*, *Tamarix usneoides*, discard coal and their blends can be seen in Table 4.11. The concentrations of As, Co, Cr, Cu, Mn, Nd, Rb and Zr decrease with an increase in the amount of discard coal in the blend. The concentrations of Hg and Se were similar in all samples ranging between 1 and 2 ppm. No relationship was observed between the concentrations of Ni and V with the amount of discard coal in the blend. Demirbas (2007) found that the concentrations of As, Cd, Cr, Cu, Pb, and Hg in

various biomass species to range from 0.72 and 92.49 ppm. The maximum concentrations of Cu and Cr in *Searsia lancea* were 918 and 529 ppm, respectively. This was much higher than the concentrations in discard coal and biomasses investigated by Demirbas (2007). The higher concentrations of trace elements in *Searsia lancea* and *Tamarix usneoides* may be attributed to the fact that they were planted in an AMD contaminated sites. In this research, *Searsia lancea* was found with the higher concentrations of trace elements than *Tamarix usneoides*.

Table 4.11: Concentration of trace elements in *Searsia lancea*, *Tamarix usneoides*, discard coal and their blends

	Trace element concentration (ppm)							
	Discard coal	***Searsia* blend**	***Tamarix* blend**	**75% S + 25% D**	**50% S + 50% D**	**25% S + 75% D**	***Searsia* leaves**	***Tamarix* Leaves**
As	13	10	1	9	5	4	1	0
Ba	713	125	48	414	516	512	57	7
Br	1	63	20	12	3	1	265	146
Ce	71	2	9	44	36	50	3	2
Co	14	50	15	30	19	16	3	12
Cr	254	529	141	303	253	219	1320	55
Cu	67	918	398	223	146	81	156	107
Ga	52	4	5	35	41	42	11	3
Hg	2	2	1	2	1	2	1	1
Mn	437	2316	1988	943	509	347	4115	2927
Mo	10	17	6	10	7	7	33	4
Nb	39	5	2	27	31	30	4	1
Ni	200	80	85	173	186	166	74	56
Nd	95	320	104	95	75	58	97	25
Pb	57	540	25	344	136	62	93	11
Rb	50	65	56	55	49	43	98	66
Sb	4	19	22	11	9	7	25	12
Se	1	1	0	2	2	2	1	1
Sn	18	26	33	20	17	14	36	20
Sr	1285	477	337	783	819	773	220	191
Th	47	17	7	34	36	34	9	4
V	192	89	11	180	209	165	65	3
Y	2	118	37	12	13	1	25	2
Zn	65	13	7	46	50	48	5	3
Zr	48	496	747	156	82	61	2205	542

S: *Searsia lancea*, D: Discard coal

4.4.3 Fouling and slagging in biomass, discard coal and their blends

The biomass ash was analyzed for fouling and slagging potentials, which are cardinal when co-firing biomass with coal in boilers. Table 4.12 below shows the fouling and slagging indices of ashes of biomass, biomass leaves, coal-biomass blends and discard coal. The biomass samples that were analyzed for fouling and slagging propensity were taken from the West complex site for both *Searsia lancea* and *Tamarix usneoides.* The leaves, biomass blends without leaves and discard coal were ashed before being analyzed for their elemental composition. The data obtained from their elemental composition was used in determining the slagging and fouling indices of the samples.

Table 4.12: Fouling and slagging indices of biomass and coal ashes

Sample	Fouling index	Slagging index
Tamarix leaves	544	3.32
Searsia leaves	214	14.9
100% *Tamarix* blend	103	11.4
100% *Searsia* blend	57.9	18.9
75% S + 25% D	2.96	60.3
50% S + 50% D	1.03	73.3
25% S + 75% D	0.48	79
Discard	0.53	75.1

S: *Searsia lancea*, D: Discard coal

The fouling index, F_u, which was used to determine the fouling potential of the coal and biomass was calculated based on the base to acid ratio according to equation (3.1) as follows:

$$F_u = R_{B/A} \times (N_2O + K_2O) \quad (3.1)$$

The base to acid ratio was determined by equation (3.2) as follows:

$$R_{B/A} = \frac{(Fe_2O_3 + CaO + MgO + K_2O + Na_2O)}{(SiO_2 + TiO_2 + Al_2O_3)} \quad (3.2)$$

For the fouling potential of a fuel, fouling is low for the $F_u \leq 0.6$, medium for $0.6 < F_u \leq 1.6$, high for $1.6 < F_u \leq 40$, and extremely high with tendency to deposits sintering when $F_u > 40$ (Texeira *et al.*, 2012). The slagging ratio was determined according to equation (3.3) as follows:

$$S_R = \frac{SiO_2}{SiO_2+Fe_2O_3+CaO+MgO} \times 100 \quad (3.3)$$

The degree of a fuel slagging propensity is based on, if $S_R > 72$ indicate low, medium if $65 < S_R \leq 72$ and high when $S_R < 65$ (Febrero *et al*., 2014).

The acidic oxides (SiO_2, TiO_2 and Al_2O_3) are noted to increase the melting temperature of ash, thereby lowering its slagging potential, while the basic oxides (Fe_2O_3, CaO, MgO, K_2O and Na_2O) reduce the melting temperature and thereby increase the likelihood of slagging (Texeira *et al*., 2012). The leaves of both *Searsia lancea* and *Tamarix usneoides* displayed extremely high likelihood of fouling with fouling indices of 214 and 514, respectively. High fouling propensity of leaves is due to the plants' ability to accumulate salt minerals such as NaCl and $CaSO_4$ in their leaves (Weiersbye, 2006). As a result, the biomass leaves harvested from the AMD sites in this study have a high concentration of basic oxides. The blends of both *Searsia lancea* and *Tamarix usneoides* with different coal percentage also showed extremely high fouling tendencies, although they are four times lower than their leaves counterparts. The results from both the leaves and the blends suggested that *Tamarix usneoides* has a higher fouling likelihood than *Searsia lancea*. This can be attributed to its better capacity to absorb minerals (Weiersbye, 2006). Comparatively, discard coal had a low fouling index of 0.53. The results on the slagging propensity of the species were similar to those of fouling; species that had high fouling propensity also had high slagging propensity. Unlike fouling, a lower slagging index indicate a higher slagging propensity. The leaves of *Searsia lancea* and *Tamarix usneoides* displayed high slagging capacity with low slagging indices of 14.9 and 3.32, respectively. 100% blend of *Searsia lancea* and *Tamarix usneoides* also had high slagging capacity with slagging indices of 18.9 and 11.4, respectively. In contrast, discard coal had a low slagging potential with a slagging index of 75.1.

Figure 4.18 shows the effect of coal inclusion on the fouling and slagging capacities of biomass. Figure 4.18 depicts the effect of addition of coal to coal-biomass blend on the fouling propensity of biomass. As seen on the graph, 100% biomass has extremely high fouling index of 57.9 compared to the low fouling index of discard (0.53). Addition of coal significantly lowered the fouling indices of biomass. This can be attributed to the lower alkali composition of the coal. Texeira *et al*. (2012) also found that the addition of coal can lower the fouling potential of biomass which can make woody biomass suitable for co-firing. Interestingly, the sample which had 25% biomass and 75% coal had the lowest fouling index, even lower than that of discard coal. This might suggest that co-firing at the right proportion might reduce not only the fouling capacity of biomass, but also of coal. The effect of coal inclusion on the slagging ratio can also be seen in Figure 4.18. The slagging ratio drastically increased with an increase in the coal proportion in the biomass. This means that the slagging potential of biomass was also lowered by the addition of coal. The addition of 25% coal increased the fouling index by three times. As in the case of fouling, the sample with 25% biomass and 75% coal blend had the lowest slagging potential with a high slagging index of 79.

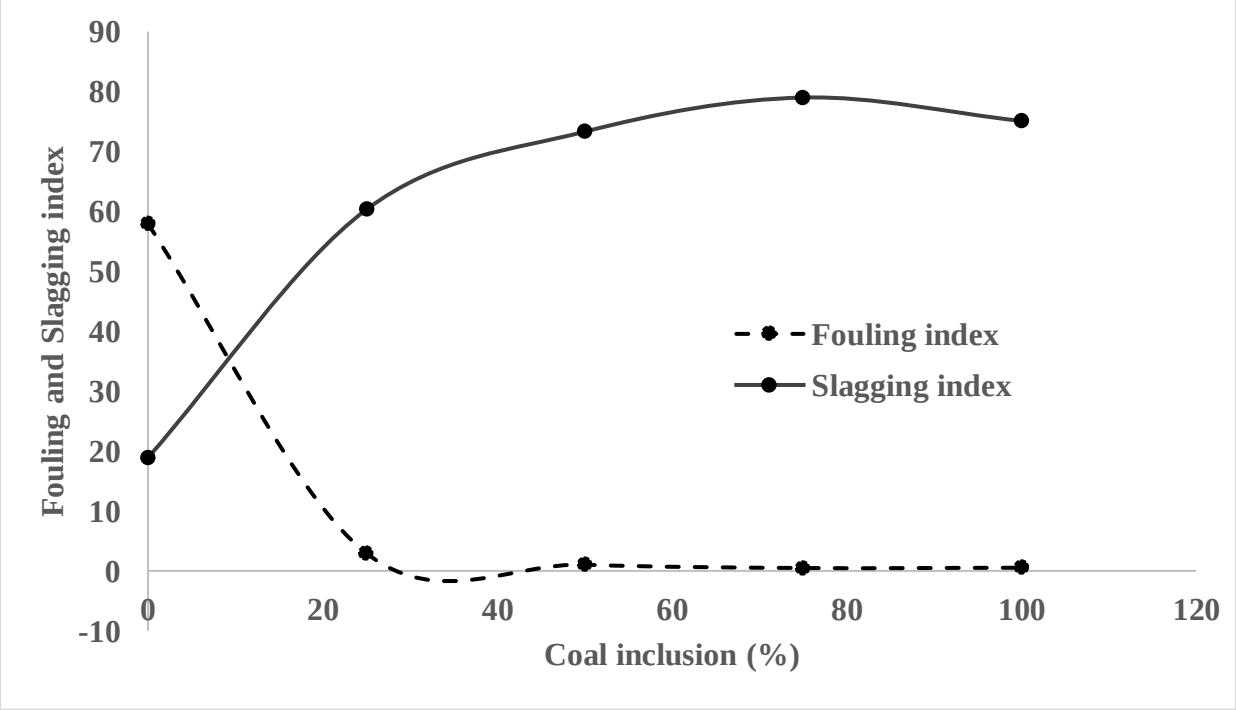

Figure 4.18: Effect of discard coal inclusion on fouling and slagging potentials of *Searsia lancea*

4.5 Gas Emission Profiles

The biomass, discard coal and their blends were combusted in a batch process for 10 minutes per sample at 850°C in a stainless-steel horizontal tube reactor. A Multi Gas Analyzer was connected to the reactor to monitor the concentrations of CO_2, SO_2, NO_x and CO emitted during combustion and co-combustion. The results of the tests conducted are presented and discussed below.

4.5.1 Gas emission profiles of raw biomass and discard coal

The gas emission profiles of biomass (*Tamarix usneoides* from Madala site) and discard coal are shown in Figures 4.19 to 4.22. Figure 4.19 shows the CO_2 emission profile for the raw biomass and discard coal. The biomass tested was found with a lower CO_2 emission of 3% compared to 5% released by the discard coal. An investigation conducted by Rokni *et al*. (2018) reported a biomass and coal with CO_2 emission of 2% and 9%, respectively. The lower CO_2 emission reported in this research for the discard coal may be due to the lower carbon content in the coal compared to that of the sub-bituminous coals used by Rokni *et al*. (2018). The lower emission noted in the biomass may also be attributed to its lower fixed carbon content compared to the coal.

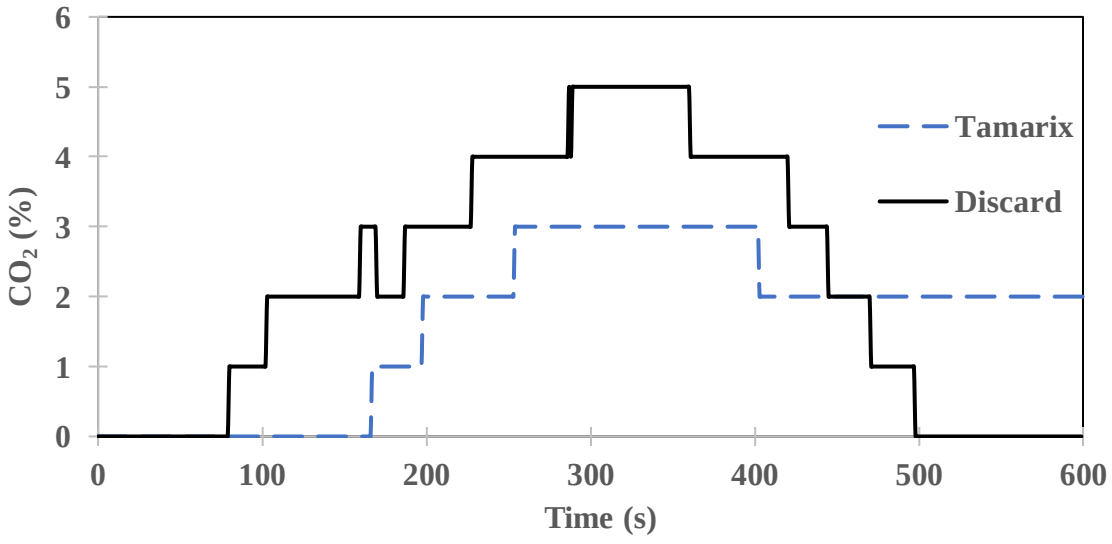

Figure 4.19: CO_2 emission profiles of *Tamarix usneoides* and discard coal.

The SO_2 emission profiles of the biomass and discard coal are shown in Figure 4.20 below. The SO_2 emitted from the biomass was found with a lower emission of 5 ppm compared to 51 ppm obtained from the discard coal. The concentration of the SO_2 obtained from this coal was remarkably low compared to that from the literature. A study conducted by Ren *et al*. (2016) and Rokni *et al*. (2018) on the SO_2 emitted from coal, shows a concentration of 188 ppm and 3180 ppm, respectively. The total sulfur content of the Bituminous Illinois coal utilized by Rokni *et al*. (2018) was 5.53%, compared to 1.34% sulfur in the coal utilized in this study. The lower sulfur emitted by this discard coal, which contains a 42% ash content is the result of low sulfur-forming swamps at the time of peat accumulation, namely, the peats formed in fresh water environments fed by clay-rich snow-melt waters from local glaciers unlike the acidic and maritime-linked swamps of the Carboniferous coals in the EU and USA (Falcon, 1986). The SO_2 concentration from the *Tamarix usneoides* utilized in this investigation was within the range reported by Rokni *et al*. (2018), with raw rice husk (10 ppm) and corn straw (17 ppm).

The lower SO_x emissions in biomass can be attributed to the lower levels of sulfur and higher sulfur retention capacity of biomass compared to discard coal (Ren *et al*., 2016). The presence of alkali metals like sodium, calcium and potassium in biomass inhibit SO_x emissions as these metals combine with sulfur to form sulphates (Ren *et al*., 2016). SO_x emissions are influenced by both the amount of sulfur in the fuel and amount of alkali in the fuel (Ren *et al*., 2016). The emission for both biomass and discard coal utilized in the study was found to be lower than the South African emission standard limit of 1350 ppm for existing plants and 9460 ppm for new plants (NEMA, 2010).

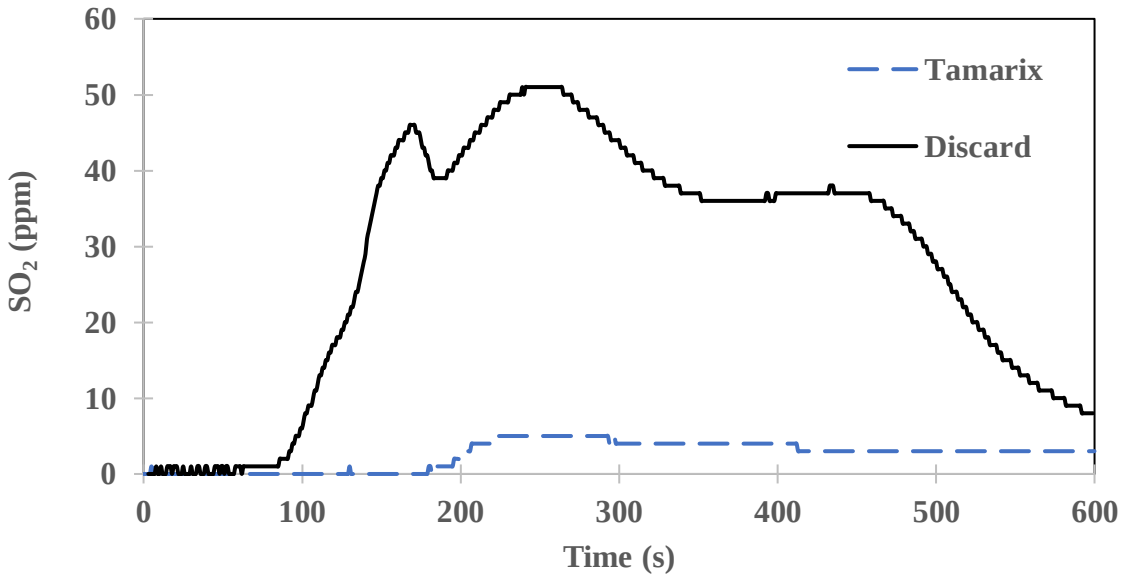

Figure 4.20: SO_2 emission profiles of *Tamarix usneoides* and discard coal.

The NO_x emission profiles for the biomass and discard coal are depicted in Figure 4.21. The biomass emitted 30 ppm of NO_x compared to 350 ppm emitted by discard coal. Ren *et al*. (2016) found NO_x emissions of most biomass to be lower than 200 ppm. Lower NO_x emissions in biomass may be attributed to lower fuel nitrogen compared to discard coal. Additionally, Ren *et al*. (2016) found NO_x emission levels of sub-bituminous coal to be 570 ppm. Furthermore, the NO_x emission levels of both biomass and discard coal was also found to be lower than the South African emission standard of 1410 ppm for existing coal plants and 2070 ppm for new coal plants (NEMA, 2010).

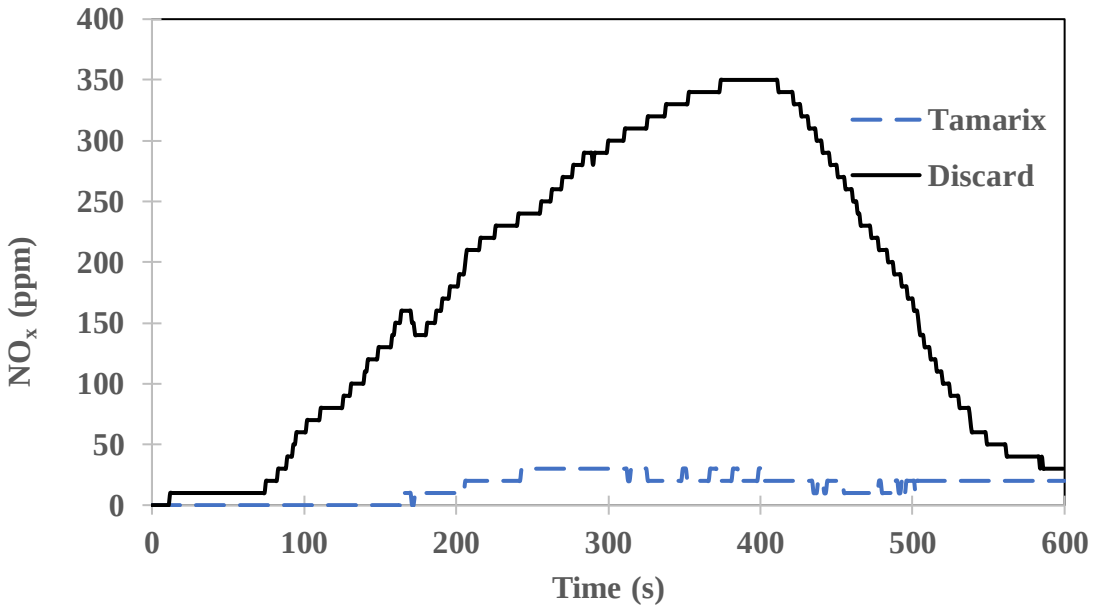

Figure 4.21: NO_x emission profiles of *Tamarix usneoides* and discard coal

4.5.2 Gas emission profiles of coal-biomass blends

Biomass was blended with discard coal at biomass inclusions of 25, 50 and 75% to investigate the effect of co-firing on CO_2, SO_2 and NO_x emission levels. The results of the tests are presented in Figures 4.22 to 4.24. Figure 4.22 presents CO_2 emission profiles of coal-biomass blends. The 100% biomass samples had the lowest CO_2 emission, while the sample with the lowest biomass inclusion (25%T + 75%D) had the highest CO_2 emissions. There was no clear trend in the CO_2 emission profiles when biomass was added to coal.

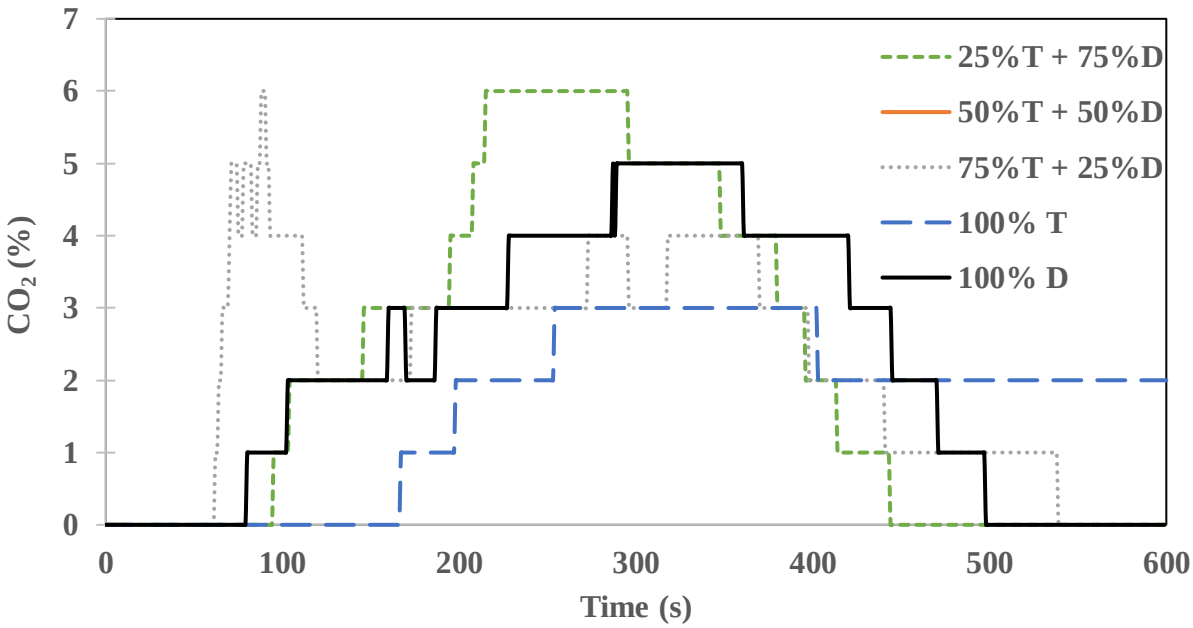

Figure 4.22: CO_2 emission profiles of coal-biomass blends (T: *Tamarix usneoides*, D: Discard coal).

Figure 4.23 presents the SO_2 emission profiles of coal-biomass blends. 100% *Tamarix* had the lowest SO_2 emission, while the discard coal had the highest SO_2 emissions. Proximate results also showed that 100% biomass had lower sulfur content than coal-biomass blends. This was due to high sulfur content of discard coal compared to biomass. The profiles also show a decrease in the SO_2 emission levels with an increase in biomass in the blend. According to Bhuiyan *et al*. (2016), SO_x emissions decrease during co-firing due to less amount of sulfur in biomass and the presence of alkali metals which promote sulfur retention in biomass. Rokni *et al*. (2018) also obtained similar results when they evaluated emissions of raw and torrefied biomass during co-firing. A previous study by Ren *et al*. (2016) also founder lower SO_x emissions in biomass than in coal, further supporting that co-firing of biomass can reduce SO_x emissions associated with electricity generation.

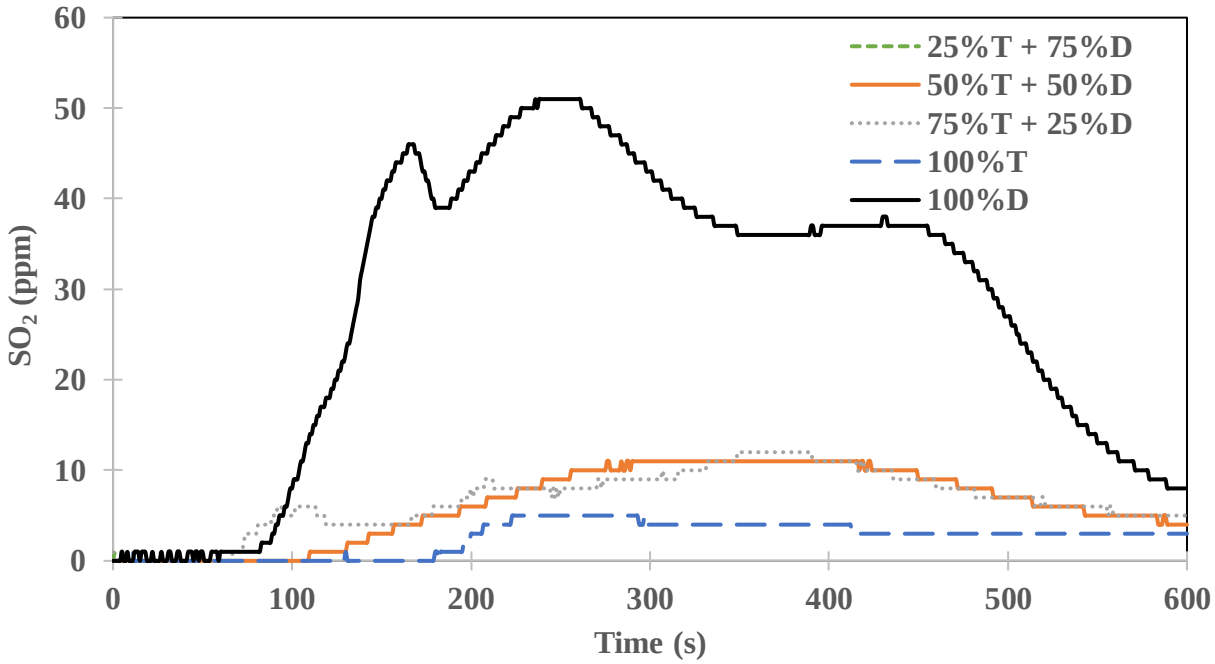

Figure 4.23: SO_2 emission profiles of coal-biomass blends (T: *Tamarix usneoides*, D: Discard coal).

NO_x emission profiles of coal-biomass blends are presented in Figure 4.24 below. 100% *Tamarix* had the lowest NO_x emission, while the discard coal had the highest NO_x emissions. Compared with discard coal and coal-biomass blends, proximate results showed that 100% biomass had the lowest nitrogen content. The profiles also show a decrease in the NO_x emission levels with an increase in biomass proportion in the blend. This can be attributed to lower levels of nitrogen in the biomass compared to the discard coal. Ren *et al*. (2016) had found that differences in nitrogen content lead to significant NO_x reduction when they are large. However, the authors found lower NO_x emissions in biomass compared to coal.

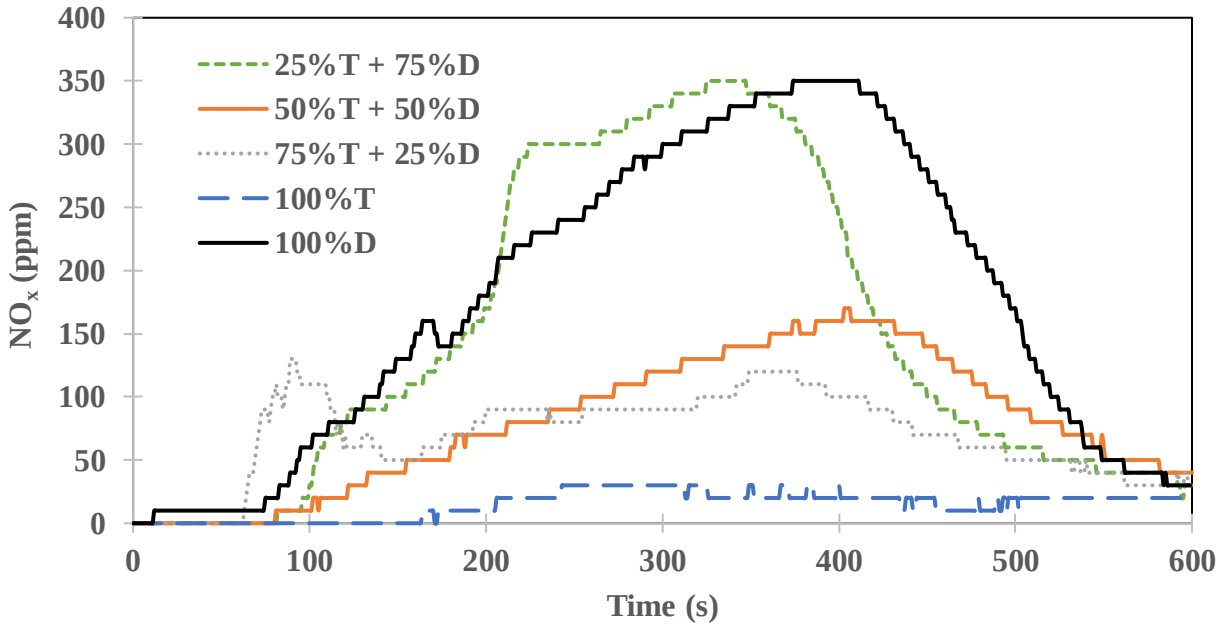

Figure 4.24: NO_x emission profiles of coal-biomass blends (T: *Tamarix usneoides*, D: Discard coal).

4.5.3 Effect of *Tamarix usneoides* leaves on gaseous emissions

A study carried out by Lin and Hsieh (1985) during the combustion of oil, showed that NaCl presence in the air enhances the formation of excess O_2, CO and SO_2. In contrast, the authors noted that the emission of CO_2 also reduced during this process. With the above stated fact, the effect of NaCl known to be in the range of 2 to 10% in *Tamarix usneoides* leaves (Weiersbye and Witkowski, 2007) was investigated in order to ascertain the potential of the leaves in reducing the emissions of SO_2, CO and CO_2. This test was conducted by combusting 100% leaves and blend of *Tamarix* leaves with discard coal at different ratios (25, 50 and 75%). Figure 4.25 below presents SO_2 emission profiles for *Tamarix* leaves, discard coal, and their blends. The co-firing of *Tamarix* leaves with discard coal (D) was found to decrease the concentration of SO_2 emitted from coal for high leaves (L) inclusion (75% L + 25% D). However, the lower the leaves inclusions (50% L + 50% D and 25% L + 75% D) in the blend, the higher the SO_2 emission levels of biomass-discard coal blends. The 100% leaves had the lowest SO_2 emission, and this may be attributed to the high concentration of alkali elements in the leaves (Weiersbye and Witkowski, 2007). Alkali metals like sodium, calcium and potassium combine with sulfur to form sulfates which inhibits SO_x

emissions (Ren *et al*, 2016). The SO_2 emission levels of the blend with 75% *Tamarix* leaves and 25% discard was found to be lower than that of the blend with 75% *Tamarix* tree blend and 25% discard coal. However, the SO_2 emissions from the other *Tamarix* tree blends of 25% and 50% are found to reduce the discard emissions about 5 times more than their leaves counterparts (Figure 4.23).

The influence of *Tamarix* leaves co-fired with discard coal on the CO emission was also investigated, with the emission profiles depicted in Figure 4.26 The 100% *Tamarix* leaves and the sample with 25% *Tamarix* leaves + 75% discard coal were found with the lowest CO emissions, while discard coal and a sample with 50% *Tamarix* leaves + 50% discard coal had the highest CO emissions. No trend was observed on the CO emission levels as the proportion of leaves in the blend increased. Generally, as observed in this study, the addition of *Tamarix* leaves decreases CO emissions.

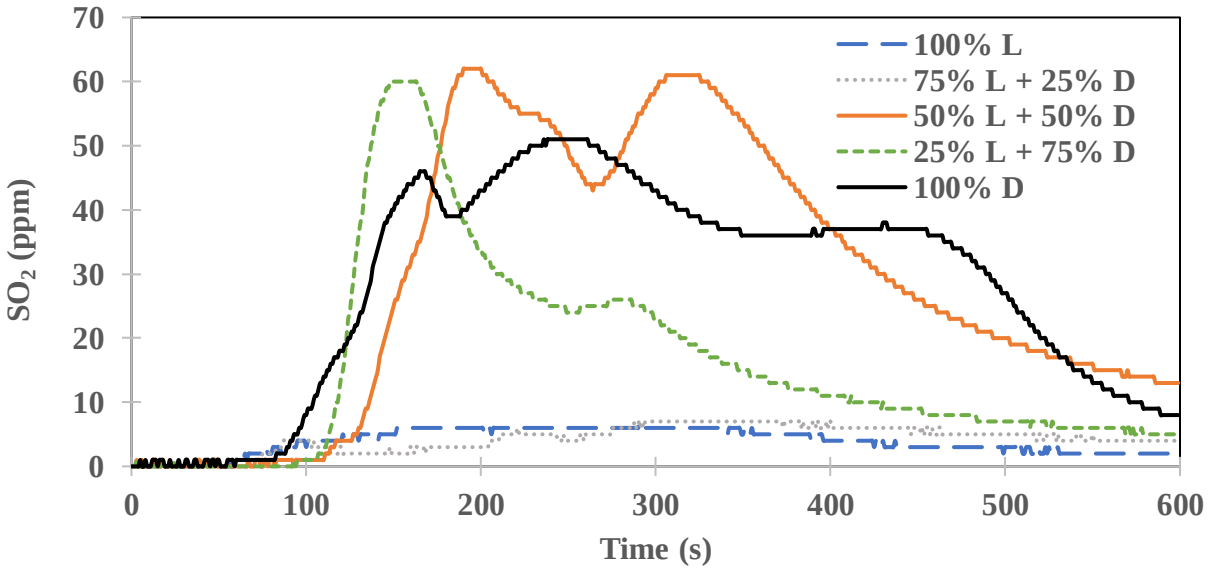

Figure 4.25: SO_2 emission profiles of *Tamarix usneoides* leaves blended with coal (L: *Tamarix* leaves D: Discard coal)

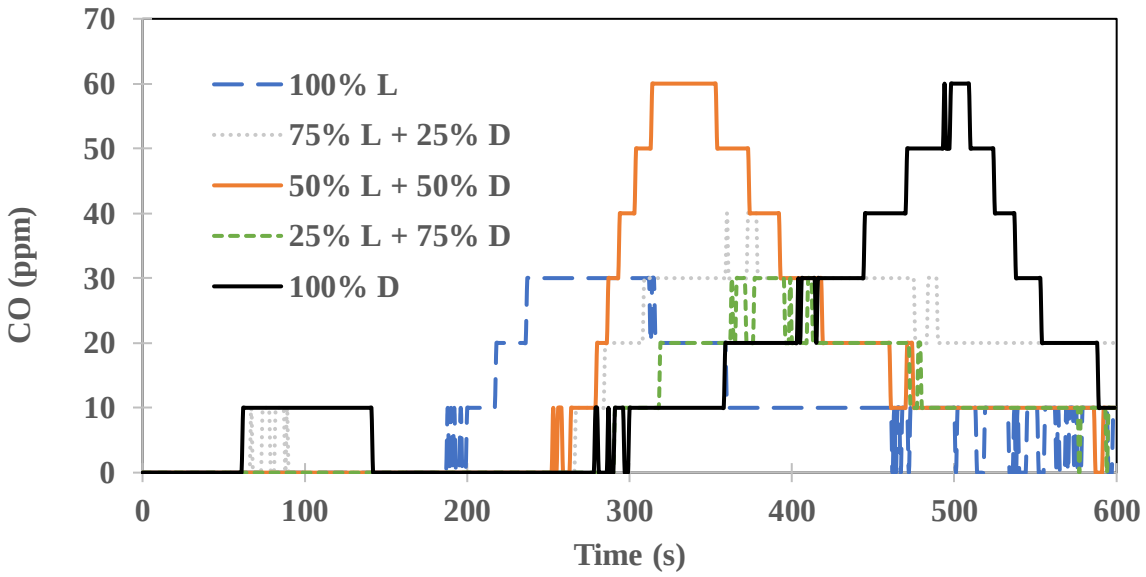

Figure 4.26: CO emission profiles of *Tamarix usneoides* leaves blended with coal. (L: *Tamarix* leaves D: Discard coal).

Figure 4.27 also presents the concentration of CO_2 from the combustion of *Tamarix leaves*, discard coal, and their co-combustion at different blending ratios. The 100% *Tamarix* leaves and a sample with 25% *Tamarix* leaves + 75% discard coal had the highest CO_2 emissions while addition of *Tamarix* leaves in discard was found to increase emission levels of discard coal. Contrary to the findings of Lin and Hsieh (1985), the presence of NaCl in the *Tamarix* leaves used in this study could be said to be responsible for the reduction of SO_2 when high proportion of leaves is blended and CO emissions while promoting CO_2 formation.

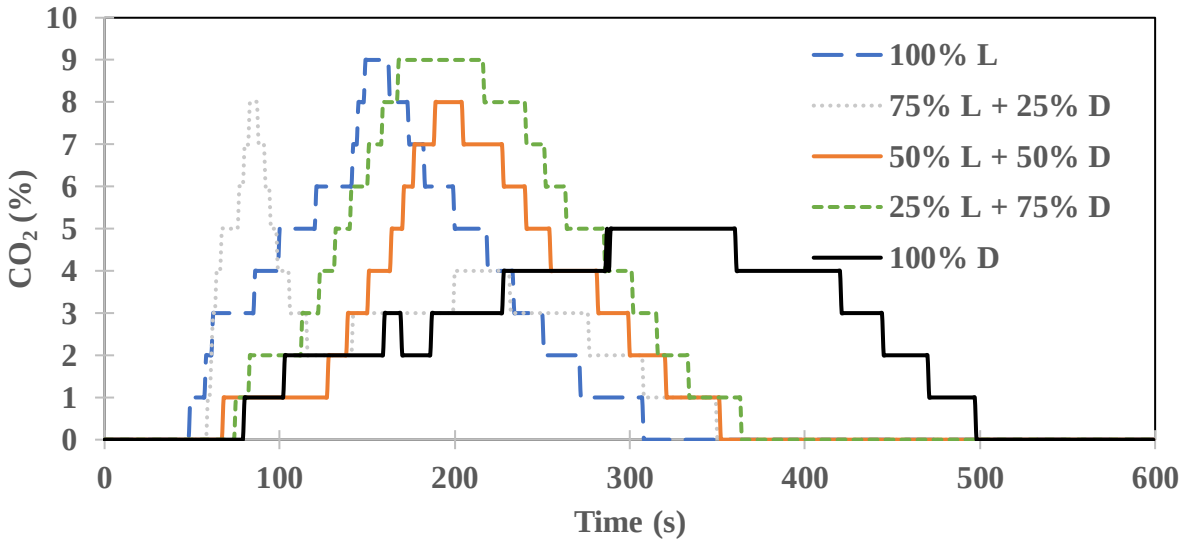

Figure 4.27: CO_2 emission profiles of *Tamarix usneoides* leaves blended with coal (L: *Tamarix* leaves D: Discard coal).

In summary, 100% discard coal had higher SO_x, NO_x and CO_2 emissions than biomass (*Tamarix usneoides*) mainly due to higher sulfur, nitrogen and carbon content as seen in the ultimate analysis results. Addition of biomass to coal in coal-biomass blends was found to decrease SO_x, NO_x and CO_2 emissions of discard coal. This means *Tamarix usneoides* can potentially be blended with coal to reduce emissions in coal-fired power stations. Meanwhile, addition of *Tamarix* leaves was found to decrease SO_x emissions from the discard coal when 75% leaves were blended with discard coal. However, SO_x emissions increased when 50 and 25% *Tamarix* leaves were blended with coal. Since only high amount of leaves in the blend would lower the energy value during co-firing, it would not be advisable to blend coal with *Tamarix* leaves.

CHAPTER 5: CONCLUSIONS AND RECOMMENDATIONS

The main findings from this study, along with the recommended future research are presented in this chapter.

5.1 Conclusions

The aim of this research was to determine the suitability of *Searsia lancea* and *Tamarix usneoides* planted for AMD rehabilitation in Witwatersrand's Vaal River and West complex mining sites as a fuel for combustion and co-combustion. This aim was achieved by accomplishing the set four major objectives, as outlined in Chapter 1.

The first objective was to determine the physicochemical characteristics of *Searsia lancea* and *Tamarix usneoides* together with discard coal and a run of mine coal. The proximate analysis conducted on each tree part, shows that the roots, rootball and the leaves contained the highest ash content of all the tree parts, while the wood and twigs had the least ash content. Of the two species, the *Searsia lancea* had a lower ash content than *Tamarix usneoides* in all tree parts. The wood and twigs from both tree species were found with high fixed carbon and volatile matter contents. All the biomass samples utilized are seen with lower ash content and similar calorific value relative to the coal utilized in this study. For the ultimate analysis test, *Searsia lancea* was found with higher total carbon content and hydrogen composition than *Tamarix usneoides* which might be responsible for the higher heating value noted from *Searsia lancea*. Both biomasses had higher hydrogen and oxygen content than both coals. The sulfur and nitrogen contents in the *Searsia lancea* and *Tamarix usneoides* were found to be less than those of discard coal and run of mine coal. Meanwhile, *Searsia lancea* had lower sulfur and nitrogen contents than *Tamarix usneoides.*

The differential thermogravimetric (DTG) and thermogravimetric analysis (TGA) thermographs for the *Searsia lancea, Tamarix usneoides* and the two different South African coals utilized in this study were used to compare the thermal characteristics of the biomass and the two coals. Two peaks were observed for biomass combustion compared to one for coal combustion. The coals were seen to ignite and burnout at higher temperatures than biomass. *Searsia lancea* and *Tamarix usneoides* displayed higher reactivities than discard and run of mine coals. *Searsia lancea*

harvested from the Mispah site and *Tamarix usneoides* harvested from the Madala site are better fuels, in terms of reactivity compared to all other samples. It was observed that, with volatile matter content greater than 60% in both biomasses, the co-firing of these biomasses with the discard coal utilized in this study appears to have led to increasingly lower temperatures for the release and combustion of volatiles in the coal discard. An improvement was also noted to the combustion characteristics of the discard coal when blended with *Tamarix usneoides.* There was a decrease in the devolatilization and ignition temperatures of the blend when discard coal was co-fired with T*amarix usneoides.* In addition, the difference in the AMD concentration between the two sites did not appear to have had an obvious major effect on the energy and combustion characteristics of the *Tamarix* samples utilized in this study, apart from the fact that the *Tamarix* sample planted on Madala was shown to exhibit a 2% higher reactivity and weight loss rate than that grown on the Mispah site.

The combustion efficiency of the raw plant samples and the coal/biomass blends were determined at four temperatures, namely; 300°C, 400°C, 500°C and 600°C. At a blend of 75% coal + 25% biomass, an increase in combustion efficiency from 14% at 300°C to 96.21% at 600°C was observed for the coal discard. *Tamarix*, on the other hand, showed a marginally higher efficiency than the *Searsia* at lower temperature and lower biomass proportion in the blends, but both samples followed a similar efficiency pattern. Both species are also noted to have better combustion efficiency compared to the discard coal between the temperature of 300-500°C, but similar efficiency with the discard coal at 600°C. Based on this observation, it can be concluded that both plant species can be co-fired with discard coal for power generation.

The second main objective was to determine the combustion and co-combustion reaction kinetics of the two tree species with and without coal in different proportions. The activation energies for the 100% biomasses were found to be lower than the activation energies for the coals utilized in this study, indicating that less energy is required for biomass combustion than for coal combustion. The activation energy for the first stage combustion of *Searsia lancea* was 32.98 kJ/mol, and 24.94 kJ/mol for its second stage combustion reaction. *Tamarix usneoides* had an activation energy of 37.39 and 26.23 kJ/mol in its first and the second stage combustion, respectively. The first stage

activation energy was lower than the second stage activation energy, but as the biomass percentage in the blend increased further, the second stage activation energy was seen reduced.

The third objective was to evaluate trace elements in the ash of biomass, coal and their blends and the impact thereof on the slagging and fouling potential of biomass. SiO_2, Al_2O_3, Fe_2O_3 and CaO were found to be the predominant oxides in the discard coal utilized in this study. Biomass had higher amounts of Na_2O and K_2O than discard coal, suggesting that the use of biomass for power generation might be detrimental to boilers. The addition of coal used in the study during co-firing reduces the concentrations of Na_2O and K_2O from 12.19 and 2.52% in 100% *Searsia* to 1.34 and 1.23%, respectively in a sample which had 75% discard coal + 25% biomass. The ash obtained from the *Tamarix* leaves was found to possess higher Na_2O, SO_3^{2-}, Cl and Ca than *Searsia* leaves. Therefore, this result justifies why the leaves from both species, especially *Tamarix* were not added to the tree compartments during blending. The blends of *Tamarix* and *Searsia* at different coal ratio also had higher chlorine levels compared to the discard coal, with less composition than those in the leaves. The addition of coal reduced the concentration of chlorine from 0.47% in 100% biomass sample to 0.01% in a sample with 75% discard coal + 25% biomass inclusion. Interestingly, coal ash had less SO_3^{2-} than both *Searsia lancea* and *Tamarix usneoides* blends.

The leaves of both *Searsia lancea* and *Tamarix usneoides* displayed extremely high likelihood of fouling with fouling indices of 214 and 514, respectively. The blends of both *Searsia lancea* and *Tamarix usneoides* with different coal percentage also showed extremely high fouling tendencies, although they are four times lower than their leaves counterparts. The results from both the leaves and the blends suggested that *Tamarix usneoides* has a higher fouling likelihood than *Searsia lancea*. The slagging ratio drastically increased with an increase in the coal proportion in the biomass, which indicate lower slagging potential for the biomass/coal blend.

The fourth objective was to investigate the effect of biomass inclusion on the CO_2, SO_x and NO_x emission levels of discard coal. The biomass tested was found with a lower CO_2 emission of 3% compared to 5% released by the discard coal. SO_2 emitted from the biomass was found with a lower emission of 5 ppm compared to 51 ppm obtained from the discard coal. The emission for both biomass and discard coal utilized in the study was found to be lower than the South African

emission standard limit of 1350 ppm for existing plants and 9460 ppm for a new plant. The biomass emitted 30 ppm of NO_x compared to 350 ppm emitted by discard coal. In conclusion, all CO_2, SO_x and NO_x emissions of discard coal were reduced by the addition of biomass in the blend. Therefore, *Tamarix usneoides* can be co-fired with coal to lower the emissions of CO_2, SO_x and NO_x in coal-fired power stations.

The effect of *Tamarix* leaves was investigated in order to ascertain the potential of the leaves in reducing the emissions of SO_2, CO and CO_2. The 100% *Tamarix* leaves had the highest CO_2 emissions, and the addition of *Tamarix* leaves with the discard coal was found to increase emission levels of discard coal. Contrary to the findings of Lin and Hsieh (1985), the presence of NaCl in the *Tamarix* leaves used in this study could be said to be responsible for the reduction of SO_2 and CO emissions while promoting CO_2 formation.

5.2 Recommendations

Based on the findings and limitations of this research, the following areas are recommended for further research:

- Pre-treatment as a way of improving the thermal and physicochemical characteristics of trees planted for AMD rehabilitation before using the plants for combustion and co-combustion.
- Techno-economic evaluation and life cycle assessment to assess the viability of using *Searsia lancea* and *Tamarix usneoides* as fuels for combustion and co-combustion.
- Gasification of *Searsia lancea* and *Tamarix usneoides* to determine the impact of the trace elements on the product yields

REFERENCES

Agrawal, A., and Chakraborty, S., (2013), *A kinetic study of pyrolysis and combustion of microalgae Chlorella vulgaris using thermo-gravimetric analysis*, Bioresource Technology, Vol.128, 72-80.

Akcil, A., and Koldas, S., (2006), *Acid Mine Drainage (AMD): Causes, Treatment and Case Studies*, Journal of Cleaner Production, Vol.14, 1139-1145.

Akinyeye, R., Odunayo, R., Pereao, O., Petrik, L. and Olaofe, O., (2016), *Comparative Chemical and Trace Element Composition of Coal Samples from Nigeria and South Africa*, American Journal of Innovative Research and Applied Sciences.

Alvarez, A., Pizarro, C., Garcia, R., Bueno, J.L. and Lavin, A.G., (2016), *Determination of kinetic parameters for biomass combustion*, Bioresource Technology, Vol.216, 36-43.

AngloGold Ashanti (AGA), (2007), *Vaal River Groundwater Plume Delineation Update*, Internal reference number ANGGA.07.175/70563 VRW, Vaal River, South Africa.

Arendze, S., (2015), *The effect of trees on physical and chemical properties of substrata contaminated by gold mine waste disposal*, MSc dissertation, University of the Witwatersrand, Johannesburg.

ASMT International, (2019), *Standard Test Method for Gross Calorific Value of Coal and Coke*, https://www.astm.org/DATABASE.CART/HISTORICAL/D5865-04.htm, [Accessed on 10 November 2019].

ASMT International, (2019), *Standard Test Methods for Instrumental Determination of Carbon, Hydrogen, and Nitrogen in Laboratory Samples of Coal and Coke*, https://www.astm.org/DATABASE.CART/HISTORICAL/D5373-02.htm, [Accessed on 10 November 2019].

ASMT International, (2019), *Standard Test Methods for Proximate Analysis of the Analysis Sample of Coal and Coke by Instrumental Procedures*, https://www.astm.org/Standards/D5142.htm, [Accessed on 10 November 2019].

ASMT International, (2019), *Standard Test Methods for Sulfur in the Analysis Sample of Coal and Coke Using High Temperature Tube Furnace Combustion Methods*,

https://www.astm.org/DATABASE.CART/HISTORICAL/D4239-05.htm, [Accessed on 10 November 2019].

Bada, S.O., Falcon, R.M.S. and Falcon, L.M., (2014), *Investigation of combustion and co-combustion characteristics of raw and thermal treated bamboo with thermal gravimetric analysis*, *Thermochimica Acta*, Vol.589, 207–214.

Bada, S.O., Falcon, R.M.S., and Falcon, L.M., (2014), *Investigation of combustion and co-combustion characteristics of raw and thermal treated bamboo with thermal gravimetric analysis*, Thermochimica Acta, Vol.589, 207–214.

Bada, S.O., Falcon, R.M.S., and Falcon, L.M., (2015), *Characterization and co-firing potential of a high ash coal with Bambusa balcooa*, Fuel, Vol.151, 130-138.

Bada, S.O., Falcon, R.M.S., Falcon, L.M. and Bergmann, P., (2016), *Co-firing potential of raw and thermally treated Phyllostachys aurea bamboo with coal*, Energy Sources, Part A: Recovery, Utilization, and Environmental Effects, Vol. 38(10), 1345-1354.

Bai, F., Guo, W., Lu, X., Liu, Y., Guo, M., Li, Q. and Sun, Y., (2015), *Kinetic study on the pyrolysis behaviour of huadian oil shale via non-isothermal thermogravimetric data*, Fuel, Vol.146, 111-118.

Barbanera, M., Cotana, F. and Di Matteo, U., (2018), *Co-combustion performance and kinetic study of solid digestate with gasification biochar*, Renewable Energy, Vol.121, 597-605.

Barnes, I., (2012), *Understanding pulverised coal, biomass and waste combustion*, CCC/205, London, UK, IEA Clean Coal Centre.

Barnes, I., (2018), *HELE perspectives for selected Asian countries*, CCC/287, London, UK, IEA Clean Coal Centre.

Baum, B., (1978), *The Genus Tamarix*. Israel Academy of Sciences and Humanities, Jerusalem.

Baxter, L., (2005), *Biomass-coal co-combustion: opportunity for affordable renewable energy*, Fuel, Vol.84(10), 1295-1302.

Baxter, L., (2011), *Biomass-coal cofiring: An overview of technical issues*, In: Grammelis P, editor. Solid biofuels for energy, London: Springer, 43–73.

Bhavsar, P.A., Jagadale, M.H., Khandetod, Y.P. and Mohod, A.G., (2018), *Proximate Analysis of Selected Non Woody Biomass*, International Journal of Current Microbiology and Applied Sciences, Vol.7(9), 2846-2849.

Bhuiyan, A. A., Blicblau, A.S., Islam, S.A.K.M. and Naser, J., (2016), *A review on thermo-chemical characteristics of coal/biomass co-firing in industrial furnace*, Journal of the Energy Institute, Vol.91, 1-18.

Biagini, E., Lippi, F., and Tognotti, L., (2002), *Devolatilisation rate of biomasses and coal biomass blends: An experimental investigation*, Fuel, Vol.81, 1041-1050.

Boumanchar, I., Chhiti, Y., Alaoui, F.E.M., Elkhouakhi, M., Sahibed-dine, A., Bentiss, F., Jama, C. and Bensitel, M., (2019), *Investigation of (co)-combustion kinetics of biomass, coal and municipal solid wastes*, Vol.97, 10-18.

Bracmort, K., (2016), *The renewable fuel standard (RFS), in brief*, https://nationalaglawcenter.org/wp-content/uploads//assets/crs/R43325.pdf, [Accessed 10 November 2019].

Bredenkamp, C.L. and Phepho, N., (2008), *Hybridization of Tamarix usneoides and Tamarix ramosissima*, Unpublished, South African National Botanical Institute (SANBI) Herbarium, Pretoria.

Bredenkamp, C.L., (2003), *Personal Communication*, South African National Botanical Institute Herbarium, Pretoria.

Brodie, M.J., Robertson, A. Mac, G. & Gadsby, J.W., (1992), Cost Effective Closure Plan Management for Metal Mines, Steffen Robertson and Kirsten Inc., Vancouver, B.C.

Brotherson, J.D. and Field, D., (1987), *Tamarix: Impacts of a Successful Weed*, Rangelands, Vol. 9(3),110-112.

BSI group, (2019), Solid biofuels. Determination of ash content, https://shop.bsigroup.com/ProductDetail/?pid=000000000030198062 , [Accessed on 10 November 2019].

Cai, J., Wang, Y., Zhou, L., Huang, Q., (2008), *Thermogravimetric analysis and kinetics of coal/plastic blends during co-pyrolysis in nitrogen atmosphere*, Fuel Processing Technology, Vol.89, 21–27.

Cai, R., Ke, X., Lyu, J., Yang, H., Zhang, M., Yue, G., Ling, W., (2017), *Progress of circulating fluidized bed combustion technology in China: a review*, Clean Energy, Vol.1(1), 36–49.

Caillat, S. and Vakkilainen, E., (2013), *Large scale biomass combustion plants: An overview*, Chapter 8, In: Rosendahl, L, (Ed.), Biomass Combustion Science, Technology and Engineering. Woodland Publishing Series in Energy, London, 274-296.

Campbell, P.A., Mitchell, R.E. and Ma, L., (2002), *Characterisation of coal char and biomass char reactivities to oxygen*, Proc Combust Inst, Vol.29, 519-526.

Chamber of Mines of South Africa, (2018), National Coal Strategy for South Africa, Available at: http://www.mineralscouncil.org.za/component/jdownloads/send/25-downloads/535-coal-strategy-2018 [Accessed on 08 November 2019].

Chandrasekaran, C., (2017), *Rubber lining for sulfur dioxide systems*, Anticorrosive rubber lining, Applied Science Publishers, 73-76.

Chen W.H., Huang M.Y., Chang J.S., Chen C.Y. and Lee W.J., (2015), *An energy analysis of torrefaction for upgrading microalga residue as a solid fuel*, Bioresource Technology, Vol.185, 285-293.

Chen, D., Zhen, Y. and Zhu, X., (2013), *In-depth investigation on the pyrolysis kinetics of raw biomass. Part I: Kinetic analysis for the drying and devolatilization stages*, Bioresource Technology, Vol.131, 40-46.

Chen, W. and Wu, J., (2009), *An evaluation on rice husk and pulverized coal blends using a drop tube furnace and a thermogravimetric analyzer for application to a blast furnace*, Energy. Vol.34, 1458-1466.

Cheng, J., Zhou, J., Liu, J., Zhou, Z., Huang, Z., Cao, X., Zhao, X., Cen, K., (2003), *Sulfur removal at high temperature during coal combustion in furnaces: A review*, Prog. Energy. Combust. Sci., Vol.29, 381–405.

Coats, A.W. and Redfern, J.P., (1964), *Kinetic parameters from thermogravimetric data*, Nature, Vol. 201, 68-69.

Coyne, D., (2018), *World Coal 2018-2050: World Energy Annual Report (Part 4)*, http://peakoilbarrel.com/world-coal-2018-2050-world-energy-annual-report-part-4/, [Accessed on 08 November 2019].

Cumming, J.W., McLaughlin, J., (1982), *The thermogravimetric behaviour of coal*, Thermochima Acta, Vol.57, 253–272.

De Klerk, A., (2014), Chapter 12 - *Transport Fuel: Biomass-, Coal-, Gas- and Waste-to-Liquids Processes*, Future Energy, second edition, 245-270.

Demirbas, A., (2007), *Progress and Recent Trends in Biofuels*, Progress in Energy and Combustion Science, Vol.33(10), 1-18.

Dennis, A., (2008), *Salt glands and elemental concentration in leaves of Tamarix usneoides E. Mey, ex Bunge (Tamaricaceae) grown on seepage from Highveld gold mines*, BSc. Honours Project: University of the Witwatersrand, Johannesburg.

Department of Mineral Resources, (2009), *The future role of the Waterberg Coalfield in South Africa's Coal Industry*, Report R76/2009, https://www.dmr.gov.za/LinkClick.aspx?fileticket=75uia_ngmek%3D&portalid=0, [Accessed on 08 November 2019].

Department of Mineral Resources, Republic of South Africa, (2014), *South Africa's coal industry*. https://www.dmr.gov.za/LinkClick.aspx?fileticket=uePTS1drX6A%3D&portalid=0, [Accessed on 09 November 2019].

DOE (U.S. Department of Energy), (2001), *Coal technologies are cost competitive*.

Dong N.S., (2011), *Utilisation of low rank coals*. CCC/182, London, UK, IEA Clean Coal Centre.

Dye, P.1. & Weiersbye, I.M., (2010), *The Mine Woodlands Project in the Witwatersrand Basin Gold Fields of South Africa: Strategy and Progress, Ecological Engineering and Phytotechnology Programme*, School of Animal, Plant and Environmental Sciences, University of the Witwatersrand, Johannesburg.

Dye, P.1., Jarmain, C., Oageng, B., Xaba, J. and Weiersbye, I.M., (2008a), A.B. Fourie, M. Tibbett, I.M. Weiersbye, P.1. Dye (eds), *The Potential of Woodlands and Reed-beds for Control of Acid Mine Drainage in the Witwatersrand Gold Fields*, South Africa, Mine Closure -Australian Centre for Geomechanics, Perth, ISBN 978-0-9804185-6-9.

Easterly, J.L. and Burnham, M., (1996), *Overview of biomass waste fuel resources for power production*, Biomass Bioenergy, Vol.10(2-3), 79-92.

Eastman, M.L., (2003), Clean coal power initiative, presented at the Clean Coal Power Conference, www.netl.doe/gov/coalpower/ccpi/program_info.html, November 18, 2003, [Accessed on 09 November 2019].

Eberhard, A., (2011), *The future of South African coal: Market, investment and policy challenges*, program on energy and sustainable development, PESD Stanford, https://fsi-live.s3.us-west-1.amazonaws.com/s3fs-public/WP_100_Eberhard_Future_of_South_African_Coal.pdf [Accessed on 08 November 2019].

EIA, (2009), International Energy Outlook, U.S. Department of Energy, May 2009.

El May, Y., Jeguirim, M., Dorge, S., Trouve, G. and Said, R., (2011), *Thermogravimetric analysis and kinetic study on palm of Phoenix dactyliferal*, MCS, Vol.7, 11-15.

Eriksson, T., Barisic, V., Nuortimo, K., Jäntti, T., (2018), *Advanced utility CFB technology for challenging new solid biomass fuels*, Conference: Power Gen Europe 2015, at Amsterdam, The Netherlands.

Eskom, (2018), *Medupi Flue Gas Desulfurization, Technology Selection Study Report*, http://www.eskom.co.za/OurCompany/SustainableDevelopment/EnvironmentalImpactAssessments/medupi/Final%20Scoping%20Report%20Appendicies/Appendix%20D%20-%20Medupi%20FGD%20Technology%20Selection%20Study%20Report.pdf , [Accessed on 09 November 2019].

Eskom, (2019), Coal Power, Available at: http://www.eskom.co.za/AboutElectricity/ElectricityTechnologies/Pages/Coal_Power.aspx [Accessed on 08 November 2019].

export.gov. (2019). *South Africa-Electrical Power Systems*, https://www.export.gov/article?id=South-Africa-electrical-power, [Accessed on 09 November 2019].

Exxaro, (2018), Exxaro resources limited integrated report 2018, https://www.exxaro.com/investor/integrated-reports2018/overview-of-our-business.php, [Accessed on 08 November 2019].

Falcon RM.S., (1986), *A brief review of the origin, formation. and distribution of coal in southern Africa*. In: Mineral and Deposits of Southern Africa. Anhaeusser CR and Maske S. (Eds.). Vols I and II. Geol. Soc. S. Afr. Johannesburg. 1879-1898.

Falcon, L., (1992), *The complexities of Coal*, Gold Fields of South Africa in house magazine.

Falcon, R.M.S. and Ham A.J, (1988), *The Characterisation of South African Coals*, Journal of the South African Institute for Mining and Metallurgy, Vol.88(5), 145-161.

Falcon, R.M.S., (1977a), *Coal in South Africa Part I, The Quality of South African Coal in Relation to its Uses and World Energy Resources*, Mineral Sci. Engng. Part 1, Vol.9, 198-217.

Falcon, R.M.S., (1977b), *Coal in South Africa Part II, The Application of Petrography to the Characterisation of Coal*, Mineral Sci. Engng. Part 2, Vol.10(1), 29-52.

Falcon, R.M.S., (2013), *Coal, coke and carbon in the metallurgical industry*. Lecture. University of the Witwatersrand. Delivered July 2013.

Febrero, L., Granada, E., Regueiro, A., Miguez, J.L., (2015), *Influence of Combustion Parameters on Fouling Composition after Wood Pellet Burning in a Lab-Scale Low-Power Boiler*, Energies, Vol.8, 9794-9816.

Federal Energy Regulatory Commission, (2010), *Oil, coal and natural gas daily spot prices*, www.ferc.gov/market-oversight/, [Accessed on 30 April 2019].

Flagan R.C. and Seinfeld JH., (1988), *Fundamentals of air pollution engineering*, Courier Corporation.

Gani, A., Morishita, K., Nishikawa, K. and Naruse, I., (2005), *Characteristics of co-combustion of low-rank coal with biomass*, Energy Fuels, Vol.19, 1652–1659.

Gera, D., Mathur, M.P., Freeman, M.C. and Robinson, A., (2002), *Effect of large aspect ratio of biomass particles on carbon burnout in a utility boiler*, Energy Fuels, Vol.16, 1065-1075.

Ghetti, P., (1986), Fuel, Vol.65, 636.

Gil, M.V., Casal, D., Pevida, C., Pis, J.J. and Riveida, F., (2010), *Thermal behaviour and kinetics of coal/biomass blends during combustion*, Bioresource Technology, Vol. 101, 5601-5608.

Government Gazette, Republic of South Africa, No. 39 of 2004: National Environment Management Act: Air Quality Act, 2004, Vol.476, Cape Town ,24 February 2005.

Grammelis, P., Agraniotis, M. and Kakaris, E., (2010), *Co-utilization of Biomass Based Fuels in Pulverized Coal Power Plants in Europe*, https://doi.org/10.1002/9783527628148.hoc07, [Accessed on 10 November 2019].

Guo, F. and Zhong, Z., (2018), *Co-combustion of anthracite coal and wood pellets: Thermodynamic analysis, combustion efficiency, pollutant emissions and ash slagging*, Environmental Pollution, Vol.239, 21-29.

Hancox P.J., Götz A.E., (2014), *South Africa's coalfields-A 2014 perspective*., Int. J. Coal. Geol., Vol.132, 170–254.

Harvey, C. and Heikkinen, N., (2018), *Congress Says Biomass Is Carbon-Neutral, but Scientists Disagree*, E & E News, https://www.scientificamerican.com/article/congress-says-biomass-is-carbon-neutral-but-scientists-disagree/, [Accessed 10 November 2019].

Hazra, S. K., (2002) *High Temperature Carbonization of Coal.* In: Two-Day Programme for Small and Tiny Sector on Eco-friendly Technologies for better Environmental Management, January 30-31, 2002, CSIR-NML.

Hedden, S., (2015), *How do we solve South Africa's energy crisis?* https://www.weforum.org/agenda/2015/09/how-do-we-solve-south-africas-energy-crisis, [Accessed on 09 November 2019].

Heim, K.R.G. and Bemtgen, J.M., (1998), *EU Clean coal technology: Co-combustion of coal and biomass*, Fuel Processing Technology, Vol.54, 159-169.

Heywood, V.H., Brummit, R.K, Culham, A. and Seberg, O., (2007), *Flowering plant families of the world*. Firefly Books Ltd, Buffalo, USA.

Hu, J., Yan, Y., Evrendilek, F., buyukada, M. and Liu, J., (2019), *Combustion behaviors of three bamboo residues: Gas emission, kinetic, reaction mechanism and optimization patterns*, Journal of Cleaner Production, Vol.235, 549-561.

Hughes, E., (2000), *Biomass co-firing economics, policy and opportunities*, Biomass Bioenergy, Vol.19, 457-465.

Hurskainen, M., and Vainikka, P., (2016), *Technology options for large-scale solid-fuel combustion*. in J Oakey (ed.), *Fuel Flexible Energy Generation: Solid, Liquid and Gaseous Fuel*, Woodhead Publishing, Woodhead publishing series in energy, Vol.91, 177-199.

Hurt, R.H. (1998), *Structure, properties and reactivity of solid fuels*, Proc Combust Inst, Vol.27, 2887-904.

IEA (International Energy Agency), (2017), World Energy Outlook 2017.

IEA Bioenergy, (2013), Bioenergy, *Land Use Change and Climate Change Mitigation*, https://www.ieabioenergy.com/wp-content/uploads/2013/10/Bioenergy-Land-Use-Change-and-Climate-Change-Mitigation-Background-Technical-Report.pdf , [Accessed 10 November 2019].

IEA, (2012), *Technology Roadmap - High-Efficiency, Low-Emissions Coal-Fired Power Generation*, International Energy Agency – IEA 9 rue de la Federation, 75015 Paris, France.

IEA, (2018), Global Energy & CO2 Status Report: The latest trends in energy and emissions in 2018, https://www.iea.org/geco/, [Accessed on 08 November 2019].

IEA-ETSAP, (2013), *Biomass co-firing in coal power plants*, https://www.iea-etsap.org/index.php/etsap-tools/acquiring-etsap-tools/10-home/74-co-firing-biomass [Accessed on 09 November 2019].

ISO, (2019), *Solid mineral fuels-Determination of ash*, https://www.iso.org/standard/55944.html, [Accessed on 10 November 2019].

Jeffrey, L.S., (2005), *Characterisation of the coal resources in South Africa*, The Journal of The South African Institute of Mining and Metallurgy, 95-102.

Johnson, M., (2014), *10 disadvantages of wind energy: Not as clean as you thought*, Udemy, https://blog.udemy.com/disadvantages-of-wind-energy/, [Accessed on 09 November 2019].

Joubert, M.K., (2017), *Contaminant fate in Searsia lancea woodlands on acid mine drainage in the Witwatersrand basin goldfields*, MSc dissertation, University of the Witwatersrand, Johannesburg.

K.C. Cottrell, (2016), *Flue gas desulfurization, Wet limestone-gypsum process*, https://www.eecpowerindia.com/codelibrary/ckeditor/ckfinder/userfiles/files/KC%20Cottrell.pdf [Accessed on 09 November 2019].

Kabakci, S.B. and Hacıbektasoglu, S.G., (2017), *Catalytic pyrolysis of biomass*, Intech Open, DOI: 10.5772/67569.

Kaplan, S.M., (2010), *Displacing coal with generation from existing natural gas fired power plants*, Congressional Research Service.

Kastanaki, E., Vamvuka, D., Grammelis, P. and Kakaras E., (2002), *Thermogravimetric studies of the behavior of lignite biomass blends during devolatilization*, Fuel Process Technology, Vol.77-78, 159-66.

Keating, M., (2011), *Cradle to grave: The environmental impacts from coal*, Clean Air Task Force, http://www.catf.us/resources/publications/files/Cradle_to_Grave.pdf, [Accessed on 09 November 2019].

Kleinhans, U., Wieland, C., Frandson, F. and Spliethoff, H., (2018), *Ash formation and deposition in coal and biomass fired combustion systems: Progress and challenges in the field of ash particle sticking and rebound behavior*, Progress in Energy and Combustion Science, Vol.68, 65-168.

Ko, S. and Lautala, P., (2018), *Advanced Woody Biomass Logistics for Co-Firing in Existing Coal Power Plant: Case Study of the Great Lakes States*, Journal of the Transportation Research Board, Vol-2672.

Kok, M. and Ozgur, E., (2013), *Thermal analysis and kinetics of biomass samples*, Fuel Processing Technology, Vol.106, 739-743.

Kumar, P.B.A.N., Motto, H. and Raskin, I., (1995), *Rhizofiltration: The Use of Plants to Remove Heavy Metals from Aqueous Streams*, Environmental Science and Technology, Vol.29(5), 1239-1245.

Lang, T. and Hurt, R.H., (2002), *Char combustion reactivities for a suite of diverse solid fuels and char forming organic model compounds*, Proc Combust Inst, Vol.29, 423–431.

Lange, C.A., Kotte, K., Smit, M., van Deventer, P.W. and van Rensburg, L., (2012), *Effects of different soil ameliorants on karee trees (Searsia lancea) growing on mine tailings dump soil-Part I: Port Trials*, International Journal of Phytoremediation, Vol.14(9), 908-924.

Li, J., Brzdekiewics, A., Yang, W. and Blasiak, W., (2012), *Co-firing based on biomass torrefaction in a pulverized coal boiler with aim of 100% fuel switching*, Applied Energy, Vol.99, 344–354.

Lin, C.Y. & Hsieng, M.J., (1995), *Emissions of oil-fired furnaces burning with sodium chloride-contained air*, Journal of Environmental Science and health. Part A: Environmental Science and Engineering and Toxicology, Vol.30, 1473-1497.

Lisnic, R. and Jinga, S.I., (2018), *Study on current state and future trends of flue gas desulfurization technologies: A review*, Romanian Journal of Materials, Vol.48(1), 83 – 90.

Liu, D.C., Mi, T., Shen, B.X. and Feng, B., (2002), *Reducing N_2O emission by co-combustion of coal and biomass*, Energy Fuels, Vol.16, 525-526.

Liu, N.A., Fan, W., Dobashi, R., Huang, L., (2002), *Kinetic modelling of thermal decomposition of natural cellulosic materials in air atmosphere*, Journal of Applied Pyrolysis, Vol.63, 303–325.

Luo, X., Wu, T., Shi, K., Song, M. and Rao, Y., (2018), *Biomass Gasification: An overview of technological barriers and socio-environmental impact*, InTech Open.

Luque, R. and Speight, J.D., (2015), *Gasification and synthetic liquid fuel production: an overview*, Fundamentals, Processes and Applications, 3-27.

Lyu, J., Yang, H., Ling, W., Nie, L., Yue, G., Li, R., Chen, Y., Wang, S., (2017), *Development of a supercritical and an ultra-supercritical circulating fluidized bed boiler*, Front. Energy 2019, Vol.13(1),114–119.

Ma, W., Zhou, H., Zhang, J., Zhang, K., Liu, D., Zhou, C. and Cen, K., (2018), *Behavior of Slagging Deposits during Coal and Biomass Co-combustion in a 300 kW Down-Fired Furnace*, Energy Fuels, Vol.32(4), 4399-4409.

Mahlaba, J.S., Kearsley, E.P. and Kruger, R.A., (2011), *Physical, chemical and mineralogical characterisation of hydraulically disposed fine coal ash from SASOL Synfuels*, Fuel, https://repository.up.ac.za/bitstream/handle/2263/16641/Mahlaba_Physical%282011%29.pdf?sequence=1 , [Accessed on 10 November 2019].

Makgato, S.S. and Chirwa, E.M.N., (2017), *Characteristics of Thermal Coal used by Power Plants in Waterberg Region of South Africa*, The Italian Association of Chemical Engineering, Vol.57, 510-516.

Makwarela, O., (2016), *Combustion and physicochemical properties of raw and thermally treated bamboo with coal*, MSc dissertation, University of the Witwatersrand, Johannesburg.

Maledi, N., (2017), *Characterisation of Mineral Matter in South African Coals Using MicroRaman Spectroscopy and Other Techniques*, Ph.D. dissertation, University of the Witwatersrand, Johannesburg.

Mayonde, S.G., (2013), *Genotypic and phylogeographic investigation of indigenous and alien Tamarix species in Southern Africa*, MSc dissertation, University of the Witwatersrand, Johannesburg.

Melissari, B., (2014), *Ash related problems with high alkali biomass and its mitigation: Experimental evaluation*, http://www.um.edu.uy/docs/3_ash_related_problems_with_high_alkalii_biomass_mitigation.pdf , [Accessed on 10 November 2019].

Meng, A., Zhou, H., Qin, L., Zhang, Y. and Li, Q., (2013), *Quantitative and kinetic TG-FTIR investigation on three kinds of biomass pyrolysis*, Journal of Analytical and Applied Pyrolysis, Vol.104, 28-37.

Miller, B.G., (2010), *Clean Coal Engineering Technology*, first edn, Butterworth-Heinemann, Oxford.

Miller, B.G., (2011), *Clean Coal Engineering Technology*, first edn, Butterworth-Heinemann, Oxford.

Miller, B.G., (2017), *Clean Coal Engineering Technology*, first edn, Butterworth-Heinemann, Oxford.

Mills S., (2016), *Low quality coals- Key commercial, environmental and plant considerations.* CCC/270, London, UK, IEA Clean Coal Centre.

Mills S.J., (2011), *Global perspective on the use of low quality coals*. CCC/180, London, UK, IEA Clean Coal Centre.

Mills S.J., (2008), *Meeting the demand for new coal-fired power plants*, IEA Clean Coal Centre.

Mining Weekly, (2016), *AngloGold Ashanti (AGA) Surface Operations*, https://www.miningweekly.com/article/vaal-river-surface-operations-south-africa-2016-07-15/rep_id:3650 , [Accessed on 10 November 2019].

Mock, C., Lee, H., Choi, S., Yang, W., Choi, S. and Manovic, V., (2018), *Combustion Behavior of Single Pellets of Coal–Wood Mixtures in a Hot Gas Flow Field*, *Energy and fuels*, Vol. 32(11), 11913-11923.

Mohan, D., Pittman, C.U. and Steele, P.H., (2006), *Pyrolysis of wood/biomass for bio-oil: A critical review*, Energy Fuels, Vol.20, 848-889.

Morisson, G., (2012), *Global outlook for Clean Coal Technologies and the work of the IEA Clean Coal Centre*, 4th EU - South Africa Coal and Clean Coal Working Group Meeting 5 to 6 November 2012, Johannesburg.

Mosito N.S.V., (2016), *Risk assessment of above ground biomass for fuel use in Eucalptus species cultivated on acid mine drainage in the Witwatersrand Basin gold fields*, MSc dissertation, University of the Witwatersrand, Johannesburg.

MRFR, (2019), *Biomass gasification market expected to reach 8.50% CAGR by size, share, growth, trends, forecast to 2023, https://www.reuters.com/brandfeatures/venture-capital/article?id=91531*, [Accessed on 08 November 2019].

Munir, S., Daood, S.S., Nimmo, W., Cunliffe, A.M. and Gibbs, B.M., (2009), *Thermal analysis and devolatilization kinetics of cotton stalk, sugar cane bagasse and shea meal under nitrogen and air atmospheres*, Bioresource Technology, Vol.100(3), 1413-1418.

Munir, S., Nimmo, W. and Gibbs, B.M., (2011), *The effect of air staged, co-combustion of pulverised coal and biomass blends on NOx emissions and combustion efficiency*, Fuel, Vol.90, 126-135.

Muthuraman, N., Namioka, T. and Yoshikawa, K., (2010), *A comparison of co-combustion characteristics of coal with wood and hydrothermally treated municipal solid waste*, Bioresource Technology, Vol.101(7), 2477-2482.

Nalbandian, H., (2011), *Expert systems and coal quality in power generation*, CCC/186, London, UK, IEA Clean Coal Centre.

Nassar, M.M., (1999), *Thermal analysis kinetics of bagasse and rice straw*, Energy Sources, Vol. 21, 131-137.

National Energy Technology Laboratory, (2019), *Fischer-Tropsch Synthesis*, https://www.netl.doe.gov/research/coal/energy-systems/gasification/gasifipedia/ftsynthesis, [Accessed on 08 November 2019].

National Geographic, (2019), *Causes of global warming explained: Human activity is driving climate change, including global temperature rise*, https://www.nationalgeographic.com/environment/global-warming/global-warming-causes/ , [Accessed 10 November 2019].

Niksa, S., Liu, G. and Hurt, R.H., (2003), *Coal conversion submodels for design applications at elevated pressures, Part I, Devolatilisation and char oxidation*, Prog Energy Combust Sci, Vol.29, 425-77.

Norton, G.A., (1992), *A review of the derivative thermogravimetric technique (burning profile) for fuel combustion studies*, Thermochimica Acta, Vol.214, 171-182.

Nunez, C., (2019), *Carbon dioxide levels at a record high. Here's what you need to know*, National Geographic, https://www.nationalgeographic.com/environment/global-warming/greenhouse-gases/, [Accessed November 8, 2019].

Nuortimo, K., (2015), *State of the art CFB technology for flexible large-scale utility power production*, Amec Foster Wheeler, Presented at Power Gen, Moscow, Russia, 3-5 March 2015.

Obe, A.M., (2017), *Development and deployment of HELE coal power technologies*, London, UK, IEA Clean Coal Centre.

Obernberger, I., Dahl, J. and Brunner, T., (1999), *Formation, composition and particle size distribution of fly ashes from biomass combustion plants*, In: Proceedings of the 4th biomass conference of the Americas, Oakland (CA): Elsevier, Science Ltd, 1377–85.

Oladejo, J., Shi, K., Meng, Y., Adegbite, S. and Wu, T., (2019), *Biomass constituents' interactions with coal during co-firing*, Energy Procedia, Vol.158, 1640-1645.

Ozawa, T., (1965), *A new method of analyzing thermogravimetric data*, Chem. Soc. Jpn, Vol. 38, 1881-1886.

Ozawa, T., (1992), *Estimation of activation energy by isoconversion methods*, Thermochimica Acta, Vol.203, 159-165.

Palgrave, K.C., (2002), *Keith Coates Palgrave: Trees of Southern Africa*, edn 3. Struik, Cape Town.

Park, S.W. and Jang, C.H., (2012), *Effects of pyrolysis temperature on changes in fuel characteristics of biomass char*, Energy, Vol.39, 187-195.

Pederson, L.S., Morgan, D.J, van de Kamp, W.L., Christensen, J., Jespersen, P. and Dam-Johansen K., (1997), *Effects on SO_x and NO_x emissions by co-firing straw and pulverized coal*, Energy Fuels, Vol.11, 439-446.

Pederson, L.S., Nielsen, H.P., Kills, S., Hansen, S., Dam-Johansen, K. and Kildsig, F. et al. (1996), *Full-scale co-firing of straw and coal*, Fuel, Vol.75, 1584-90.

Plantinfo, http://plantinfo.co.za/plant/searsia-lancea/ , [Accessed 10 November 2019].

Power Technology, (2019), *Drax Power Station, Cleanest And Most Efficient Coal-Fired Power Station In the United Kingdom*, https://www.power-technology.com/projects/drax/ , [Accessed on 09 November 2019].

Prairie State Energy Campus, (2010), Power Plant, www.prairiestateenergycampus.com, [Accessed on 09 November 2019].

Pretorius, I., Piketh, S., Burger, R., Neomagus, H., (2015), *A perspective of South African coal fired power stations emissions*, Journal of Energy in South Africa, Vol.26, N.3.

Quan, C. and Gao, N., (2016), *Copyrolysis of Biomass and Coal: A Review of Effects of Copyrolysis Parameters, Product Properties, and Synergistic Mechanisms*, BioMed Research International, Vol.2016.

Radenovic, A., (2006), Inorganic Constituents in Coal. *Kemija u Industriji*. Vol.55(2).

Ren, X., Sun, R., Meng, X., Vorobiev, N., Schiemann, M. and Levendis, Y.A., (2016), *Carbon, sulfur and nitrogen oxide emissions from combustion of pulverized raw and torrefied biomass*, Fuel, Vol.188, 310-323.

Research and Markets, (2019), *Global Flue Gas Desulfurization (FGD) Market Forecast to Reach $12 Billion by 2024 - Wet FGD System Category is Anticipated to Account for the Majority Share During the Forecast Period*, https://www.globenewswire.com/news-release/2019/05/01/1813319/0/en/Global-Flue-Gas-Desulfurization-FGD-Market-Forecast-to-Reach-12-Billion-by-2024-Wet-FGD-System-Category-is-Anticipated-to-Account-for-the-Majority-Share-During-the-Forecast-Period.html, [Accessed on 08 November 2019].

Riaza, J., Gibbins, J. and Chalmers, H., (2017), *Ignition and combustion of single particles of coal and biomass*, Energy Procedia, Vol.114, 6067-6073.

Rokni, E., Ren, X. and Levendis, Y.A, (2018), *Emissions of SO_2, NO_x, CO_2, and HCl from Co-firing of coals with raw and torrefied biomass fuels*, Fuel, Vol.211, 363-374.

Roni, M.S., Chowdhury, S., Mamun, S., Marufuzzaman, M., Johnson, S., Lein, W., (2017), *Biomass co-firing technology with policies, challenges and opportunities: A global review*, https://www.osti.gov/pages/servlets/purl/1407416 , [Accessed on 09 November 2019].

Rostam-Abadi, M., DeBarr J.A. and Chen, W.T., (1990), Thermochima Acta, Vol.166, 351

Rycroft, M., (2015), *Co-firing biomass with coal for power generation*, EE publishers, http://www.ee.co.za/article/co-firing-biomass-coal-power-generation.html [Accessed on 09 November 2019].

Rycroft, M., (2019), *Biomass gasification for large-scale electricity generation*. EE Publishers. https://www.ee.co.za/article/biomass-gasification-for-large-scale-electricity-generation.html, [Accessed on 08 November 2019].

Sahu, S.G., Chakraborty, N. and Sarkar, P., (2014), *Coal–biomass co-combustion: An overview*, Renewable and Sustainable Energy Reviews, Vol.39, 575–586.

Sahu, S.G., Sarkar, P., Mukherjee, A., Adak, A.K. and Charkraborty, N., (2013), *Studies on the co-combustion behaviour of coal/biomass blends using thermogravimetric analysis*, International Journal of Emerging Technology and Advanced Engineering, Vol.3, 131-138.

Saidur, R., Abdelaziz, E.A., Demirbas, A., Hossain, M.S. and Mekhilef, S., (2011), *A review on biomass as a fuel for boilers*, Renewable and Sustainable Energy Reviews, Vol.15(5), 2262-2289.

Saleh, S., Flensborg, J., Shoulaifar, T., Sárossy, Z., Hansen, B.B, Egsgaard, H., DeMartini, N., Jensen, P.A., Glarborg, P., Dam-Johansen, K., (2014), *Release of Chlorine and Sulfur during Biomass Torrefaction and Pyrolysis*, Energy and Fuels, Vol.28(6), 3738-3746.

Sarkar, D. K., (2015). *Thermal power plant: design and operation*, 1-84.

Sasol, 2019, https://www.sasol.com/innovation/gas-liquids/technology, [Accessed on 08 November 2019].

Satyendra, (2014), *Carbonization of coal for metallurgical coke production*. ISPAT GURU. https://www.ispatguru.com/carbonization-of-coal-for-metallurgical-coke-production/ [Accessed on 08 November 2019].

Saxena, P., (2013), *The optimum mix. Impact of coal quality variation on power plants*. Power Line Magazine; July 2013, 2 pp.

Sayigh, A., (2013), *Comprehensive Renewable Energy: Biomass Power Generation*. first ed. Elsevier Inc.

Sharma, K. K., (2015), *Enhancing value through better coal quality*. Coal Preparation Society of India Journal, Vol.7(17), 36-50.

Shen, D.K., Gu, S., Luo, K.H., Bridgwater, A.V. and Fang, M.X., (2009*), Kinetic study on thermal decomposition of woods in oxidative environment*, Fuel, Vol.88, 1024–1030.

Shrilekha, P.R. and Soni, A.H., (2015), *An approach on determination of coal quality using digital image processing*, Journal of Engineering Approach and Application, Vol.5(12), 38-41.

Singh, A., Sharma, V., Mittal, S., Pandey, G., Mudgal, D. and Gupta, P., (2017), *An overview of problems and solutions for components subjected to fireside of boilers*, International Journal of Industrial Chemistry, Vol.9, 1-15.

Slabbert, A. (2017). Expert warns SA on too much renewable energy, *Tech Central*. [Online]. Available from: https://www.techcentral.co.za/expert-warns-on-too-much-renewable-energy/72586/, [Accessed on 09 November 2019].

Slopiecka, K., Bartocci, P. and Fantozzi, F, (2011), *Thermogravimetric analysis and Kinetic study of poplar wood pyrolysis*, Third International Conference on Applied Energy, 16-18 May 2011, Perugia, Italy, 1687-1698.

South Africa state government, (2015), Energy Advocacy. http://www.energy.gov.za/files/media/Pub/Energy-Advocacy-May2015-Issue-1-newsletter.pdf [Accessed on 09 November 2019].

South African National Biodiversity Institute, http://pza.sanbi.org/tamarix-usneoides , [Accessed on 10 November 2019].

Speight, J.G., (2016), *High-temperature and low-temperature Fischer–Tropsch*, Fuel Flexible Energy Generation, 145-174.

Speight, J.G., (2017), *Industrial organic chemistry*, *Environmental organic chemistry for engineers*, Elsevier, 87-151.

Splienthoff, H. and Heim, K.R.G., (1998), *Effect of co-combustion of biomass on biomass emission in pulverized fuel furnaces*, Fuel Process Technology, Vol.54, 189-205.

Stahl, R., Henrich, E., Gehrmann, H.J., Vodegel, S. and Koch, M., (2004), *Definition of a standard biomass*, Integrated Project, Sustainable Energy Systems, Report prepared under the framework of project: RENEW – Renewable fuels for advanced power trains.

Statista, (2018), *Capacity of biomass power plants in selected countries and worldwide in 2018*, https://www.statista.com/statistics/264637/world-biomass-energy-capacity/ , [Accessed on 09 November 2019].

Strivastava, R.K. and Jozewics, W., (2001), *Flue gas desulfurization: the state of the art*, Journal of Air and Waste Management Association, Vol.51(12), 1676-88.

Strydom, C.A., Sehume, T.Z., Bunt, J.R. and van Dyk, J.C., (2015), *The influence of selected biomass additions on the co-pyrolysis of an inertinite-rich medium rank C grade South African coal*, The Journal of The Southern African Institute of Mining and Metallurgy, Vol.115, 707-716.

Sumitomo, (2017), *CFB Technology for Biomass and Waste Fuels*, Power Gen Asia, Bangkok, 19-21 September.

Sun, C.L. and Zhang, M.Y., (1998), *Ignition of coal particles at high pressure in a thermo gravimetric analyzer*, CombustFlame, Vol.115, 267–274.

Sung, Y., Lee, S., Kim, C., Jun, D., Moon, C., Choi, G. and Ki, D., (2016), S*ynergistic effect of co-firing woody biomass with coal on NOx reduction and burnout during air-staged combustion*, Experimental Thermal and Fluid Science, Vol.71, 114-125.

Tahmasebi, A., Kassim, M.A., Yu, J. and Bhattacharya, S., (2013), *Thermogravimetric study of the combustion of Tetraselmis suecica microalgae and its blend with a Victorian brown coal in O_2/N_2 and O_2/CO_2 atmospheres*, Bioresource Technology, Vol.150, 15-27.

Tanggara, D., Amijaya, D.H. and Surjono, S.S., (2018), *Evaluation of coking properties bituminous medium volatile coal*, Bata Ayau Formation, Kutai Basin, Central Kalimantan. IOP Conference Series: Earth and Environmental Science Sci. 212 012032.

Tanigichi, M., (2012), *Fundamental Experiments of Coal Ignition for Engineering Design of Coal Power Plants*, Intech Open, DOI: 10.5772/28477.

Taole, R., (2014), *The impact of coal quality and operating conditions on the efficiency of a spreader stoker boiler*, MSc thesis, University of the Witwatersrand, Johannesburg [Accessed November 8, 2019].

Tchapda, A.H. and Pisupati, S.V., (2014), *Characterization of coal and biomass chars from high temperature pyrolysis in CO_2 atmosphere*, Paper presented at 3first Annual International Pittsburgh Coal Conference: Coal - Energy, Environment and Sustainable Development, PCC 2014, Pittsburgh, United States, 10/6/14 - 10/9/14.

Teixeira, P., Lopes, H., Gulyurtlu, I., Lapa, N. and Abelha, P., (2012), *Evaluation of slagging and fouling tendency during biomass co-firing with coal in a fluidized bed*, Biomass and Bioenergy, Vol. 3, 192-203.

Tillman, D., Duong, D., Harding, N.S., (2012), *Solid Fuel Blending*, first ed. Imprint: Butterworth Heinemann.

Tillman, D.A., (2000), *Biomass Co-firing: The Technology, the Experience, the Combustion Consequences*, Biomass and Bioenergy, Vol.19(6),365-384.

Tillman, D.A., (2012). *The Combustion of Solid Fuels and Wastes. The Combustion of Solid Fuels and Wastes*, 1-378.

Tomimatsu, H., Iio, A., Adachi, M., Saw, L., Fletcher, C. and Tang, Y., (2014), *High CO_2 concentration increases relative leaf carbon gain under dynamic light in Dipterocarpus sublamellatus seedlings in a tropical rain forest, Malaysia*, Tree Physiology, Volume 34(9), September 2014, Pages 944–954.

USEA (U.S. Energy Association), (2002), *National Energy Security Post* 9/11, U.S. Energy Association, June 2002.

van Loo, S., and Koppejan, J., (2008), The Handbook of Biomass Combustion and Cofiring.

Varol, M., Antimtay, A.T., Bay, B. & Olgun, H., (2010), *Investigation of co-combustion characteristics of low quality lignite coals and biomass with thermogravimetric analysis*, *Thermochimica Acta*, Vol.510, 195-201.

Vasilev, S.V., Vassileva, C.G. and Baxter, D., (2014), *Trace element concentrations and associations in some biomass ashes*, Fuel, Vol.129, 292-313.

Venter, F. and Venter, J.A., (1996), *Making the most of indigenous trees*, Briza Publications, Pretoria.

VGB Powertech. (2008), *Advantages and limitations of biomass co-combustion in fossil fired power plants*, https://www.vgb.org/vgbmultimedia/Biomass_Co_combustion_March_2008-p-2141.pdf [Accessed on 09 November 2019].

Vhathvarothai, N., Ness, J. and Yu, J, (2014), *An investigation of thermal behaviour of biomass and coal during thermogravimetric analysis (TGA)*, International Journal of Energy Research, Vol.38(6), 804-812.

Vyazovkin, S. and Wight, C.A., (1999), *Model-free and model-fitting approaches to kinetic analysis of isothermal and nonisothermal data*, Thermochimica Acta, Vol.340-341, 53-68.

Wagoner, C.L. and Winegartner, E.C., (1973), J. Eng. Power, Vol.95, 119.

Wanenge, M.T., (2009*), Growth, biomass production and, carbon, sulfur and nitrogen contents of two Rhus species (Anacardiaceae) planted to control acid mine drainage: A case study on Highveld gold mines*, BSc Honours research report, University of the Witwatersrand, Johannesburg.

Wang, C., Wang, F., Yang, Q., Liang, R., (2009), *Thermogravimetric studies of the behavior of wheat straw with added coal during combustion*, Biomass Bioenergy, Vol.33, 50–56.

Wang, G., Zhang, J., Shao, J., Liu, Z., Zhang, G., Xu, T., Guo, J., Wang, H., Xu, R. and Lin, H., (2016), *Thermal behavior and kinetic analysis of co-combustion of waste biomass/low rank coal blends*, Energy Conversion and Management, Vol.124, 414-426.

Wang, J., Laborie, M.G. and Wolcott, M.P., (2005), *Comparison of model-free kinetic methods for modelling the cure kinetics of commercial phenol-formaldehyde resins*, Thermochimica Acta, Vol. 439, 68-73.

Weiersbye, I. M., (2007), In A, Fourie, M. Tibbett. and J. Wiertz [Eds]. *Global review and cost comparison of conventional and phyto-technologies for mine closure*, Mine Closure 2007, Australian Centre for Geomechanics, Perth, ISBN 978-0-9804 185-0-7.

Weiersbye, I.M. & Witkowski, E.T.F., (2007), *Impacts of acid mine drainage on the regeneration potential of Highveld phreatophyte trees*, In J.J. Bester, Seydack, A.H.W., Voster T., Van der Merwe, I.J., and Dzivhani S., Multiple use management of natural forests and woodlands: Policy Refinement and scientific progress IV. Department of Water Affairs and Forestry of South Africa, 224- 237.

Weiersbye, I.M., Cukrowska, E.M., Margalit, N., Feingersh, T., Revivo, G., Braun, 0., Stark, R., and Zur, Y., (2006), *Acid Mine Drainage (AMD) and Phreatophyte Vegetation: Cycling of Pollutants and Implications for Land-Use Planning*, Invited Paper Presented at the Natural Woodlands and Forests Symposium IV, Summerstrand, Port Elizabeth 2006, Department of Water Affairs and Forestry.

Weiersbye, I.M., Witkowski, E.T.F. and Reichardt, M., (2006b), *Floristic Composition of Gold and Uranium Tailings Dams, and Adjacent Polluted Areas, on South Africa's Deep Level Mines*, Bothalia. Vol.36 (I), 101-127.

Williams, B., (2013), *3 Challenges facing the solar energy industry*, Save on energy, https://www.saveonenergy.com/green-energy/3-challenges-facing-the-solar-energy-industry/ , [Accessed on 09 November 2019].

Wilson, H., Mycock, D. and Weiersbye, I., (2017), *The salt glands of Tamarix usneoides E. Mey. ex Bunge (South African Salt Cedar)*, International Journal of Phytoremediation, Vol.19(6).

Workman, D., (2019), *Coal Exports by Country*, http://www.worldstopexports.com/coal-exports-country/, [Accessed on 08 November 2019].

Yao, F., Wu, Q., Lei, Y., Guo, W. and Xu, Y., (2008), *Thermal decomposition kinetics of natural fibres: activation energy with dynamic thermogravimetric analysis*, Polymer Degradation and Stability, Vol. 93, 90-98.

Zhang, J., Ito, T., Okada, T., Oono, E. and Suda, T., (2013), *Improvement of NO_x formation model for pulverized coal combustion by increasing oxidation rate of HCN*, Fuel, Vol.113, 697-706.

Zheng, J.L., Zhu, Y.H., Zhu, M.Q., Kang, K. and Sun R.C., (2019), *A review of gasification of bio-oil for gas production*, Sustainable Energy and Fuels, Vol.3, 1600-1622.

Zhou, L., Wang, Y., Huang, Q. and Cai, J, (2006), *Thermogravimetric characteristics and kinetic of plastic and biomass blends co-pyrolysis*, Fuel Process Technology, Vol. 87, 963-969.

Zolin, A., Jensen, A.D. and Dam-Johansen, K., (2002), *Experimental study of char thermal deactivation*, Fuel, Vol.81, 1065-1075.

APPENDICES

Appendix A

Table A. 1: Proximate analysis of *Tamarix usneoides* in Red soil site

		FIRST RUN				**SECOND RUN**				**STANDARD DEVIATION**			
Tree name	**Tree part**	**TM (%)**	**VM (%)**	**ASH (%)**	**FC (%)**	**TM (%)**	**VM (%)**	**ASH (%)**	**FC (%)**	**TM (%)**	**VM (%)**	**ASH (%)**	**FC (%)**
	Twigs	6.97	71.13	8.24	13.67	6.9	70.67	8.62	13.82	0.05	0.33	0.27	0.11
	Wood	7.03	70.01	2.41	20.55	6.81	70.25	2.56	20.38	0.16	0.17	0.11	0.12
	Roots	8.9	60.16	11.53	19.41	8.99	59.53	11.54	19.94	0.06	0.45	0.01	0.37
	Blend 1	N/A											
T4	**Blend 2**	7.99	66.32	9.57	16.13	7.86	64.94	9.83	17.37	0.09	0.98	0.18	0.88
	Wood	7.03	69.51	2.56	20.89	6.81	70.8	2.47	19.92	0.16	0.91	0.06	0.69
	DB	8.32	60.81	14.06	16.8	7.72	59.55	17.5	15.22	0.42	0.89	2.43	1.12
	Roots	7.74	60.21	17.54	14.52	8.36	60.65	14.55	16.45	0.44	0.31	2.11	1.36
	Blend 1	N/A											
T6	**Blend 2**	7.32	62.89	12.33	17.45	7.35	64.48	10.49	17.68	0.02	1.12	1.30	0.16
T4 +T6 BLEND		8.31	64.15	9.07	18.47	8.58	63.64	8.88	18.9	0.19	0.36	0.13	0.30

Table A. 2: Proximate analysis of *Searsia lancea* in Red soil site

		FIRST RUN				SECOND RUN				STANDARD DEVIATION			
Tree name	**Tree part**	**TM (%)**	**VM (%)**	**ASH (%)**	**FC (%)**	**TM (%)**	**VM (%)**	**ASH (%)**	**FC (%)**	**TM (%)**	**VM (%)**	**ASH (%)**	**FC (%)**
S4	**Leaves**	4.18	68.95	4.36	22.51	4.18	68.34	4.46	23.03	0.00	0.43	0.07	0.37
	Twigs	7.39	70.41	1.65	20.56	6.96	70.59	2.4	20.05	0.30	0.13	0.53	0.36
	DB	7.27	71.65	2.13	18.95	7.22	70.41	2.56	19.81	0.04	0.88	0.30	0.61
	Roots	7.17	70.15	2.72	19.96	7.12	68.93	2.83	21.12	0.04	0.86	0.08	0.82
	Blend 1	6.12	70.68	2.66	20.55	6.06	69.85	2.96	21.13	0.04	0.59	0.21	0.41
	Blend 2	6.86	70.86	2.51	19.76	7.01	70.65	2.46	19.89	0.11	0.15	0.04	0.09
S5	**Leaves**	4.92	69.45	3.95	21.68	5.04	68.57	3.97	22.42	0.08	0.62	0.01	0.52
	Twigs	6.63	69.25	3.32	20.8	7.04	69.06	3.25	20.64	0.29	0.13	0.05	0.11
	Wood	8.08	67.72	3.58	20.63	7.94	68.23	3.39	20.45	0.10	0.36	0.13	0.13
	DB	6.11	77.01	1.11	15.77	6	77.62	1.26	15.12	0.08	0.43	0.11	0.46
	Stump	9.01	60.36	6.46	24.16	9.16	62.82	6.57	21.45	0.11	1.74	0.08	1.92
	Roots	6.96	67.25	4.5	21.3	6.97	67.42	4.59	21.02	0.01	0.12	0.06	0.20
	Blend 1	5.79	70.08	2.91	21.22	6.08	70.26	2.97	20.69	0.21	0.13	0.04	0.37
	Blend 2	7.42	68.88	3.73	19.98	7.26	69.11	3.54	20.1	0.11	0.16	0.13	0.08
S4 +S5 BLEND		8.42	66.53	3.8	21.25	8.4	67.01	3.74	20.85	0.01	0.34	0.04	0.28

Table A. 3: Proximate analysis of *Tamarix usneoides* in Mispah site

		FIRST RUN				SECOND RUN				STANDARD DEVIATION			
Tree name	**Tree part**	**TM (%)**	**VM (%)**	**ASH (%)**	**FC (%)**	**TM (%)**	**VM (%)**	**ASH (%)**	**FC (%)**	**TM (%)**	**VM (%)**	**ASH (%)**	**FC (%)**
	Leaves	8.66	67.44	15.84	8.06	9.08	66.58	15.44	8.90	0.30	0.61	0.28	0.59
	Twigs	6.80	70.00	8.07	15.14	7.31	69.88	7.85	14.95	0.36	0.08	0.16	0.13
	Wood	9.00	68.28	7.28	15.44	8.90	69.04	6.63	15.43	0.07	0.54	0.46	0.01
	Roots	7.33	59.22	21.46	11.99	7.71	59.08	21.48	11.73	0.27	0.10	0.01	0.18
	Root Ball	7.80	57.31	22.97	11.91	7.86	56.81	23.54	11.79	0.04	0.35	0.40	0.08
	Blend 1	7.58	63.59	15.58	13.26	8.81	62.84	15.32	13.03	0.87	0.53	0.18	0.16
T11	**Blend 2**	7.27	63.15	16.06	13.53	8.54	62.52	15.20	13.74	0.90	0.45	0.61	0.15
	Leaves	8.93	67.14	14.23	9.71	8.98	66.35	14.24	10.44	0.04	0.56	0.01	0.52
	Twigs	8.02	72.05	7.67	12.27	8.07	69.71	7.66	14.57	0.04	1.65	0.01	1.63
	Wood	8.17	66.67	8.25	16.91	8.22	66.90	8.97	15.92	0.04	0.16	0.51	0.70
	Roots	6.62	56.42	26.26	10.70	6.36	54.88	27.47	11.29	0.18	1.09	0.86	0.42
	Root Ball	8.39	61.50	16.65	13.46	8.36	61.49	16.58	13.58	0.02	0.01	0.05	0.08
	Blend 1	7.56	64.07	15.10	13.27	8.88	63.53	15.02	12.57	0.93	0.38	0.06	0.49
T12	**Blend 2**	7.27	63.33	15.21	14.18	7.34	63.56	15.39	13.71	0.05	0.16	0.13	0.33
T11+T12 BLEND		8.35	68.26	7.44	15.95	8.39	68.77	7.51	15.33	0.03	0.36	0.05	0.44

Table A. 4: Proximate analysis of *Searsia lancea* in Mispah site

		FIRST RUN				SECOND RUN				STANDARD DEVIATION			
Tree name	**Tree part**	**TM (%)**	**VM (%)**	**ASH (%)**	**FC (%)**	**TM (%)**	**VM (%)**	**ASH (%)**	**FC (%)**	**TM (%)**	**VM (%)**	**ASH (%)**	**FC (%)**
S11	**Leaves**	7.97	65.58	5.71	20.74	8.03	65.85	5.65	20.47	0.04	0.19	0.04	0.19
	Twigs	7.37	67.77	3.96	20.90	7.50	68.44	3.89	20.17	0.09	0.47	0.05	0.52
	Wood	7.67	70.35	2.51	19.47	7.77	69.68	2.49	20.06	0.07	0.47	0.01	0.42
	DB	7.04	73.92	2.80	16.24	7.65	67.59	5.01	19.75	0.43	4.48	1.56	2.48
	Roots	8.17	67.72	2.67	21.44	8.17	67.77	2.67	21.44	0.00	0.04	0.00	0.00
	Blend 1	7.76	67.02	5.00	20.23	7.67	67.53	4.97	19.83	0.06	0.36	0.02	0.28
	Blend 2	7.40	68.85	4.68	19.07	7.44	67.99	4.78	19.79	0.03	0.61	0.07	0.51
S12	**Leaves**	8.12	65.49	5.90	20.49	8.86	64.55	5.84	20.75	0.52	0.66	0.04	0.18
	Twigs	7.58	68.82	3.67	19.93	8.00	71.73	3.48	16.80	0.30	2.06	0.13	2.21
	Wood	7.80	69.90	3.11	19.19	8.19	69.71	2.91	19.20	0.28	0.13	0.14	0.01
	DB	8.40	69.04	5.27	17.29	8.92	67.67	5.14	18.26	0.37	0.97	0.09	0.69
	Stump	7.19	71.54	2.03	19.24	7.78	71.19	2.01	19.02	0.42	0.25	0.01	0.16
	Roots	8.13	61.76	10.61	19.50	8.51	61.28	10.78	19.43	0.27	0.34	0.12	0.05
	RB	7.35	62.40	10.83	19.42	7.74	62.85	9.60	19.81	0.28	0.32	0.87	0.28
	Blend 1	7.70	66.24	6.03	20.03	8.60	66.57	5.60	19.24	0.64	0.23	0.30	0.56
	Blend 2	7.60	67.13	5.93	19.33	8.64	66.89	5.51	18.96	0.74	0.17	0.30	0.26
S11+S12 BLEND		8.30	69.12	3.84	18.74	8.29	69.67	3.97	18.07	0.01	0.39	0.09	0.47

Table A. 5: Proximate analysis of *Tamarix usneoides* in West complex site

		FIRST RUN				SECOND RUN				STANDARD DEVIATION			
Tree name	**Tree part**	**TM (%)**	**VM (%)**	**ASH (%)**	**FC (%)**	**TM (%)**	**VM (%)**	**ASH (%)**	**FC (%)**	**TM (%)**	**VM (%)**	**ASH (%)**	**FC (%)**
	Leaves	7.67	69.84	12.95	9.54	7.34	68.94	13.75	9.97	0.23	0.64	0.57	0.30
	Twigs	6.77	71.33	6.13	15.76	6.41	71.64	6.27	15.68	0.25	0.22	0.10	0.06
	Wood	5.98	71.70	6.54	15.78	5.77	73.09	6.88	14.26	0.15	0.98	0.24	1.07
	Roots	8.48	70.07	8.44	13.00	8.65	64.75	11.32	15.28	0.12	3.76	2.04	1.61
	Rootball	8.41	65.00	11.40	15.20	8.36	64.40	11.39	15.85	0.04	0.42	0.01	0.46
	Blend 1	7.10	68.47	9.71	14.72	7.02	69.59	9.86	13.52	0.06	0.79	0.11	0.85
T7	**Blend 2**	7.41	67.85	8.92	15.81	7.33	68.35	8.76	15.56	0.06	0.35	0.11	0.18
	Leaves	8.36	68.37	15.59	7.69	8.65	66.75	15.59	9.01	0.21	1.15	0.00	0.93
	Twigs	4.94	71.93	5.22	17.91	5.20	72.02	5.09	17.68	0.18	0.06	0.09	0.16
	Wood	7.20	69.22	8.33	15.25	7.35	67.80	8.38	16.47	0.11	1.00	0.04	0.86
	Blend 1	6.49	70.12	9.76	13.63	6.63	68.87	9.84	13.65	0.10	0.88	0.06	0.01
T9	**Blend 2**	7.39	67.59	8.36	16.67	7.25	69.04	7.96	15.75	0.10	1.03	0.28	0.65
T7 +T9 BLEND		8.11	68.14	8.31	15.43	8.24	68.92	8.38	14.46	0.09	0.55	0.05	0.69

Table A. 6: Proximate analysis of *Searsia lancea* in West complex site

		FIRST RUN				SECOND RUN				STANDARD DEVIATION			
Tree name	**Tree part**	**TM (%)**	**VM (%)**	**ASH (%)**	**FC (%)**	**TM (%)**	**VM (%)**	**ASH (%)**	**FC (%)**	**TM (%)**	**VM (%)**	**ASH (%)**	**FC (%)**
S7	**Leaves**	6.37	66.70	4.59	22.33	7.36	66.15	4.55	21.94	0.70	0.39	0.03	0.28
	Twigs	5.05	68.72	3.67	22.56	6.65	67.51	4.18	21.62	1.13	0.86	0.36	0.66
	Wood	7.40	70.19	1.65	20.77	7.30	68.13	2.66	21.90	0.07	1.46	0.71	0.80
	DB	7.58	68.57	2.99	20.86	7.35	69.99	3.14	19.52	0.16	1.00	0.11	0.95
	Roots	7.80	63.16	7.08	21.96	8.32	62.55	7.03	22.10	0.37	0.43	0.04	0.10
	Root Ball	7.18	60.01	8.55	24.27	7.78	59.42	8.71	24.08	0.42	0.42	0.11	0.13
	Blend 1	6.83	65.75	4.82	22.61	7.00	65.50	5.06	22.44	0.12	0.18	0.17	0.12
	Blend 2	7.22	65.32	5.43	22.03	7.22	65.35	5.37	22.06	0.00	0.02	0.04	0.02
S8	**Leaves**	5.81	66.92	4.15	23.11	5.91	67.43	4.46	22.19	0.07	0.36	0.22	0.65
	Twigs	7.53	69.62	1.65	21.20	6.80	71.05	2.23	19.92	0.52	1.01	0.41	0.91
	Wood	6.99	72.04	0.57	20.40	6.30	72.29	2.09	19.33	0.49	0.18	1.07	0.76
	DB	8.35	67.71	1.95	21.99	7.79	68.16	3.18	20.88	0.40	0.32	0.87	0.78
	Roots	8.26	66.55	3.24	21.95	7.48	65.85	4.72	21.95	0.55	0.49	1.05	0.00
	Blend 1	7.23	67.91	3.11	21.75	7.32	68.20	3.29	21.20	0.06	0.21	0.13	0.39
	Blend 2	7.99	68.61	3.00	20.40	7.86	68.42	3.00	20.71	0.09	0.13	0.00	0.22
S7+S8 BLEND		8.30	66.68	3.92	21.10	8.39	66.21	3.95	21.45	0.06	0.33	0.02	0.25

Table A. 7: Proximate analysis of *Tamarix usneoides* in Madala site

		FIRST RUN				SECOND RUN				STANDARD DEVIATION			
Tree name	**Tree part**	**TM (%)**	**VM (%)**	**ASH (%)**	**FC (%)**	**TM (%)**	**VM (%)**	**ASH (%)**	**FC (%)**	**TM (%)**	**VM (%)**	**ASH (%)**	**FC (%)**
	Leaves	9.05	67.09	14.10	9.79	8.40	66.88	15.59	9.13	0.46	0.15	1.06	0.47
	Twigs	6.97	69.61	6.59	16.83	6.96	69.60	6.66	16.78	0.01	0.01	0.05	0.04
	Wood	7.45	70.45	6.45	15.65	7.42	70.12	6.19	16.28	0.02	0.23	0.18	0.45
	DB	7.91	69.15	7.45	15.49	7.81	69.73	7.31	15.14	0.07	0.41	0.10	0.25
	Roots	7.64	70.28	7.42	14.67	7.42	69.31	8.17	15.10	0.16	0.69	0.53	0.30
	Blend 1	7.66	68.04	9.11	15.19	7.47	68.23	9.15	15.14	0.13	0.13	0.03	0.04
T1	**Blend 2**	7.58	69.60	7.13	15.70	7.60	69.32	7.37	15.72	0.01	0.20	0.17	0.01
	Leaves	7.67	67.95	15.09	9.30	7.54	71.55	15.33	5.59	0.09	2.55	0.17	2.62
	Twigs	5.39	72.70	4.77	17.14	4.89	72.42	5.66	17.03	0.35	0.20	0.63	0.08
	DB	6.99	71.73	6.71	14.57	7.01	72.05	6.70	14.24	0.01	0.23	0.01	0.23
	Stump	8.36	67.35	10.06	14.23	8.19	67.53	10.06	14.22	0.12	0.13	0.00	0.01
	Blend 1	7.00	70.14	9.75	13.11	6.73	68.35	9.99	14.93	0.19	1.27	0.17	1.29
T3	**Blend 2**	7.22	70.45	9.00	13.34	7.26	69.47	9.23	14.04	0.03	0.69	0.16	0.49
T1+T3 BLEND		8.28	69.14	8.05	14.53	8.24	68.78	8.30	14.68	0.03	0.25	0.18	0.11

Table A. 8: Proximate analysis of *Searsia lancea* in Madala site

		FIRST RUN				SECOND RUN				STANDARD DEVIATION			
Tree name	**Tree part**	**TM (%)**	**VM (%)**	**ASH (%)**	**FC (%)**	**TM (%)**	**VM (%)**	**ASH (%)**	**FC (%)**	**TM (%)**	**VM (%)**	**ASH (%)**	**FC (%)**
S1	**Leaves**	7.60	64.34	4.44	23.62	7.56	64.98	4.48	22.99	0.03	0.45	0.03	0.45
	Twigs	8.30	69.61	3.77	18.32	8.20	67.83	3.61	20.36	0.07	1.26	0.11	1.44
	Wood	7.99	67.80	3.70	20.51	8.05	67.89	3.49	20.57	0.04	0.06	0.15	0.04
	DB	7.25	71.87	3.23	17.66	7.22	71.22	3.22	18.35	0.02	0.46	0.01	0.49
	Stump	9.06	60.50	7.78	22.66	9.06	58.95	8.23	23.75	0.00	1.10	0.32	0.77
	Blend 1	8.14	66.45	4.43	20.97	7.92	66.69	4.64	20.75	0.16	0.17	0.15	0.16
	Blend 2	8.18	67.44	4.18	20.20	8.10	66.55	4.48	20.87	0.06	0.63	0.21	0.47
S3	**Leaves**	7.38	66.00	5.65	20.97	7.31	65.14	5.71	21.84	0.05	0.61	0.04	0.62
	Twigs	7.95	65.75	3.94	22.36	7.87	64.96	3.91	23.26	0.06	0.56	0.02	0.64
	Wood	8.09	64.90	5.82	21.19	7.98	64.43	6.23	21.36	0.08	0.33	0.29	0.12
	DB	7.57	71.67	2.88	17.87	7.57	71.98	2.76	17.69	0.00	0.22	0.08	0.13
	Roots	7.29	55.56	19.04	18.11	7.38	54.67	20.10	17.86	0.06	0.63	0.75	0.18
	Blend 1	7.70	64.51	7.91	19.89	7.57	71.98	2.76	17.69	0.09	5.28	3.64	1.56
	Blend 2	7.64	63.46	9.36	19.54	7.58	62.92	10.11	19.38	0.04	0.38	0.53	0.11
S1+S3 BLEND		8.48	64.54	6.56	20.43	8.26	64.86	6.63	20.25	0.16	0.23	0.05	0.13

Table A. 9: Ultimate analysis of tree blends, discard coal and ROM: Test 1

Sample ID	C (%)	H (%)	N (%)	S (%)	M (%)	A (%)	O %)
T1T3	40.93	5.935	0.44	0.937	8.26	8.18	35.318
S1S3	44.98	6.143	0.38	0.135	8.37	6.6	33.392
T4T6	41.99	5.769	0.97	0.843	8.45	8.98	32.998
S4S6	44.82	6.026	0.42	0.1	8.41	3.77	36.454
T7T9	43.88	6.165	1.09	1.145	8.18	8.35	31.19
S7S9	45.93	6.156	0.44	0.1	8.35	3.94	35.084
T11T12	43.34	6.44	1.02	1.29	8.37	7.48	32.06
S11S12	44.92	6.29	0.44	0.1	8.3	3.91	36.04
S1 Leaves	47.98	5.96	1.59	0.1	7.58	4.46	32.33
T1 Leaves	37.98	5.001	0.82	2.09	8.73	14.84	30.539
T7 Leaves	40.89	5.231	1.47	2.294	7.51	13.35	29.255
Discard	42.02	1.806	1.08	4.139	2.06	41.95	6.945
ROM	49.01	3.376	1.24	1.768	2.24	29.42	12.946

Table A. 10: Ultimate analysis of tree blends, discard coal and ROM: Test 2

Sample ID	C (%)	H (%)	N (%)	S (%)	M (%)	A (%)	O %)
T1T3	40.9	5.892	0.41	0.979	8.26	8.18	35.379
S1S3	45.71	6.207	0.42	0.152	8.37	6.6	32.541
T4T6	42.78	5.836	1.01	0.78	8.45	8.98	32.164
S4S6	45.5	6.137	0.45	0.1	8.41	3.77	35.633
T7T9	43.21	6.18	1.01	1.173	8.18	8.35	31.897
S7S9	45.52	6.243	0.48	0.1	8.35	3.94	35.367
T11T12	42.98	6.32	0.96	1.32	8.37	7.48	32.57
S11S12	45.31	6.4	0.43	0.1	8.3	3.91	35.55
S1 Leaves	47.87	5.986	1.6	0.1	7.58	4.46	32.404
T1 Leaves	38.27	5.069	0.84	2.029	8.73	14.84	30.222
T7 Leaves	40.96	5.297	1.47	2.244	7.51	13.35	29.169
Discard	41.85	1.816	1.06	4.108	2.06	41.95	7.156
ROM	48.87	3.347	1.21	1.819	2.24	29.42	13.094

Table A. 11: Calorific values of tree blends

		Test 1	Test 2
Site	**Sample ID**	**CV (MJ/kg)**	
	T1	16.25	16.21
	T3	15.79	15.99
	T1 + T3	15.79	15.99
	S1	17.20	17.09
	S3	16.48	16.49
Madala	**S1 + S3**	17.02	17.11
	T4	16.71	16.71
	T6	15.83	15.68
	T4 + T6	16.63	16.66
	S4	17.33	17.34
	S5	17.31	17.37
Red soil	**S4 + S5**	17.22	17.40
	T7	16.38	16.34
	T9	16.46	16.52
	T7 + T9	16.74	16.32
	S7	17.30	17.25
	S8	17.30	17.27
West complex	**S7 + S8**	17.22	17.33
	T11	16.37	16.26
	T12	16.23	16.12
	T11 + T12	16.29	16.23
	S11	17.56	17.62
	S12	16.34	16.86
Mispah	**S11 + S12**	17.37	17.10

Table A. 12: Calorific value of different tree parts in S4

	Test 1	**Test 2**
Tree part	**CV (MJ/kg)**	
Leaves	19.21	19.21
Twigs	18.11	18.29
Dry Biomass	16.96	16.91
Roots	17.12	17.30
Blend 1	17.57	17.08
Blend 2	17.33	17.34

Appendix B

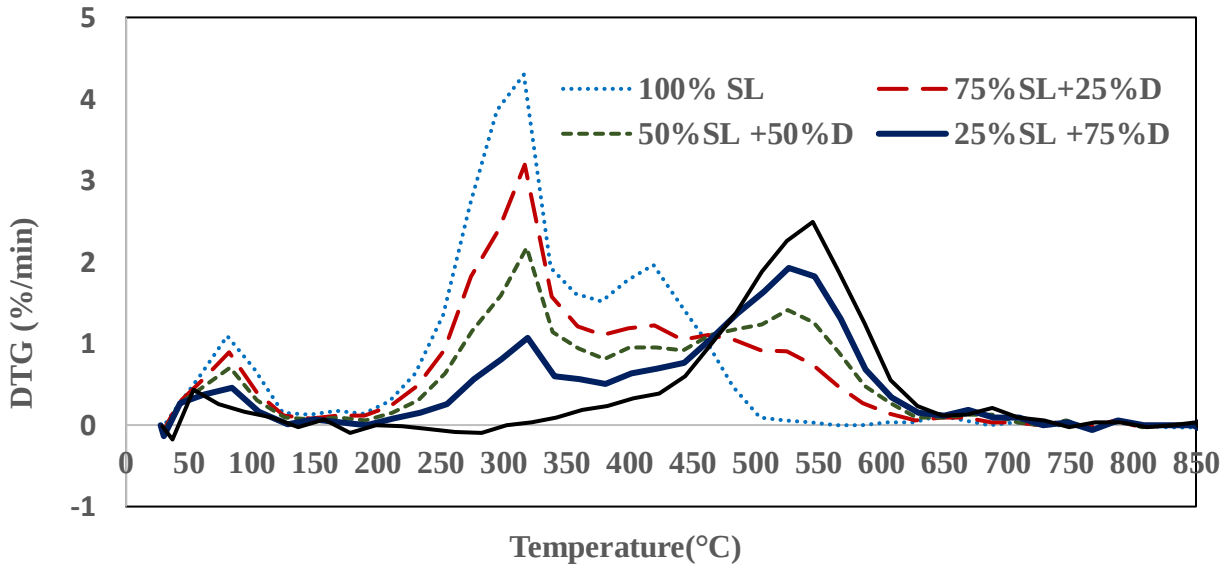

Figure B. 1 : Combustion characteristics of *Searsia lancea* on Madala site with different discard proportions.

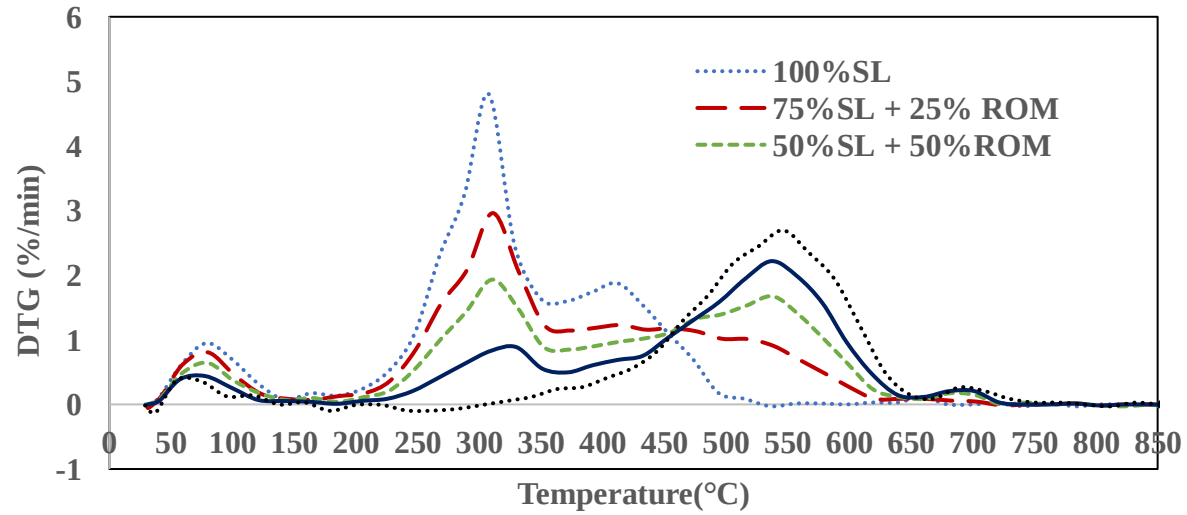

Figure B. 2: Combustion characteristics of *Searsia lancea* on Madala site with different ROM proportions

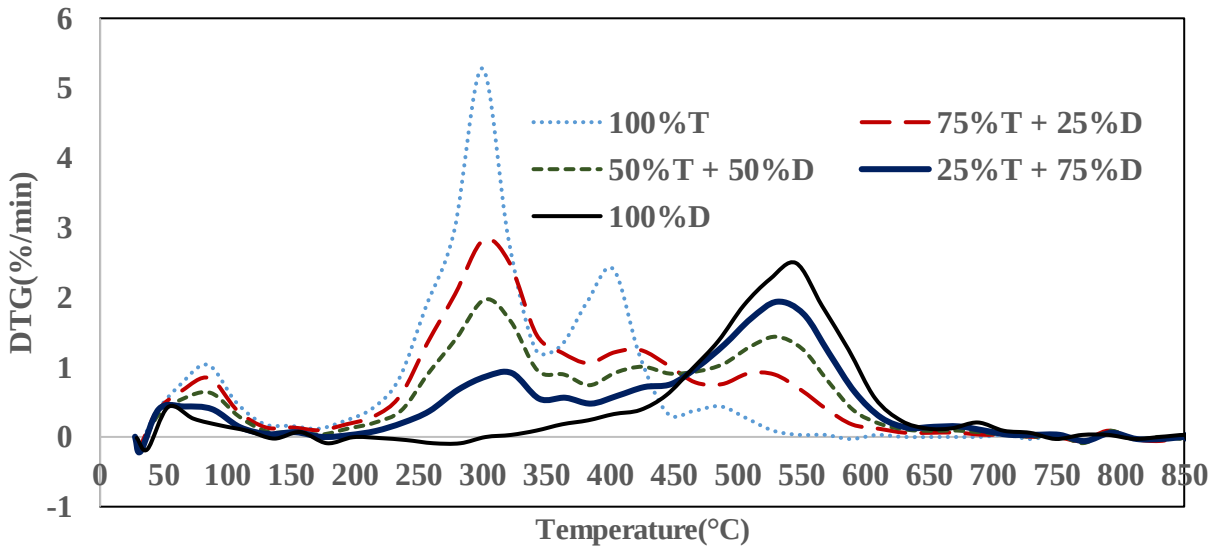

Figure B. 3: Combustion characteristics of *Tamarix usneoides* on Madala site with different discard proportions.

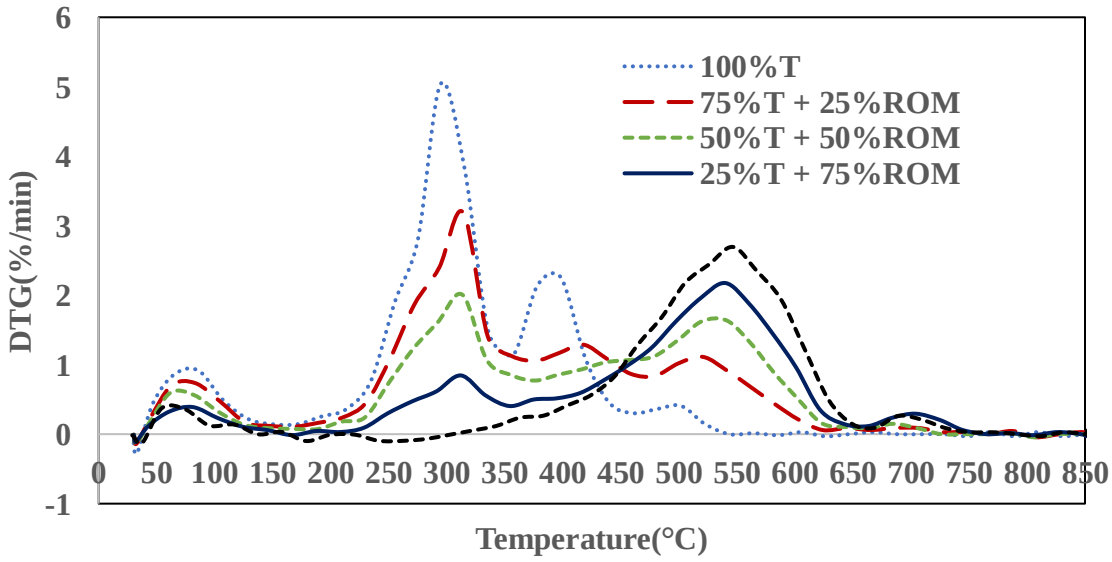

Figure B. 4: Combustion characteristics of Tamarix usneoides on Madala site with different ROM proportions

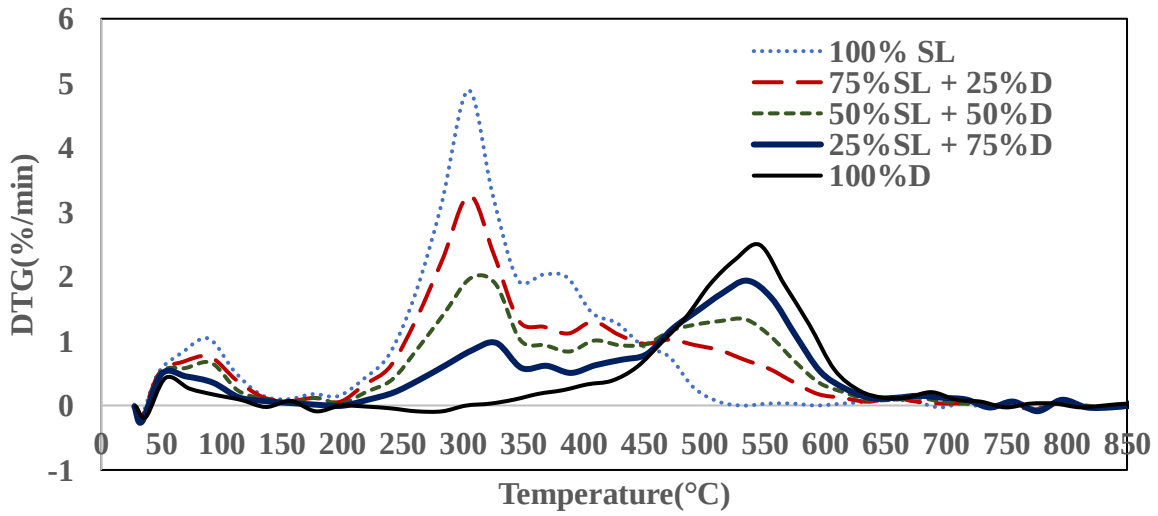

Figure B. 5: Combustion characteristics of *Searsia lancea* on red soil with different coal proportions

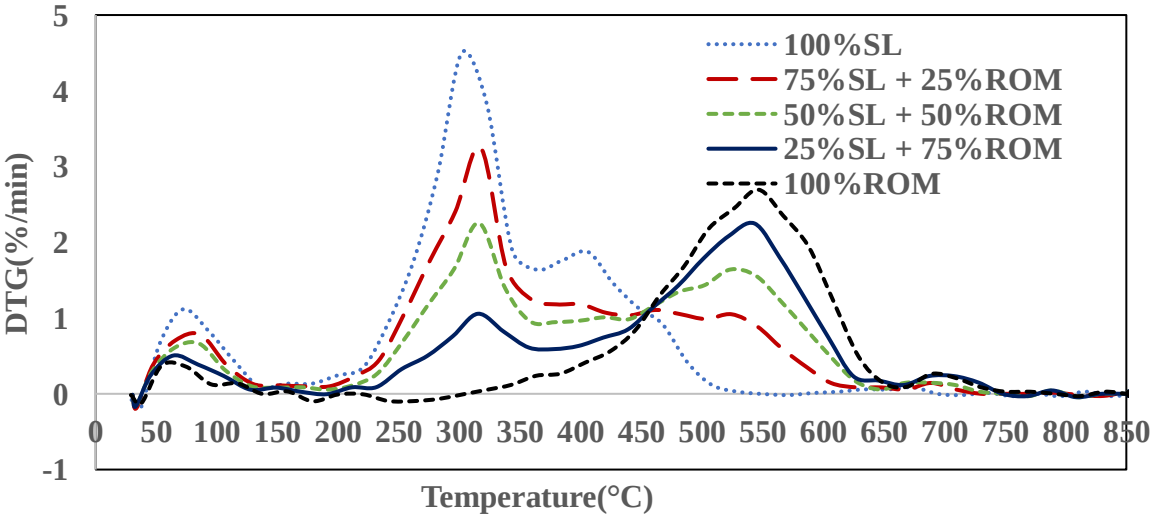

Figure B. 6: Combustion characteristics of *Searsia lancea* on red soil with different ROM proportions

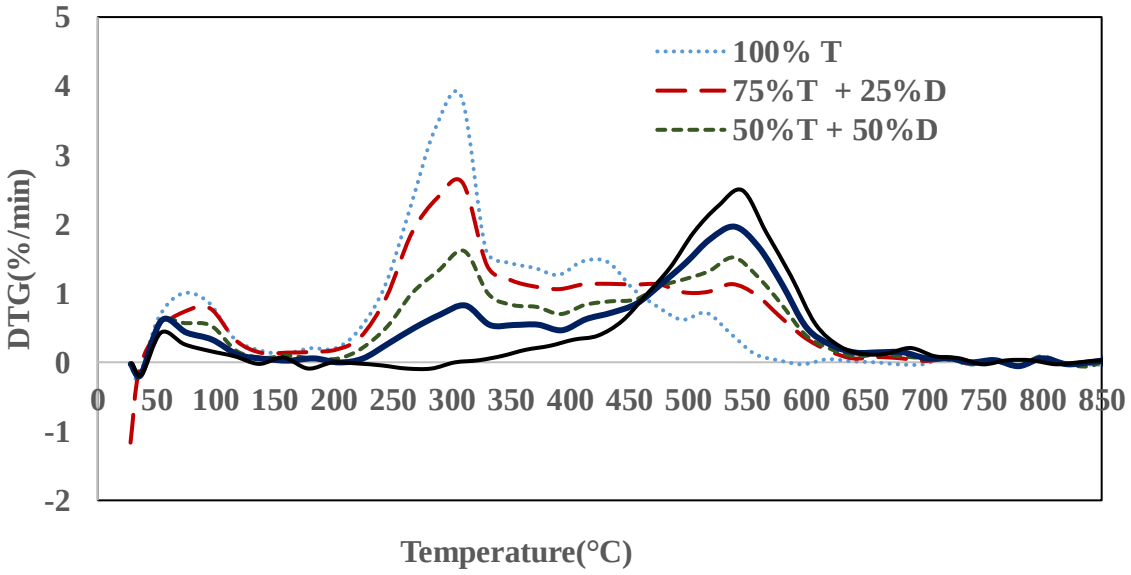

Figure B. 7: Combustion characteristics of *Tamarix usneoides* on red soil with different discard proportions

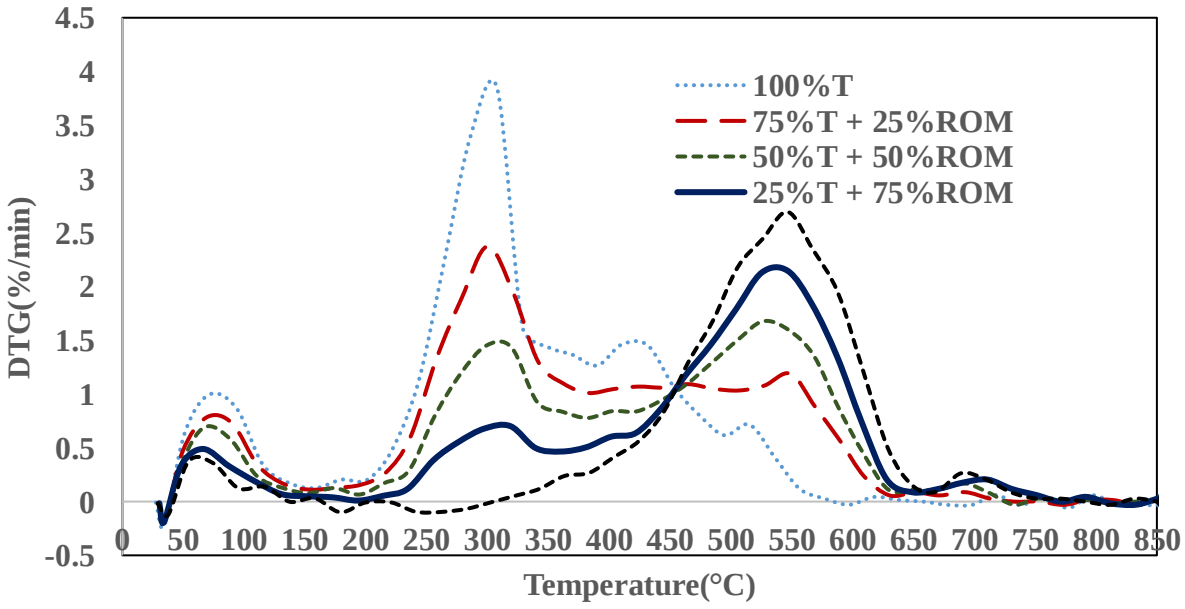

Figure B. 8: Combustion characteristics of *Tamarix usneoides* on Red soil with different ROM proportions

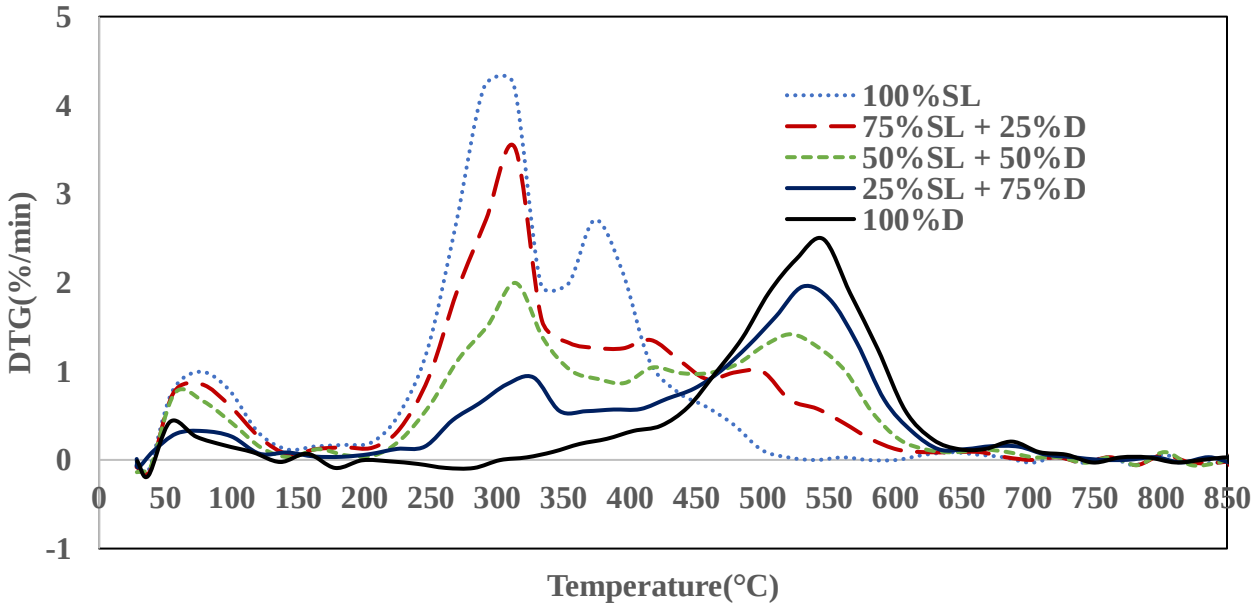

Figure B. 9: Combustion characteristics of *Searsia lancea* on West complex with different discard proportion

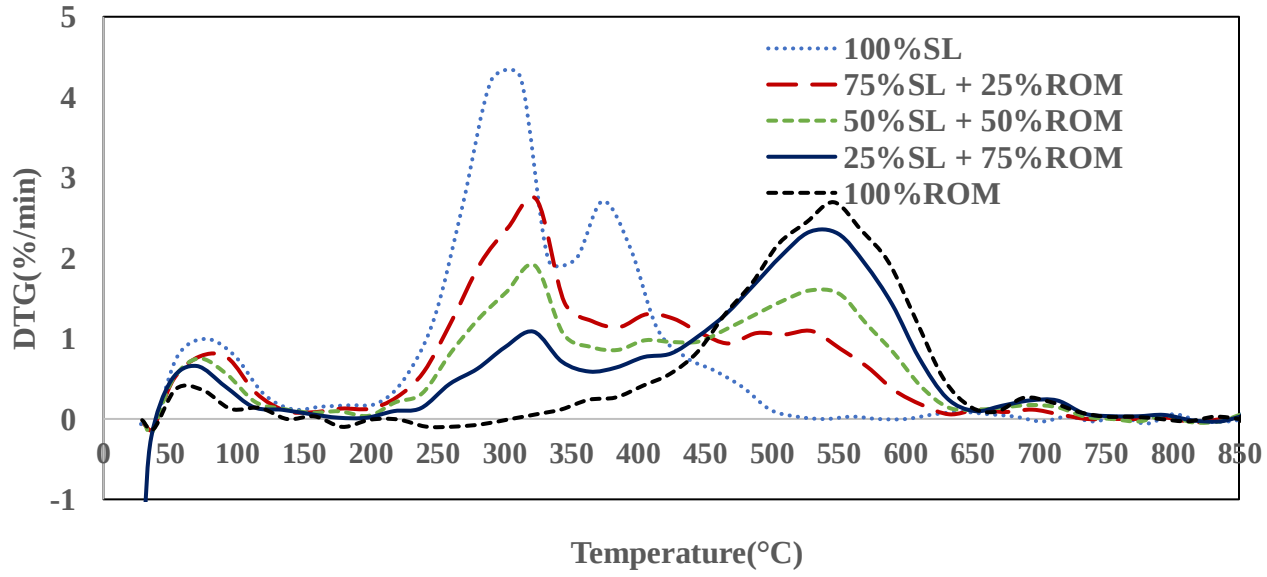

Figure B. 10: Combustion characteristics of *Searsia lancea* on West complex with different ROM proportions

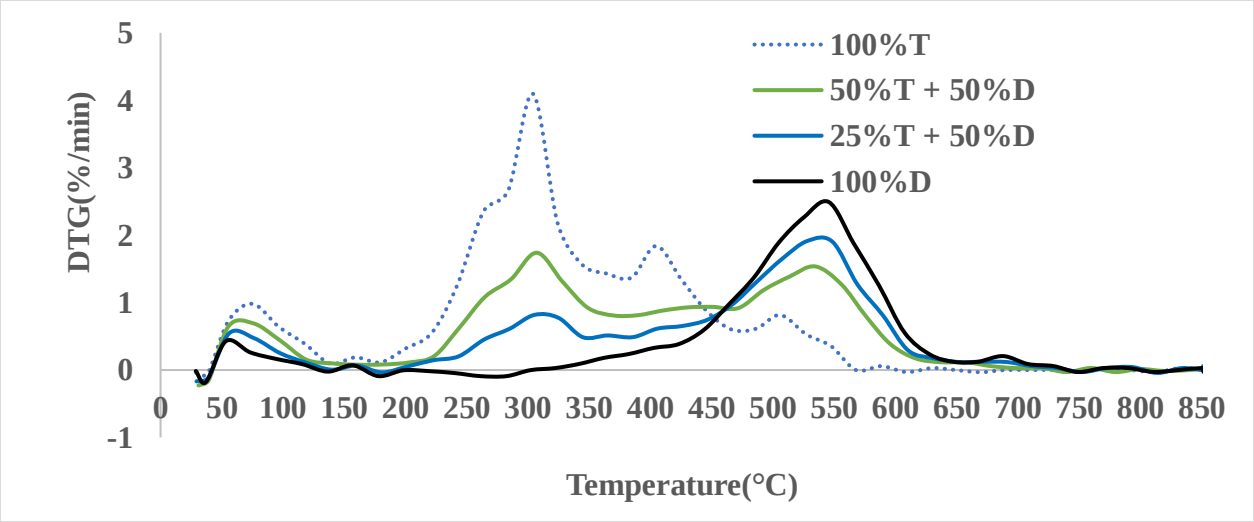

Figure B. 11: Combustion characteristics of *Tamarix usneoides* on West Complex with different discard proportions

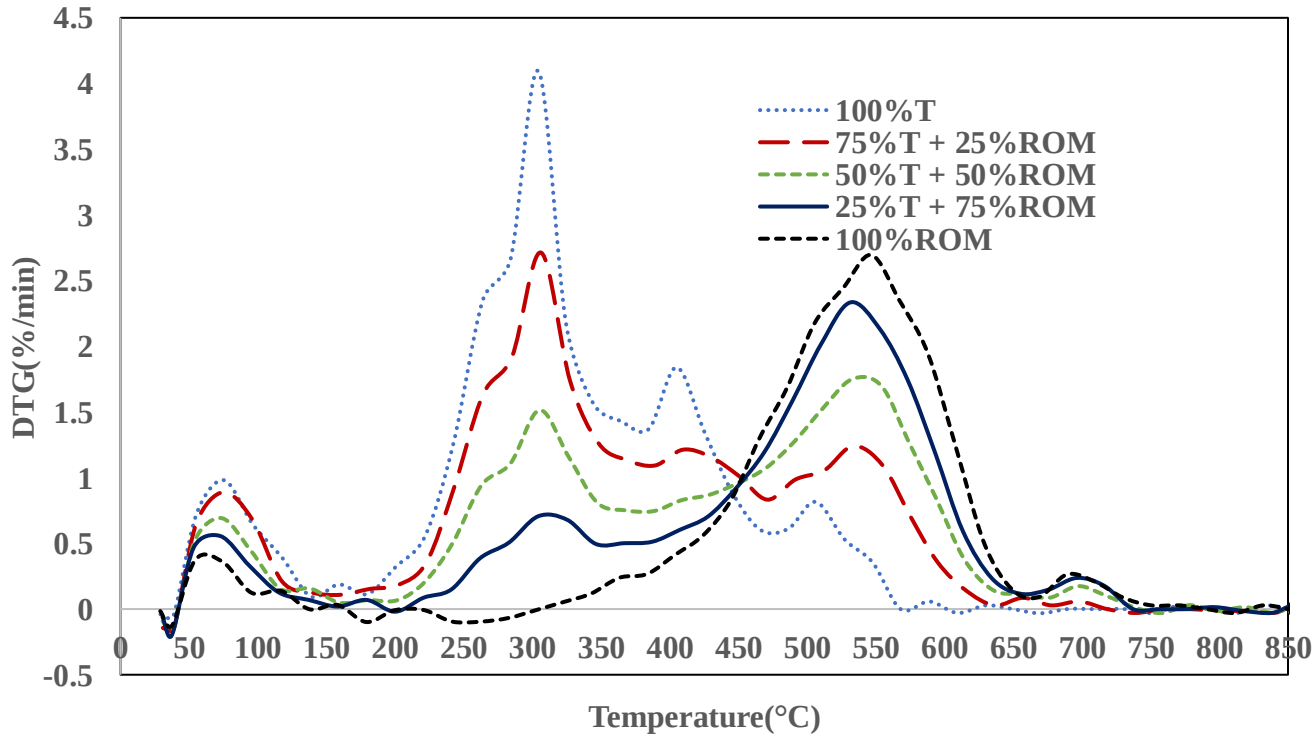

Figure B. 12: Combustion characteristics of *Tamarix usneoides* on West Complex with different ROM proportions

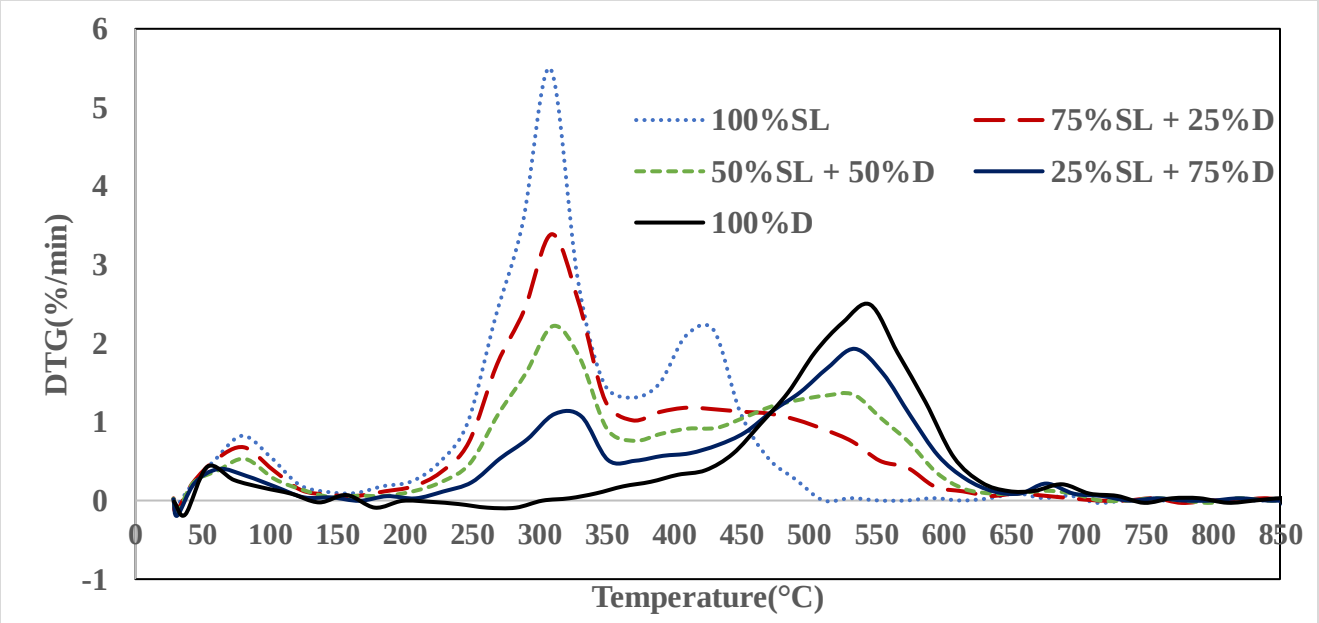

Figure B. 13: Combustion characteristics of *Searsia lancea* on Mispah with different coal discard proportions

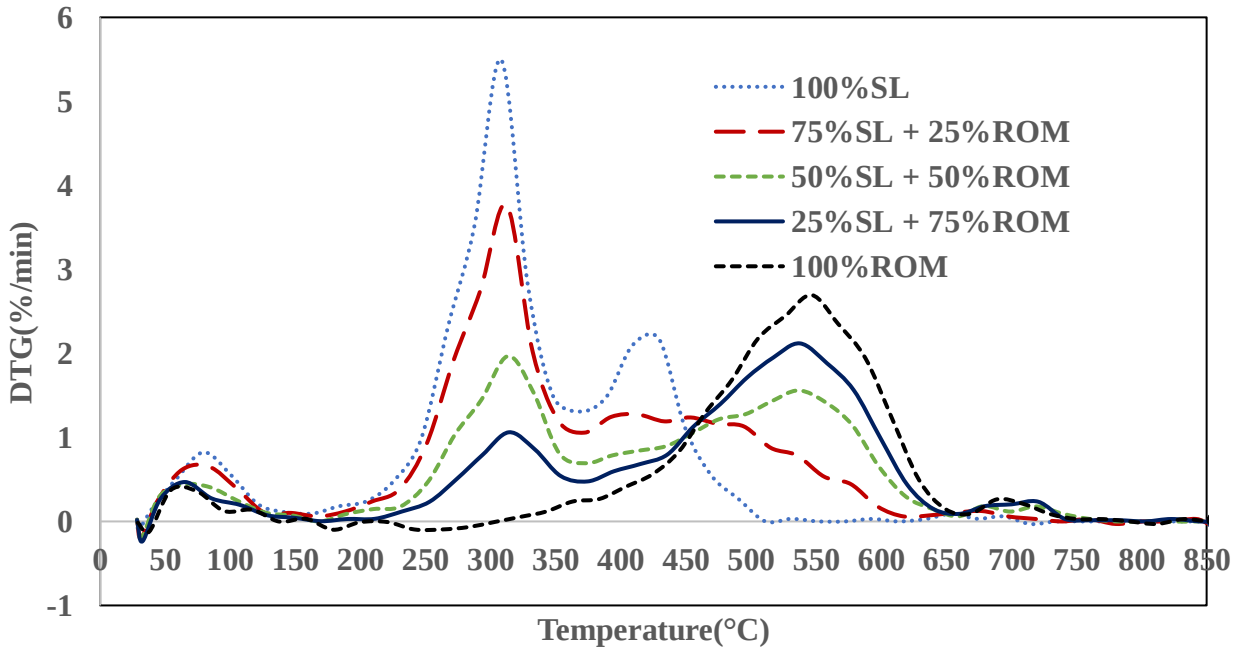

Figure B. 14: Combustion characteristics of *Searsia lancea* on Mispah with different ROM proportions

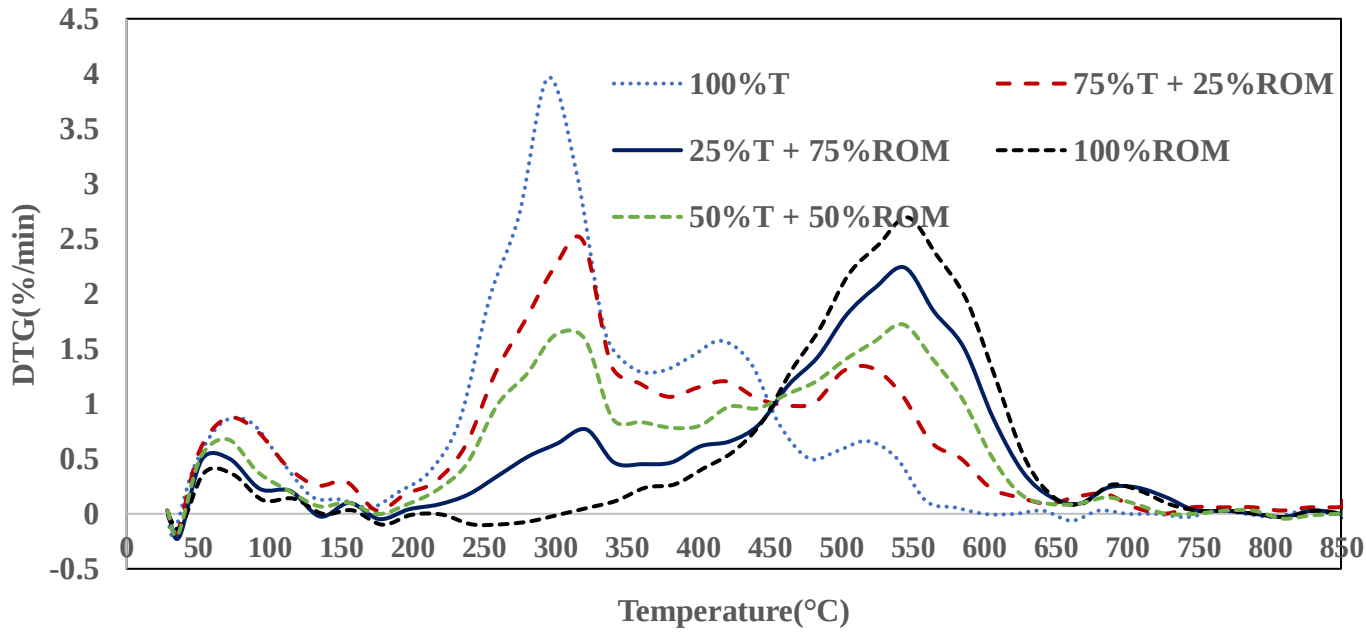

Figure B. 15: Combustion characteristics of *Tamarix usneoides* on Mispah with different ROM proportions

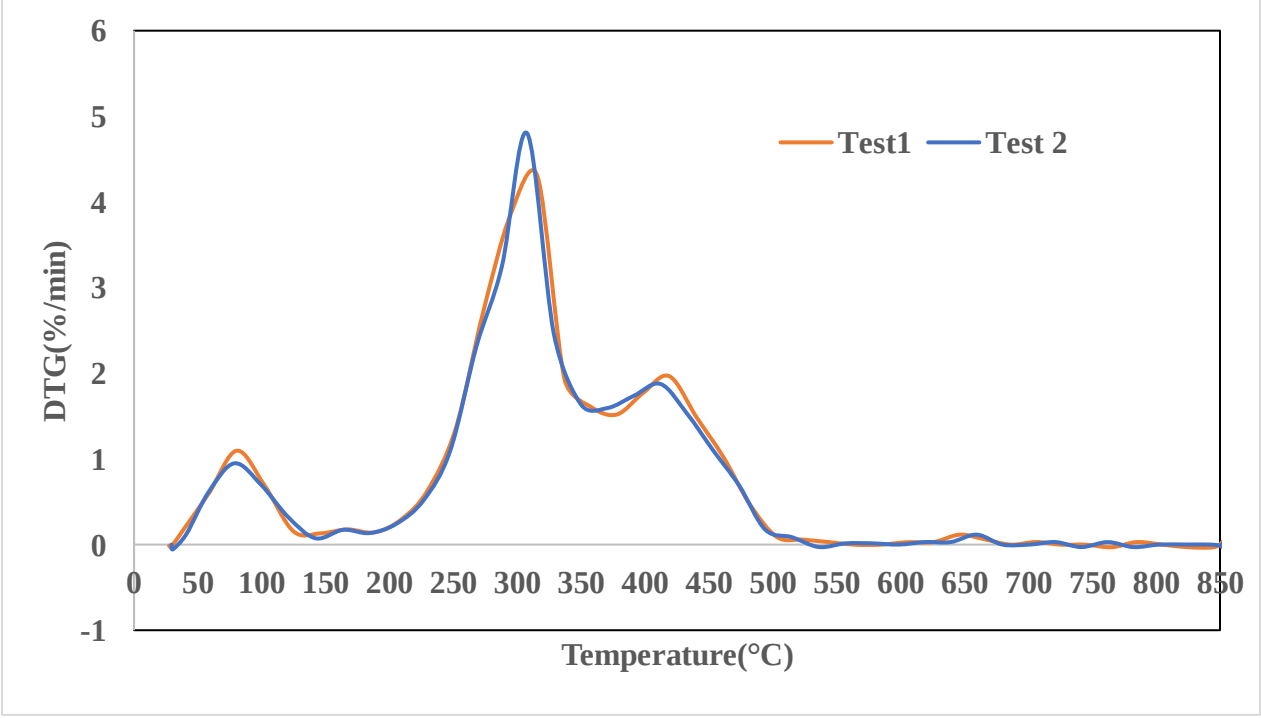

Figure B. 16: Reproducibility of combustion results using *Searsia lancea*

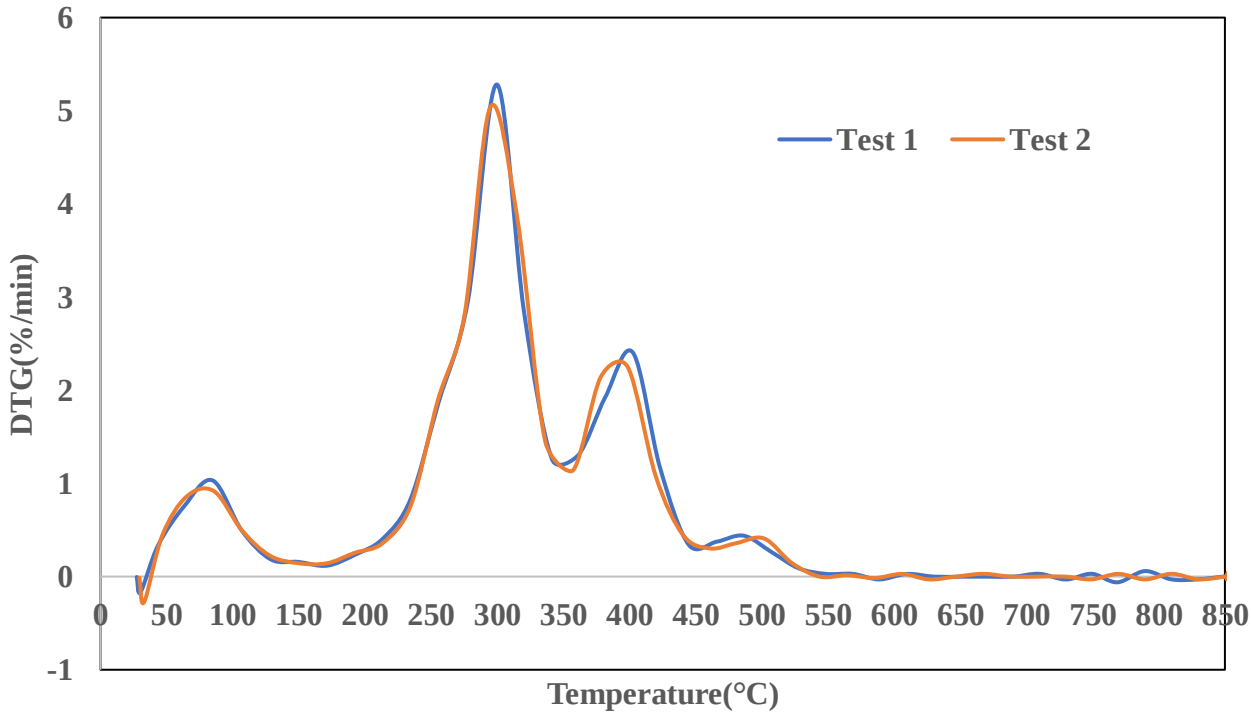

Figure B. 17: Reproducibility of combustion results using *Tamarix usneoides*